I.O.S.

RESULTS FROM A STORM SURGE PREDICTION MODEL OF THE NORTH-WEST EUROPEAN CONTINENTAL SHELF FOR APRIL, NOVEMBER AND DECEMBER 1973

by

R. A. FLATHER

REPORT NO. 24

1976

NATURAL ENVIRONMENT RESEARCH COUNCIL

INSTITUTE OF OCEANOGRAPHIC SCIENCES

RESULTS FROM A STORM SURGE PREDICTION MODEL OF THE NORTH-WEST EUROPEAN CONTINENTAL SHELF FOR APRIL, NOVEMBER AND DECEMBER 1973

by

R. A. FLATHER

REPORT NO. 24

1976

Institute of Oceanographic Sciences
Bidston Observatory
Birkenhead
Merseyside L43 7RA

CONTENTS

1. INTRODUCTION

A new scheme, employing numerical finite difference models of the atmosphere and of the sea to predict storm surges, has recently been established (Flather and Davies 1975, 1976). In applying the method to North Sea surges, a fine-mesh ten-level model of the atmosphere (Benwell, Gadd, Keers, Timpson and White 1971), currently employed in routine weather prediction at the U.K. Meteorological Office, provided the essential meteorological data, while the storm surge was computed using a sea model covering the whole of the north-west European continental shelf. First results for the periods 26-30 March 1972 and 28 March - 6 April 1973 obtained from the new scheme suggested that, although the method held some promise, there remained considerable scope for improving the accuracy of the predictions.

The purpose of the present paper is to describe some experiments aimed at determining the sensitivity of the predicted surge to changes in certain procedures of the forecasting method, and thus to indicate how the scheme may be modified to give more accurate results. The specific aspects of the method examined here correspond to those mentioned in earlier work (Flather and Davies 1975, 1976), concerning both the sea model computation itself and the derivation of the wind stress and gradients of atmospheric pressure from the basic meteorological data. The experiments were carried out by making a number of predictions for the storm surges of 28 March - 6 April 1973, each prediction differing from its predecessor in that a change was made in the forecasting procedure. By comparing results before and after each

modification, its influence on the accuracy of the prediction was assessed. The sequence of changes, thus carried out, forms a necessary part of the general development of the forecasting method.

The experiments are described and discussed in Section 2. In addition to the original result, Solution 0 (Flather and Davies 1975), five new predictions were carried out as summarised in Table 1. Specific aspects of the scheme investigated were

(i) the influence of the cross-isobar angle - the angle between the geostrophic wind and the surface wind - existing mainly because of frictional effects in the atmospheric boundary layer;

(ii) the effect of the finite difference approximation used to calculate gradients of atmospheric pressure and hence geostrophic winds - a change in the difference form employed reduces the error in estimating these gradients;

(iii) the effect of changes in depth distribution and coastal configuration incorporated in the sea model;

(iv) the influence of the presence of the tide on the predicted surge - tide-surge interaction.

A marked improvement in accuracy results from the modifications introduced.

Further verification of the revised scheme was sought by applying it to predict surges over an extended period. The period chosen was 4 November - 18 December 1973, a particularly

stormy time during which several large surges occurred. The results are presented in Section 3 and comparisons with available observations made. One of the largest surges, which reached about 3.1m at Cuxhaven on 19 November, is examined in some detail.

2. EXPERIMENTS USING THE STORM SURGES OF 2-6 APRIL 1973

2.1 THE ORIGINAL SOLUTION

Between 2 April and 6 April 1973 two storm surges occurred in the southern North Sea. The eastward passage of a small intense depression from the Atlantic across northern England, the North Sea and southern Denmark (Figure 1) produced the first surge. South-westerly winds to the south of the approaching depression decreased levels on the west side of the Southern Bight resulting in an initial negative surge at about 1200 GMT on 2 April (Figure 2a). At the same time, north-easterly winds gave a small positive surge on the north-east coast of England. The northerlies which covered the region as the depression moved east caused a positive surge, reaching 1.8m at Southend at 2000 GMT 2 April and 2.3m at Cuxhaven at 0800 GMT 3 April (Figure 2b). The passage of a frontal trough across the region on 4 April brought locally strong south-westerly winds producing a substantial negative surge in the Southern Bight at about midday.

The original forecast for this period, solution 0, is shown in Figure 2. On the English coast, the surges of 2 and 3 April are predicted reasonably well, although the double peak, possibly due to tide-surge interaction is not reproduced and the initial negative surge in the Thames Estuary is underestimated. However,

the most serious discrepancy occurs later when for a period of about 24 hours starting for Southend at 0600 GMT on 4 April the predicted surge level is up to 1.2m higher than observed. The same error can be seen (Figure 2) to a greater or lesser extent at all the ports shown, beginning a few hours earlier at Wick and later at continental ports. Thus the error appears to propagate anti-clockwise round the North Sea. As a result, the large negative surge on 4 April is completely missed and subsequently the scheme predicts a positive external surge, reaching Southend at 0000 GMT on 5 April, which did not in fact occur. Root-mean-square (RMS) errors based on hourly values of computed and observed surge for the period 0700 2/4/73 - 1900 6/4/73 have been computed for each port (see Table 2). The poor results referred to above are reflected in RMS errors of over 60 cm at Southend and Cuxhaven.

The worst discrepancies are associated with disturbances caused by the passage of a frontal trough eastwards over the continental shelf accompanied by locally strong south to south-westerly winds. Factors which it was considered might have contributed to the errors were (Flather and Davies 1975)

a) the failure of the sea model to represent adequately the shallow areas in inlets such as the Moray Firth, the Wash and the Thames Estuary on the east coast of Britain, where the offshore winds could have substantially lowered water levels locally;

b) uncertainties in the empirical relationship between the geostrophic and surface winds and in particular the angle between their directions - the cross-isobar angle;

c) failure of the scheme to resolve smaller scale atmospheric features such as fronts which might be very important in determining the surge.

Investigations of these factors are discussed in the following section.

2.2. THE EFFECT OF CHANGES IN THE SEA MODEL AND IN THE TREATMENT OF METEOROLOGICAL DATA

The influence of a), b) and c) above have been investigated by carrying out three further predictions, solutions A, B and C. The changes in the forecasting scheme incorporated before each prediction are summarised in Table 1 and described separately below with comments on the results

a) SOLUTION A

In an investigation of the M_2 tidal regime on the continental shelf (Flather 1976) it was found that a number of changes in the model as used in the original prediction were required in order to reproduce correctly the propagation of the tide from the Atlantic into the North Sea. Since storm surges and the tides are dynamically similar, both being long-waves, the characteristics of the propagation of storm surges should likewise be favourably influenced by these changes in the sea model. Accordingly, account was taken of advective accelerations, previously omitted in the equations of motion, and improvements were carried out in the representation of coastal configuration in the model. Thus, the model coastline representing the Moray Firth region, the Firths of Forth and Tay, the Thames Estuary, the Strait of Dover, the Gulf of St. Malo, the Bristol Channel and a number of other places was

changed in order to follow more closely the line of the actual land boundary. In addition, barriers were introduced to represent islands including the Isle of Man, the Hebrides, the Orkneys and the Shetlands. (The blocking effect of the Orkneys was found to have a marked effect on the tide entering the North Sea). The entrance to the Skaggerak, previously treated as a coastal boundary was also changed into an open sea boundary. The revised model is shown in Figure 3.

The forecast obtained with the altered sea model, solution A, is plotted together with solution 0 in Figure 4. The corresponding RMS errors are given in Table 2. Due to a computer error part of solution A covering the period 0700 GMT on 2 April to 0700 GMT on 3 April was lost, so that the errors exclude this interval. The changes have the effect of reducing levels during the negative surge on 4 April by typically 20 cm but as much as 50 cm at Southend. Also, the erroneous external positive surge later on 4 April is delayed by 2 to 3 hours. It is clear from Table 2 that the changes have improved the overall accuracy of the prediction, the RMS error at Southend being reduced by about 10 cm.

b) SOLUTION B

In the original prediction and in solution A, the relationship used to derive the surface wind, $\underset{\sim}{w}$, from the geostrophic wind, $\hat{\underset{\sim}{w}}$, was taken from the results of Hasse and Wagner (1971), who, on the basis of measurements in the German Bight, found that

$$\underset{\sim}{w} = a\hat{\underset{\sim}{w}} + b, \qquad (1)$$

where $a = 0.56$, and, for a neutrally stable atmospheric boundary layer, $b = 2.4$ m/s. Hasse and Wagner also commented that the angle between geostrophic and surface winds at sea was usually small and that the directional data available did not permit a meaningful investigation of these small values. On this basis it was assumed in solutions O and A that surface and geostrophic winds were in the same direction.

Recently Hasse (1974) has re-examined this relationship using an extended data set and paying particular attention to the influence of the stability of the air column as indicated by the air-sea temperature difference, ΔT . The new result gives for the coefficients in (1)

$$a = 0.54 - 0.012\,\Delta T \quad , \qquad b = 1.68 - 0.105\,\Delta T \quad m/s \tag{2}$$

where $\Delta T = T_a - T_w$ ^{o}C, T_a being the temperature of the air near the sea surface and T_w the temperature of the surface water. Clearly the difference in magnitude between the surface winds derived using the alternative values of a and b will not be very great and, in view of the uncertainties in other steps in the derivation of wind stress from the pressure distribution, may not be important. However, of greater significance, the extended data set permitted an examination of the relative directions of surface and geostrophic winds. We define the cross-isobar angle, δ , to be the angle between the directions of surface and geostrophic winds, taken as positive when the surface wind blows across the isobars from high to low pressure. Then Hasse found considerable variation

in δ , which decreases from 20^{o} for $\Delta T \doteq -5^{o}C$ to about 8^{o} when the air-sea temperature difference is small and increases again to 22^{o} at $\Delta T \doteq +3^{o}C$, with the uncertainties of directional measurements reflected in large standard deviations of 16.4^{o} for $\omega > 7$ m/s and $\sim 40^{o}$ for $\omega < 7$ m/s.

It seemed probable that a change in direction of the surface wind, and hence the wind stress, of up to 22^{o} would have a significant effect on the computed storm surge. To investigate this possibility, the formulae for computing east and north components of surface wind, ω_λ , ω_φ , from the corresponding components, $\hat{\omega}_\lambda$, $\hat{\omega}_\varphi$, of the geostrophic wind were modified as follows. First applying (1) to the geostrophic wind gives

$$\left.\begin{aligned} \omega_\lambda^c &= \hat{\omega}_\lambda (a\hat{\omega} + b)/\hat{\omega}, \\ \omega_\varphi^c &= \hat{\omega}_\varphi (a\hat{\omega} + b)/\hat{\omega}, \end{aligned}\right\} \qquad (3)$$

where ω_λ^c , ω_φ^c are the components of surface wind assuming $\delta = 0$, as used previously, and $\hat{\omega} = (\hat{\omega}_\lambda^2 + \hat{\omega}_\varphi^2)^{1/2}$. Now introducing the directional change

$$\left.\begin{aligned} \omega_\lambda &= \omega_\lambda^c \cos\delta - \omega_\varphi^c \sin\delta, \\ \omega_\varphi &= \omega_\lambda^c \sin\delta + \omega_\varphi^c \cos\delta. \end{aligned}\right\} \qquad (4)$$

(3) and (4) may be combined to give

$$\left.\begin{aligned} \omega_\lambda &= (a\hat{\omega} + b)(\hat{\omega}_\lambda \cos\delta - \hat{\omega}_\varphi \sin\delta)/\hat{\omega}, \\ \omega_\varphi &= (a\hat{\omega} + b)(\hat{\omega}_\lambda \sin\delta + \hat{\omega}_\varphi \cos\delta)/\hat{\omega} \end{aligned}\right\} \qquad (5)$$

To apply Hasse's results directly, the cross-isobar angle would

vary with both position and time, depending on air-sea temperature differences. Duun-Christensen (1975) has recently carried out surge hindcasts in which this was done, taking a simplified form of the variation of δ with ΔT given by Hasse. However, since no forecast temperatures were available here, for simplicity it was assumed that $\delta = 20^{o}$. This assumption is consistent with the values of 18^{o} used by Duun-Christensen (1971) for North Sea surges and 22^{o} adopted by Heaps and Jones (1975) for surges in the Irish Sea.

The forecast obtained using the revised meteorological data, solution B, is plotted in Figure 4, and the corresponding RMS errors are given in Table 2. Comparing solutions A ($\delta = 0^{o}$) and B ($\delta = 20^{o}$), it is clear that the cross-isobar angle has a substantial influence on the computed surge. Levels during the negative surge on 4 April are reduced by up to 50 cm, a definite improvement although the surge is still underestimated. The following positive surge, predicted incorrectly, is also delayed and reduced in magnitude as required for increased agreement with observations. The general improvement in the prediction is reflected in significantly smaller RMS errors (Table 2) and suggests that the value $\delta = 20^{o}$ may be a better approximation than $\delta = 0^{o}$ in this instance. The overall sensitivity of the results to the change in δ indicates that the spatial and temporal variations of this parameter should be taken into account. In future it is hoped that this can be achieved when additional information in the form of the predicted distribution of air temperature in the bottom layer

of the atmospheric model becomes available.

c) SOLUTION C

The basic meteorological data used in the surge prediction scheme comprises arrays of values of H, the height of the 1000 mb pressure surface, at hourly intervals, derived from the atmospheric model. The first stage in the treatment of these data consists of deriving gradients of the atmospheric pressure, p_a, assumed equal to 1000 mb + $\rho_a g H$, where ρ_a is the air density and g the acceleration due to gravity. The original formulation used spatially-centred finite differences of the form

$$\left.\begin{aligned} \left(\frac{\partial H}{\partial x}\right)_{x,y} &\doteq \{H(x+\Delta x, y) - H(x-\Delta x, y)\} / 2\Delta x, \\ \left(\frac{\partial H}{\partial y}\right)_{x,y} &= \{H(x, y+\Delta y) - H(x, y-\Delta y)\} / 2\Delta y, \end{aligned}\right\} \qquad (6)$$

to give the required gradients at the grid point x, y of the meteorological model, where $\Delta x, \Delta y$ are the distances between mesh points in the co-ordinate directions. Here the differences extend over two grid lengths, a distance of the order of 200 km, and it is easy to imagine how small scale features, such as the discontinuities associated with fronts, might be smoothed out or otherwise misrepresented by (6).

An alternative formulation which uses differences extending over only one grid length to give estimates for the required gradients at intermediate points, $x + \frac{1}{2}\Delta x, y + \frac{1}{2}\Delta y$ say, is

$$\left.\begin{aligned} \left(\frac{\partial H}{\partial x}\right)_{x+\frac{1}{2}\Delta x, y+\frac{1}{2}\Delta y} &\doteq \{H(x+\Delta x, y+\Delta y) - H(x, y+\Delta y) \\ &\quad + H(x+\Delta x, y) - H(x, y)\} / 2\Delta x, \end{aligned}\right\}$$

$$\left(\frac{\partial H}{\partial y}\right)_{x+\frac{1}{2}\Delta x,\, y+\frac{1}{2}\Delta y} \doteq \Big\{ H(x+\Delta x, y+\Delta y) - H(x+\Delta x, y) + H(x, y+\Delta y) - H(x,y) \Big\} / 2\Delta y . \tag{7}$$

Intuitively, (7), by virtue of its finer resolution, would be expected to give more accurate results than (6). This is indeed borne out in a closer examination of the errors. Straightforward expansion of the right hand side of (6) using Taylor series gives

$$\{ H(x+\Delta x, y) - H(x-\Delta x, y) \} / 2\Delta x = \left(\frac{\partial H}{\partial x}\right)_{x,y} + \frac{\Delta x^2}{3!}\left(\frac{\partial^3 H}{\partial x^3}\right)_{x,y} + O(\Delta x^4),$$

with an equivalent expression for the y-component. In other words, the errors in (6) are

$$\left.\begin{aligned} &\frac{\Delta x^2}{3!}\left(\frac{\partial^3 H}{\partial x^3}\right)_{x,y} + O(4) ; \\ &\frac{\Delta y^2}{3!}\left(\frac{\partial^3 H}{\partial y^3}\right)_{x,y} + O(4) \end{aligned}\right\}$$

Applying a similar analysis to (7) gives corresponding errors

$$\left.\begin{aligned} &\tfrac{1}{4}\left\{ \frac{\Delta x^2}{3!}\left(\frac{\partial^3 H}{\partial x^3}\right) + \frac{\Delta y^2}{3!}\left(\frac{\partial^3 H}{\partial x \partial y^2}\right)\right\}_{x+\frac{1}{2}\Delta x,\, y+\frac{1}{2}\Delta y} + O(4) . \\ &\tfrac{1}{4}\left\{ \frac{\Delta x^2}{3!}\left(\frac{\partial^3 H}{\partial x^2 \partial y}\right) + \frac{\Delta y^2}{3!}\left(\frac{\partial^3 H}{\partial y^3}\right)\right\}_{x+\frac{1}{2}\Delta x,\, y+\frac{1}{2}\Delta y} + O(4) \end{aligned}\right\}$$

Thus, for example, if $H = H(x)$ then the error in (7) is smaller than that in (6) by a factor of four.

The scheme for processing the meteorological data was modified so as to improve its resolution by incorporating (7) in place of (6). The forecast obtained using the revised scheme, solution C,

is plotted in Figure 4 and the corresponding RMS errors given in Table 2. Comparing solutions B (using (6)) and C (using (7)), substantial differences are apparent, especially in the Southern Bight. At Southend, the negative surge on 4 April is 50 cm lower than in solution B and agrees quite well with the observed level, though occurring somewhat later. However, the overall accuracy of the present solution as indicated by the RMS errors in Table 2 shows conflicting results, with reduced errors at Walton-on-Naze and Southend but correspondingly increased errors at Ijmuiden and Terschelling. At ports outside the Southern Bight solutions B and C seem to achieve similar accuracy. Nevertheless, the surge profile at individual ports is quite sensitive to the changes described so that the question of the resolution of the meteorological situation warrants serious consideration. If the atmospheric model itself does not resolve important smaller scale features, then a refinement of its computational mesh would appear to be needed - but could be impracticable because of the size of the computation. If, on the other hand, the atmospheric model data does indeed describe adequately these features, then still more accurate methods of obtaining derivatives, perhaps using higher order difference formulae or even spectral methods, might be justified.

2.3 THE EFFECT OF FURTHER CHANGES IN THE SEA MODEL AND TIDE-SURGE INTERACTION

In the light of work carried out on the tides on the continental shelf (Flather 1976), some additional changes to the sea model topography were introduced. These changes were made in an attempt

to further improve the accuracy of tidal propagation in some areas of the model of particular importance from the point of view of surge prediction. A "surge only" solution (D) obtained with these changes included is described here and compared with the equivalent solution (E) in which tide and surge were computed together, permitting the important question of tide-surge interaction to be examined.

a) SOLUTION D

The model depth distribution used in all previous solutions was taken from that used by Heaps (1969). Since in the present finite-difference schematisation depth values are required at points different from those in Heaps' model, the appropriate values for our model were obtained from those quoted by Heaps by simple averaging: a process which introduces some smoothing of bottom topography. In view of the importance of shallow water areas in tidal propagation and surge generation, a new set of depths with no artificial smoothing was prepared from navigational charts, particular attention being given to coastal areas. The representation of the land boundary in the southern North Sea and in the German Bight was also changed slightly. Tests with the M_2 tide using the revised scheme (Figure 5) showed some improvement in the Thames Estuary, though at the expense of slightly worse results elsewhere. Nevertheless, this model was used in the present solution which in all other respects was identical to solution C.

The forecast obtained with the revised scheme is plotted in Figure 6 for all 17 ports from which observational data were

available and the corresponding RMS errors are again given in Table 2. The errors are very nearly the same as in solution C, and detailed comparisons of the surge profiles show differences between C and D no larger than 15 cm.

b) SOLUTION E

The final experiment in the present series included tidal influence in the surge computations. Previous work (Proudman 1955, Banks 1974) has established that tide-surge interaction, associated with non-linearities in the hydrodynamical equations, is significant in estuaries and shallow sea regions; areas which the present model grid does not resolve well. However, the effect of interaction over a more extensive area - the continental shelf as a whole - is of interest here. Should this effect be large, then the modifications to take account of interaction, described below, would be essential to the success of the scheme.

Substantial changes in the overall method of prediction as previously described, and in the details of the sea model calculation, were required in order to account for tide-surge interaction. A basic requirement was the ability to compute the tide alone on the continental shelf, a considerable problem in itself. Calculation of the M_2 tide has been discussed in a separate paper (Flather 1976). For the present purpose the M_2 and S_2 constituents were included as described below. The procedure then, for each forecast period, is to carry out two separate model runs, one to predict the tidal distribution alone, the other to predict tide and surge together. The difference between the two solutions consists of a surge prediction

including interaction effects, which might be compared with the equivalent "surge only" prediction (solution D).

The tide on the continental shelf arises from a co-oscillation with the neighbouring North Atlantic. Thus, in order to introduce tide in addition to surge into the model, the condition applied on open sea boundaries had to be altered. Incorporating the essentials of the boundary condition applied in the tidal model (Flather 1976) and in previous surge calculations (Flather and Davies 1976), the following generalised form of radiation condition was arrived at :

$$q_n = \hat{q}_n^{(s)} + \sum_i \hat{q}_n^{(i)} + \frac{c}{h}\left\{\zeta - \hat{\zeta}^{(s)} - \sum_i \hat{\zeta}^{(i)}\right\}, \qquad (8)$$

where q_n is the component of depth mean current along the outward directed normal to the boundary, ζ is elevation, h the water depth, $c = (gh)^{1/2}$, and the input now has contributions

$\hat{\zeta}^{(s)}$, $\hat{q}_n^{(s)}$ from the surge

and $\hat{\zeta}^{(i)}$, $\hat{q}_n^{(i)}$ from the i th constituent of the tide.

The surge input is computed exactly as before, taking

$$\hat{\zeta}^{(s)} = (\bar{p}_a - p_a)/\rho g, \quad \hat{q}_n^{(s)} = 0, \qquad (9)$$

where $\bar{p}_a$ is the mean atmospheric pressure, assumed to be 1012 mb, and ρ is the density of sea water. The form of the tidal input must ensure that the tide and the meteorological forcing are correctly aligned in time. This is achieved by taking, for the i th constituent,

$$\hat{\zeta}^{(i)} = f_i H_i \cos(\sigma_i t + V_i + u_i - g_i),$$
$$\hat{q}_n^{(i)} = f_i Q_i \cos(\sigma_i t + V_i + u_i - \gamma_i), \qquad (10)$$

where the notation is :

H_i amplitude of elevation;

g_i phase of elevation relative to the corresponding constituent of the equilibrium tide at Greenwich;

Q_i amplitude of the normal component of depth mean current;

γ_i phase of current;

σ_i speed of the i th constituent;

f_i, u_i nodal factors taking account of the tidal modulation with period 18.6 years;

V_i phase of the i th constituent of the equilibrium tide at Greenwich at time $t = 0$.

The nodal factors, f_i and u_i, in fact vary with time, but since their period is much larger than the duration of any model forecast, values appropriate to the time origin, $t = 0$, were used throughout. H_i, g_i, Q_i and γ_i depend on position on the open boundaries: their values for the largest constituent, M_2, (designated $i = 1$ here) were determined earlier (Flather 1976). However, it was considered worthwhile including also the next largest constituent, S_2, ($i = 2$, say) since by computing M_2 and S_2 together a spring - neap variation in tidal range is obtained. Examination of available tidal

constants derived from offshore tidal measurements (Cartwright 1976) showed that the ratio of amplitudes and the difference between phases of M_2 and S_2 varied only slightly along the edge of the continental shelf. The mean values were $H_2/H_1 = 0.363$ ($\pm 3\%$), $g_2 - g_1 = 35.3^\circ$ ($\pm 2^\circ$); the small variation presumably is a consequence of the closeness of σ_2 to σ_1 and the absence of intervening resonances, so that the propagation of the two constituents is very similar. The input data for the S_2 tidal constituent was thus obtained by taking $H_2 = 0.363\, H_1$, $g_2 = g_1 + 35.3^\circ$, $Q_2 = 0.363\, Q_1$, $\gamma_2 = \gamma_1 + 35.3^\circ$. Subsequent analysis of the tidal solution calculated using the combined M_2 and S_2 input and comparisons between the computed constants and those derived from observations at tide gauges showed agreement.

The forecast, including the effects of tide-surge interaction, computed with the revised scheme is plotted in Figure 7. Comparing the present solution with the "surge only" solution (D; Figure 6), it is clear that the presence of the tide makes a considerable difference to the surge profiles. Generally, solution E appears to give a better fit to the observations than did solution D. For the first time in these experiments, the erroneous positive external surge, predicted as reaching Southend early on 5 April in solution D, does not appear, possibly as a result of the additional damping due to the presence of tidal currents in the quadratic law of bottom stress. Although the maximum and minimum surge heights at Southend and Ostende are adversely affected, extreme levels

at other ports seem to be unaltered; see, for example, the negative surge on 4 April at Lowestoft, Inner Dowsing and Immingham, or the positive surge at Cuxhaven and Terschelling on 3 April. The negative surge at Esbjerg at 0000 on 3 April is larger and more accurately reproduced with the interaction effects included. The RMS errors from solution E, given in Table 2, show without exception a satisfactory reduction over those from solution D, amounting to 9 cm at Southend, Ostende, Cuxhaven and Esbjerg.

Strong evidence for the eventual usefulness of the proposed surge forecasting technique can be derived from an overall look at Table 2, which exhibits a reduction in RMS errors, resulting from the sequence of modifications introduced, of almost 50% at some ports.

3. STORM SURGES BETWEEN 4 NOVEMBER AND 18 DECEMBER 1973

As a further test of the modified scheme, used in solution E, an extended prediction covering a period of 44 days was carried out. The period selected was 4 November to 18 December, 1973, a particularly stormy time which included a number of large surges. Weather charts showing the meteorological situations which caused the main surges are shown in Figures 8a-8g, and the results of the forecasts are plotted, with all available observations for comparison, in Figures 9-13. For convenience, the plots are divided into four ten day periods; 4-14 November, 14-24 November, 24 November - 4 December and 4-14 December; and one four day period; 14-18 December. The RMS error for each port for each of these periods has been computed as before and

these are presented in Table 3. In addition, a linear regression analysis has been carried out as discussed later, and the results are given in Table 4.

An examination of the weather charts, Figures 8a-8g, shows that most storms during the period were caused by rather similar meteorological events in which a large depression moved east or south east from somewhere between Iceland and the Faroes, subsequently crossing southern Scandinavia and passing on into the Baltic. Associated with these storms were surges reaching magnitudes of over 3m at Cuxhaven on 19 November and 6 December and more than 2m on another four occasions (see Figures 9b, 10b, 12b and 13b). The northerly-located track of the depressions brought the strongest winds to bear over the northern half of the North Sea, so that generally disturbances on the English coast, having the nature of travelling waves, were not much amplified between the Wash and Southend; the largest positive surges were 1.2m to 1.6m at Inner Dowsing, Lowestoft and in the Thames Estuary (see Figures 9a, 10a, 12a and 13a). The largest negative surge, -1.5m on 12 November, occurred at Southend and was associated with strong south westerly winds accompanying a frontal trough. The most significant departure from the weather pattern just described occurred on 7-8 December, when a wave depression followed a more southerly track crossing the North Sea between the Wash and northern Holland (Figure 8e) and produced an internal surge on the English coast. The period 24 November - 4 December was much less disturbed than any other.

Comparing forecast surges with those observed, see Figures 9-13,

it is clear that most disturbances are predicted quite well, although some are underestimated, as for example the negative surge on the English coast on 12 November, and others, such as the positive surge on 19 and 20 November, are overestimated. In a number of cases errors appear to propagate through the system in the same way as true disturbances. An example can be seen in Figure 10a. For about 12 hours starting at 0600 on 19 November, the predicted level at Stornoway is 20 cm to 40 cm higher than observed. This error can be followed down the east coast of Scotland and England, reaching Southend at about 2200 on the same day and making predicted levels there as much as 60 cm too high during the next few hours. Seen in this way the source of the error would appear to be either incorrect specification of the input surge on the open boundary north and west of Scotland, or erroneous meteorological data generating an external surge incorrectly on the shelf to the west of Scotland. Once generated, the error propagates through the model as an external surge producing the symptoms described. However, this could be an oversimplified explanation. As mentioned already, typical storms during the present period were due to depressions passing from west to east between the Faroes and southern Norway. Frontal systems accompanying these depressions are often aligned from north-east to south-west, see Figures 8b, 8d, 8e, 8g, so that as the depression crosses the shelf, the associated fronts appear to move from north-west to south-east, affecting first the sea areas north west of Scotland then moving down the east coast of Scotland and England

into the Southern Bight. Thus if an error in the basic meteorological data or any deficiency in its treatment causes the wind stress associated with the front to be estimated incorrectly, then errors in water level will be generated locally in the neighbourhood of the front, and these errors will appear in succession at ports coming under its influence. Clearly, it is difficult to distinguish between errors introduced externally and those introduced locally with the passage of incorrect meteorological forcing. Also, once introduced, the local errors will propagate much as external surges, further complicating the problem.

One possible means of identifying the major contribution to the discrepancies is to use a second model, perhaps covering only the North Sea (Davies, 1976). By introducing observations on the northern boundary of such a model, external errors might be reduced or even eliminated. If, as a result of using the second model, the present errors along the east coast were considerably reduced, then external errors would be indicated as being of first importance. If, on the other hand, errors on the east coast were not reduced or even increased, as they could be if incorrect forcing by wind stress were applied over the better-represented shallow water areas of a fine mesh sea model, then the second mechanism could be significant. Depending on the outcome of such an experiment, attention could be given to improving the accuracy of the meteorological input data or to a more realistic treatment of conditions at the shelf edge.

In addition to the usual computation of RMS errors from the

results, a linear regression analysis was carried out in which a relationship between predicted and observed elevations of the form

$$\zeta_{observed} = c_1 \zeta_{predicted} + c_0 \qquad (11)$$

was sought. The constants c_c and c_1 were determined by standard least squares techniques from available hourly comparisons at individual ports, the five time intervals mentioned earlier being treated separately. The resulting values of c_1 and c_c are given in Table 4. An advantage of the regression analysis over simple RMS errors is that the former gives an indication of the nature of the discrepancy. For example, a value of c_1 greater than unity indicates a tendency for the scheme to underestimate the magnitude of disturbances, while a large value of c_c suggests a constant difference between predicted and observed levels which could be accounted for by an error in the datum. It is interesting to note in Table 4 that during the periods 14-24 November, 4-14 December and 14-18 December values of c_1 were generally less than unity indicating that disturbances were overestimated, and during 24 November - 4 December values of c_1 were greater than unity suggesting the reverse. Since the first three periods mentioned were the most active and the last period the least active from the storm surge point of view, it appears that wind stresses during storms may be too large and those during quiet periods too small. The assumed variation with wind

speed of the drag coefficient (Flather and Davies 1975) could well account for this.

A further point which is apparent from Table 4 is that c_c tends to decrease steadily with increasing time over the five periods, which suggests that the predicted mean level is steadily raised relative to the datum of the observations. This trend may account for the corresponding increase in RMS errors (Table 3). If the datum in the sea model is changing, then the radiation open boundary condition (8) might be suspected of producing a net gain in volume of water within the model. A practical cure would be to restrict the duration of continuous runs to, say, one month, carrying out a 'cold start' with a two or three day running-in period to continue the predictions. Also, it might seem tempting to try to improve the accuracy of the surge forecast by using an equation such as (11). However, the variability of the regression coefficients for a given port from one period to the next (see Table 4) should be sufficient warning of the possible dangers of such a procedure. Rather, it would seem to be better to do as much as possible to make the model predictions more accurate, resorting to numerical corrections only when no further progress can be made. Finally, it should be pointed out that, with the exceptions mentioned above, the RMS errors given in Table 3 are generally similar to those obtained from the better predictions for the April period (Table 2). This is encouraging since, at continental ports, some of the surges during November and December were

much larger than any predicted previously.

To complete the present investigation of the November-December 1973 period, the storm surge on 19-20 November, one of the larger surges, is now examined in some detail. Figures 14a-14ℓ contain pairs of diagrams with contours of storm surge residual elevation (cm.) on the left and the corresponding distribution of vectors representing depth mean current on the right. Referring also to Figure 8d, which gives the appropriate weather charts and to Figures 10a, 10b and 10c, showing the time variation of surge elevation at tide gauges, the following picture of the development of the surge is obtained.

Early on 18 November, a depression approached the Faroes from the Atlantic, bringing south westerly winds over the shelf west of Scotland and generating an external positive surge; north going currents near the Hebrides reached 40 cm/s at 0100 GMT (Figure 14a). Over the North Sea, pressure was falling but winds were light and a convoluted pattern of currents, perhaps following the surge elevation contours, prevailed. As the depression moved east, the south-westerly winds affected both the Irish Sea (producing a positive surge in the Solway Firth) and the north-western part of the North Sea, causing water to flow northwards near the east coast and giving an internal negative surge in the Wash (Figure 14b). Between 0600 and 1800 the depression deepened considerably. Winds to the north of Scotland veered to westerly and the external surge crossed the top of Scotland and entered the North Sea (Figures 14c and 14d). South westerly winds extending further east had decreased levels

over much of the southern North Sea. The internal negative surge reached the Thames Estuary shortly after midday, and the level difference between the Channel and the Southern Bight produced a north going current of more than 15 cm/s through the Strait of Dover at a time when local pressure gradients were negligible and winds in the area were light.

As the depression passed north of the Shetlands in the early hours of 19 November, the wind over the shelf to the north and east of Scotland changed direction from westerly to north-westerly, reaching 45 knots at times. The current into the North Sea through the Pentland Firth and between Orkney and Shetland increased to 60 cm/s (Figures 14e and 14f) and the external surge east of Scotland moved south with increasing height reaching above 120 cm in the Wash despite locally offshore winds (up to 30 knots from the west). At 0700 south going currents extended over most of the North Sea and the northerly flow through the Strait of Dover was reversed as levels in the Southern Bight exceeded those in the eastern Channel (Figure 14f). By midday the depression was centred over the Skaggerak and north to north westerly winds covered the whole of the North Sea, the region of strongest winds acting between Scotland and Southern Norway. South-going currents reached 80-90 cm/s at some places off north east Scotland at this time (Figure 14g) producing a second positive surge which grew rapidly as it moved down the east coast. Meanwhile, the external positive surge reached the Southern Bight, giving the surge peak of about 125 cm at Southend at 1500. Levels on the continental coast increased steadily over most of the day.

Figure 14h shows the situation as the surge in the German Bight approached its maximum level with the region of strongest winds situated off the west coast of Denmark. The pressure gradient due to the slope of the sea surface evidently caused water to flow northward along the Danish coast, against the direction of the wind, with velocities up to 110 cm/s. The positive surge on the east coast of England, reaching a height of 200 cm in the Wash, moved south arriving in the Thames Estuary late on 19 November and giving a maximum level of 210 cm at Southend.

In the early hours of 20 November, the depression had reached the eastern Baltic and pressure was rising over the North Sea as an anticyclone moved east over the British Isles. Winds decreased rapidly and levels began to fall as water flowed back to the north. In the Southern Bight levels remained high and the surface slope down towards the Channel was extremely steep, producing a south-going current of 70 cm/s through the Strait of Dover (Figure 14i). An examination of the weather situation at this time shows nearly uniform atmospheric pressure and light winds over the Southern Bight and English Channel. Figures 14j, 14k and 14ℓ show the return to normal levels as the high pressure region moved over the North Sea. Residual currents during this period seem to show a tendency to follow the contours of elevation with the water surface sloping up to the right of the direction of flow (Figures 14j and 14k). This behaviour suggests that the flow is nearly geostrophic, with pressure gradients balanced by the Coriolis acceleration. Finally in Figure 14ℓ, with only small elevation differences over the shelf,

a meandering pattern of currents rather similar to that in Figure 14a obtains.

Of specific interest are the vector plots in Figures 14a-14ℓ, which show for perhaps the first time the evolution of depth mean currents over the continental shelf during a large storm surge. It is noticeable that the currents are very substantial, often with magnitudes similar to those of the strongest tidal flows as depicted in tidal stream atlases - see for example Deutsches Hydrographisches Institut, 1963. Storm surges, therefore, must contribute significantly, along with water movements associated with tides and surface waves, to the largest currents occurring in the North Sea and hence to the total drag on any offshore structure occupying a large part of the water column.

4. CONCLUDING REMARKS

The experiments described in Section 2 indicate that all aspects of the forecasting scheme, investigated here, have some influence on the predicted surge.

A change of 20^{o} in the cross-isobar angle, used to relate the direction of the surface wind to that of the geostrophic wind, produces a significant effect, so that both the temporal and spatial variations of this parameter could be important in determining the storm surge and should be taken into account in future. Using Hasse's (1974) results as a basis for deriving surface wind from geostrophic wind, only some knowledge of air-sea temperature differences would be required in addition to the presently available information. It is hoped that these data will be extracted from the meteorological

model output for use in future predictions.

The accuracy with which gradients of atmospheric pressure can be derived, by finite difference methods, from the basic pressure data also has a significant influence on the predicted surge. In addition, there is a fundamental limitation depending on the grid size of the atmospheric model. If scales of motion which this mesh cannot resolve are important in surge generation, then improved treatment of the present data need not lead to more accurate water level predictions. Nevertheless, it might be worthwhile considering the use of higher order derivatives or even surface fitting techniques in order to improve the estimates of gradients.

Extensive changes in coastal configuration and depth distribution may have quite a large effect: localised changes, on the other hand, are unlikely to have much influence on the computed surges. It is difficult to see how this aspect of the scheme could be further improved within the limitations of the present mesh size. The introduction of regions of finer resolution nested in the shelf model grid, would be needed in order to represent properly certain areas. Alternatively, completely separate finer mesh models (Davies 1976) could be used.

The influence of the tide is important, and clearly tide-surge interaction must be taken into account in all future predictions. At present only M_2 and S_2, the two largest constituents, are taken into account and it is not clear to what extent an improvement in the accuracy of tidal predictions in the model by

including further constituents would be reflected in more accurate surge forecasts. The next largest semi-diurnal constituents, N_2, might be included using similar estimates to those used for S_2. In addition, diurnal constituents K_1 and O_1 might be taken into account when measurements near the shelf edge between Ireland and Brittany become available. This would introduce a diurnal inequality into the model tide. However, since interaction is a second order effect, improvements in surge predictions might not repay the work involved.

The computations carried out for surges in November and December 1973 provided a useful test of the scheme over an extended period. The results point to some further aspects of the method which might be examined. In particular, a tendency for disturbances to be overestimated in stormy periods and underestimated in quieter periods could be a reflection of too rapid an increase of the sea-surface drag coefficient with wind speed (Flather and Davies 1975). Also, the way in which errors appearing to the north-west of Scotland seem to propagate into the Southern Bight warrants further investigation. If they are introduced on the open boundary and do indeed propagate through the model as disturbances then corrections based on observational information might be introduced on the boundaries of inner models (Davies 1976). If not, then they would appear to be generated locally by incorrect wind stresses or pressure gradients moving across the sea.

A first look at depth mean currents associated with a large storm surge suggests that they may be comparable in magnitude with tidal currents. Surge currents, then, must account for a

substantial proportion of the largest currents in the North Sea. Since, by their nature, they would tend to occur at times of strong surface wave activity, they may play an important part in determining the drag on offshore structures such as oil rigs or single buoy moorings, which occupy a large part of the water column.

In addition to those aspects of the scheme, mentioned above, which require examination in the future, several more practical questions need to be answered before operational predictions could begin. These questions, concerning such things as the length of warning which can be given of an approaching surge and the general robustness of the scheme, covering procedures to be followed in the event of computer breakdowns and similar eventualities, will be discussed in a subsequent report.

ACKNOWLEDGEMENTS

The author is indebted to Dr. N. S. Heaps for advice and comments during the course of this work and to the U.K. Meteorological Office for supplying data from the 10 level model.

The assistance of Mr. R. Smith in preparing the diagrams is gratefully acknowledged.

REFERENCES

BANKS, J.E. 1974. A mathematical model of a river-shallow sea system used to investigate tide, surge and their interaction in the Thames - Southern North Sea region. Philosophical Transactions of the Royal Society, A, 275, 567-609.

BENWELL, G.R.R., GADD, A.J., KEERS, J.F., TIMPSON, M.S. & WHITE, P.W. 1971. The Bushby-Timpson 10 level model on a fine mesh. Meteorological Office, London, Scientific Papers, No.32, 23 pp.

CARTWRIGHT, D.E. 1976. Shelf boundary tidal measurements between Ireland and Norway. Mémoires de la Société Royale des Sciences de Liège, Ser.6, 10, 133-139.

DAVIES, A.M. 1976. Institute of Oceanographic Sciences Report in preparation.

DEUTSCHES HYDROGRAPHISCHES INSTITUT 1963. Atlas der Gezeitenströme für die Nordsee, den Kanal und die Britischen Gewasser, Hamburg.

DUUN-CHRISTENSEN, J.C. 1971. Investigations on the practical use of a hydrodynamic numeric model for calculation of sea level variations in the North Sea, the Skaggerak and the Kattegat. Deutsche hydrographische Zeitschrift, 24, 210-240.

DUUN-CHRISTENSEN, J.C. 1975. The representation of the surface pressure field in a two-dimensional hydrodynamic numeric model for the North Sea, the Skaggerak and the Kattegat. Deutsche Hydrographische Zeitschrift, 28, 97-116.

FLATHER, R.A. and DAVIES, A.M. 1975. The application of numerical models to storm surge prediction. Institute of Oceanographic Sciences Report No.16. 23 pp + figs.

FLATHER, R.A. 1976. A tidal model of the north-west European continental shelf. Mémoires de la Société Royale des Sciences de Liège, Ser.6, 10, 141-164.

FLATHER, R.A. and DAVIES, A.M. 1976. Note on a preliminary scheme for storm surge prediction using numerical models. Quarterly journal of the Royal Meteorological Society, 102, 123-132.

HASSE, L. and WAGNER, V. 1971. On the relationship between geostrophic and surface wind at sea. Monthly Weather Review, 99, 255-260.

HASSE, L. 1974. On the surface to geostrophic wind relationship at sea and the stability dependence of the resistance law. Beiträge zur Physik der Atmosphäre, 45, 45-55.

HEAPS, N.S. 1969. A two-dimensional numerical sea model. Philosophical Transactions of the Royal Society, A, 265, 93-137.

HEAPS, N.S. and JONES, J.E. 1975. Storm surge computations for the Irish Sea using a three-dimensional numerical model. Mémoires de la Société Royale des Sciences de Liège, Ser.6, 7, 289-333.

PROUDMAN, J. 1955. The propagation of tide and surge in an estuary. Proceedings of the Royal Society, A, 231, 8-24.

Solution	Meteorological Input		Sea Model		Tide?
	Cross-isobar angle	Resolution	Depth distribution and coastal configuration	Advection?	
0	0^o	$2\Delta s$	Heaps (1969)	NO	NO
A	0^o	$2\Delta s$	Heaps depths; <u>new boundaries</u> <u>(see Figure 3)</u>	<u>YES</u>	NO
B	<u>20^o</u>	$2\Delta s$	Heaps depths; new boundaries	YES	NO
C	20^o	<u>Δs</u>	Heaps depths; new boundaries	YES	NO
D	20^o	Δs	<u>new depths</u>; <u>new boundaries</u> <u>(see Figure 5)</u>	YES	NO
E	20^o	Δs	new depths; new boundaries	YES	<u>$M_2 + S_2$</u>

Table 1 : Summary of experiments carried out. Changes in the prediction scheme from one solution to the next are underlined.

Port	Run 0	Run A*	Run B	Run C	Run D	Run E
Wick	16.6	16.7	16.5	17.6	18.1	13.5
Aberdeen	21.4	21.8	19.5	20.3	20.3	15.9
North Shields	26.4	25.0	18.9	21.9	22.5	17.0
Inner Dowsing	39.4	34.4	27.3	26.0	26.9	21.2
Immingham	35.4	32.4	25.6	25.6	26.6	19.5
Lowestoft	45.0	38.2	28.9	27.4	29.8	25.0
Walton-on-Naze	50.6	45.3	37.8	33.3	34.3	27.2
Southend	60.8	50.6	47.5	41.5	42.9	33.9
Ostende	45.4	41.4	33.9	35.7	36.1	25.1
Ijmuiden	50.7	43.5	37.2	42.4	42.3	34.6
Terschelling	42.7	35.3	25.2	32.2	32.3	27.2
Cuxhaven	60.9	58.5	45.5	47.9	48.0	37.4
Esbjerg	40.8	45.5	33.7	32.1	32.6	23.3
Bergen	13.6	12.4	12.6	12.0	13.3	11.1

Table 2 : RMS errors (cm) based on hourly values of computed and observed surge for the period 0700 2/4/73 - 1900 6/4/73.

(* period 0700 3/4/73 - 1900 6/4/73 only)

Port	4-14 Nov	14-24 Nov	24 Nov-4 Dec	4-14 Dec	14-18 Dec	Overall	Samples
Stornoway	20.7	16.9	21.6	24.9	28.0	21.4	498
Lerwick	8.5	9.5	12.3	14.7	23.1	12.9	1013
Wick	20.0	20.1	17.0	24.1	27.6	22.1	580
Aberdeen	15.1	17.4	15.7	21.0	26.8	18.5	1056
North Shields	21.6	16.7	13.6	18.7	21.4	18.2	1056
Immingham	20.6	23.8	19.5	28.1	40.6	25.6	1056
Inner Dowsing	18.7	22.8	13.7	26.6	38.0	23.1	1039
Lowestoft	18.0	19.5	17.4	23.2	37.3	21.8	1056
Walton-on-Naze	24.5	25.6	20.0	29.3	44.8	29.4	580
Southend	27.6	29.4	21.9	30.8	49.3	32.4	580
Dover	18.4	19.8	21.2	29.6	36.1	24.2	1056
Ostende	29.1	29.5	25.4	-	-	28.6	592
Hoek van Holland	-	23.9	-	31.3	-	28.3	360
Ijmuiden	25.2	24.0	22.1	-	-	23.9	673
Terschelling	21.7	19.6	20.8	32.9	38.0	25.0	866
Helgoland	-	41.9	-	56.1	-	50.3	360
Cuxhaven	37.1	26.0	35.0	40.6	60.5	36.4	895
Esbjerg	28.0	28.3	26.7	38.5	48.7	32.8	1049
Tregde-Mandal	-	12.4	-	13.0	-	12.7	360
Stavanger	-	15.8	-	18.5	-	17.3	360
Bergen	8.9	10.6	10.2	17.0	25.4	12.9	880
All ports	22.5	22.4	20.1	29.0	37.6	25.2	15965
Samples	3587	4301	3030	3889	1158		

Table 3 : RMS errors (cm) based on hourly values of predicted and observed surge residuals during November and December 1973.

Port	4-14 Nov		14-24 Nov		24 Nov-4 Dec		4-14 Dec		14-18 Dec	
	c_1	c_c	c_1	c_c	c_1	c_c	c_1	c_c	c_1	c_c
Stornoway	0.87	-15.2	0.95	-11.2	1.08	-18.2	0.91	-22.3	-	-
Lerwick	1.33	- 3.1	0.91	- 1.4	1.54	- 6.0	0.81	-10.0	1.35	-25.9
Wick	0.78	-11.5	0.89	-15.6	1.45	-13.2	0.99	-22.3	0.93	-24.4
Aberdeen	0.88	- 6.0	0.83	- 7.8	1.60	-10.0	0.95	-17.3	0.87	-20.4
North Shields	0.84	4.7	0.89	- 0.7	1.11	3.5	0.95	- 6.2	0.79	- 5.3
Immingham	0.86	- 6.2	0.81	- 5.5	1.16	- 9.2	0.79	-12.5	0.79	-16.0
Inner Dowsing	1.03	- 0.8	0.85	- 0.6	1.10	- 1.0	0.78	- 4.8	0.82	- 9.1
Lowestoft	1.08	- 0.2	0.91	- 2.4	1.12	- 5.8	0.89	- 8.1	0.78	-10.2
Walton-on-Naze	1.01	- 2.0	0.83	- 0.9	1.26	- 9.5	0.83	-12.3	0.73	-17.0
Southend	0.93	3.3	0.82	- 1.8	1.13	- 1.4	0.78	- 8.3	0.67	-14.0
Dover	1.10	- 4.2	0.93	- 7.7	1.04	- 9.7	0.86	-18.4	0.83	-19.9
Ostende	0.96	22.0	0.87	21.0	1.09	12.9	-	-	-	-
Hoek van Holland	-	-	0.85	4.6	-	-	0.80	- 5.6	-	-
Ijmuiden	0.99	5.5	0.95	- 3.1	1.22	-10.6	-	-	-	-
Terschelling	1.15	- 2.1	1.02	- 7.9	1.37	- 8.0	0.92	-20.8	0.84	-15.2
Helgoland	-	-	0.95	-24.8	-	-	0.88	-38.3	-	-
Cuxhaven	1.09	9.1	1.08	6.7	1.20	- 2.4	0.92	-12.2	0.70	- 6.7
Esbjerg	1.06	-16.1	0.96	-10.7	1.33	-24.0	0.91	-22.2	0.76	-16.2
Tregde-Mandal	-	-	0.62	3.8	-	-	0.75	- 3.2	-	-
Stavanger	-	-	0.82	- 9.3	-	-	0.88	-12.7	-	-
Bergen	0.80	5.8	0.76	- 1.8	1.11	- 8.0	0.72	- 9.4	1.26	-25.5

Table 4 : Regression coefficients c_1 , c_c , where $\zeta_{observed} = c_1 \zeta_{predicted} + c_c$ from analysis of the results for November - December 1973.

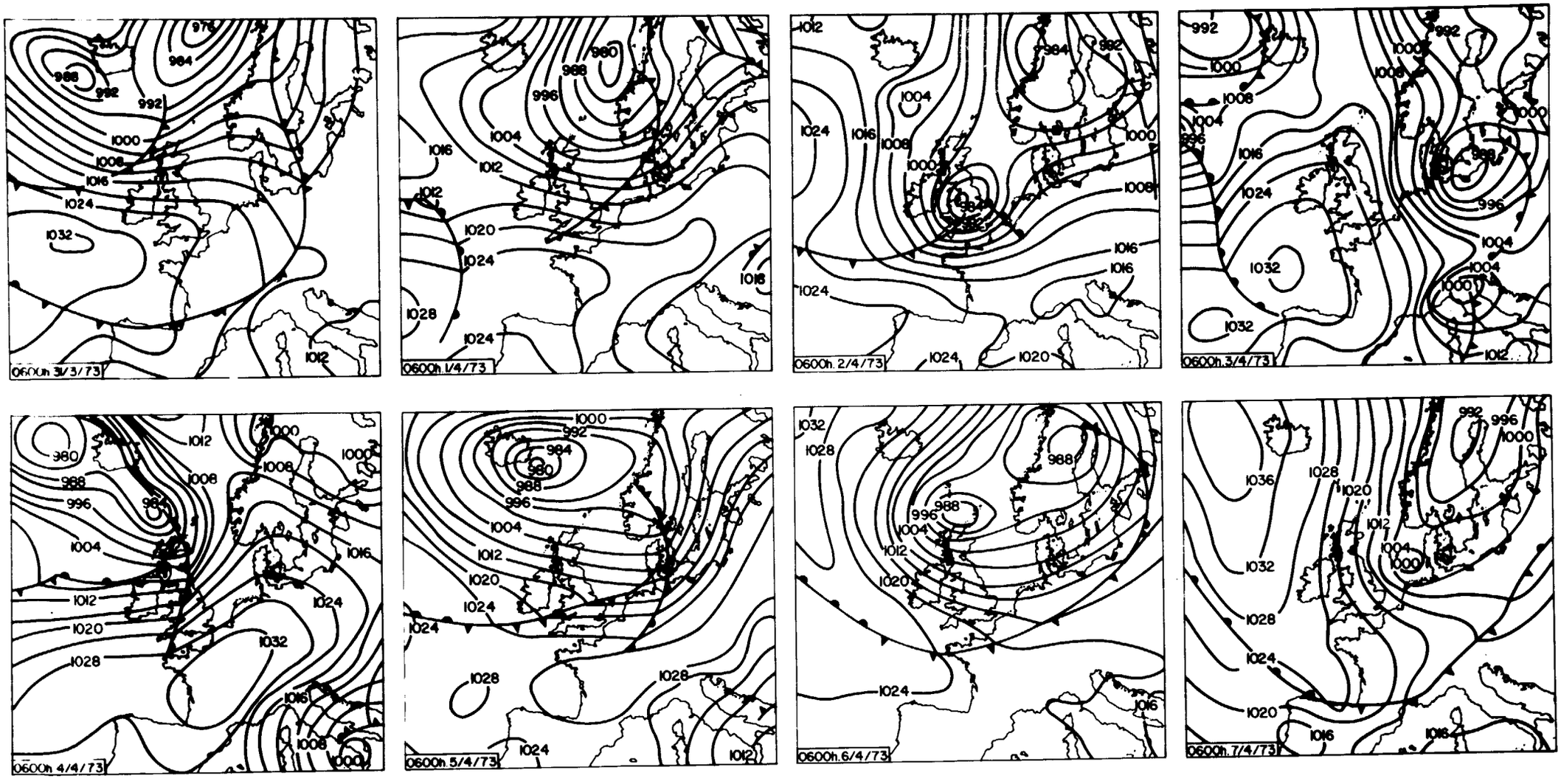

FIGURE I : WEATHER CHARTS FOR THE STORM SURGES OF 2-6/4/1973

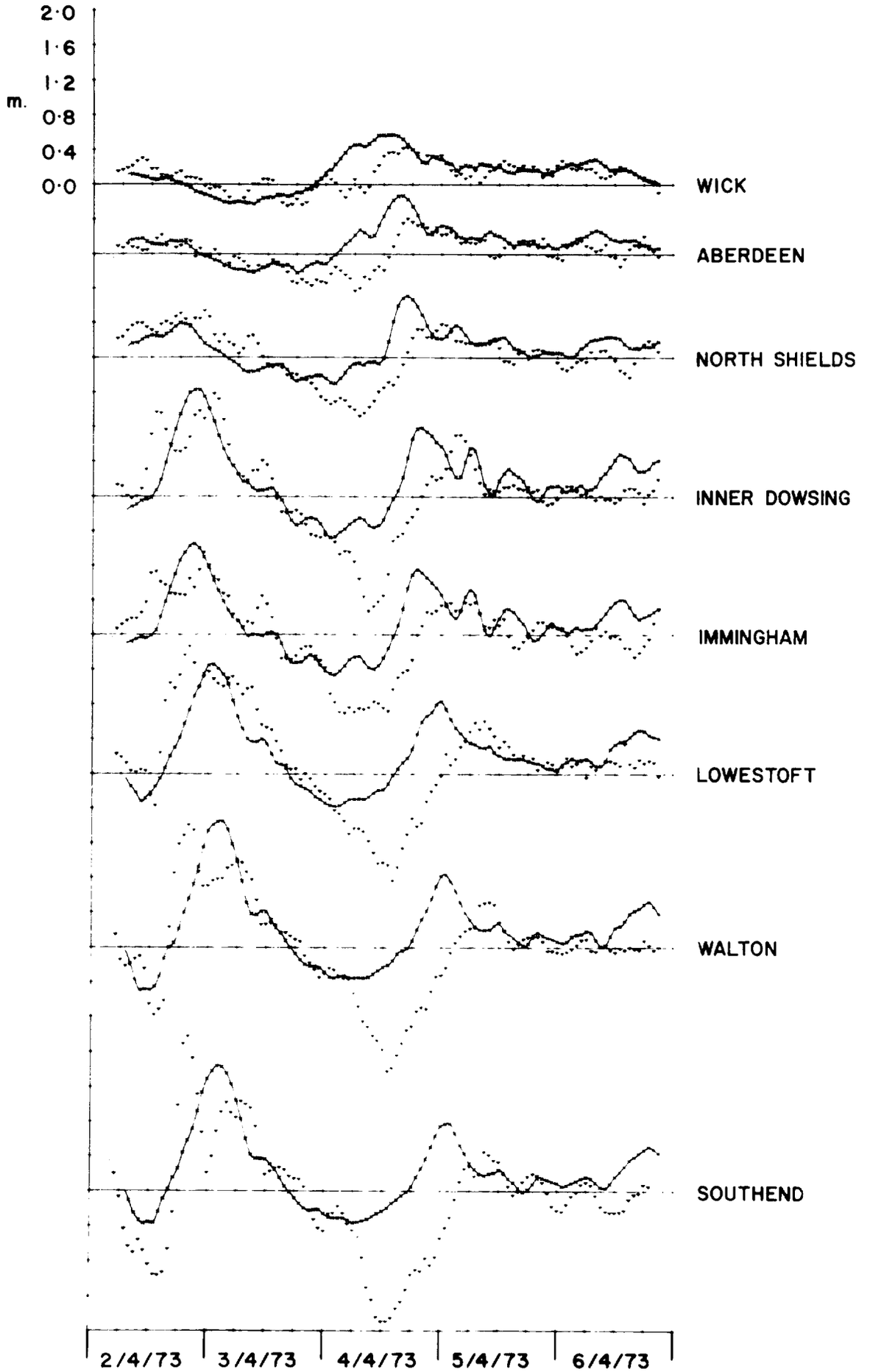

Figure 2 a : Storm surges at UK ports ; ——— original solution (O) ; ▼▼▼▼▼▼▼ observed.

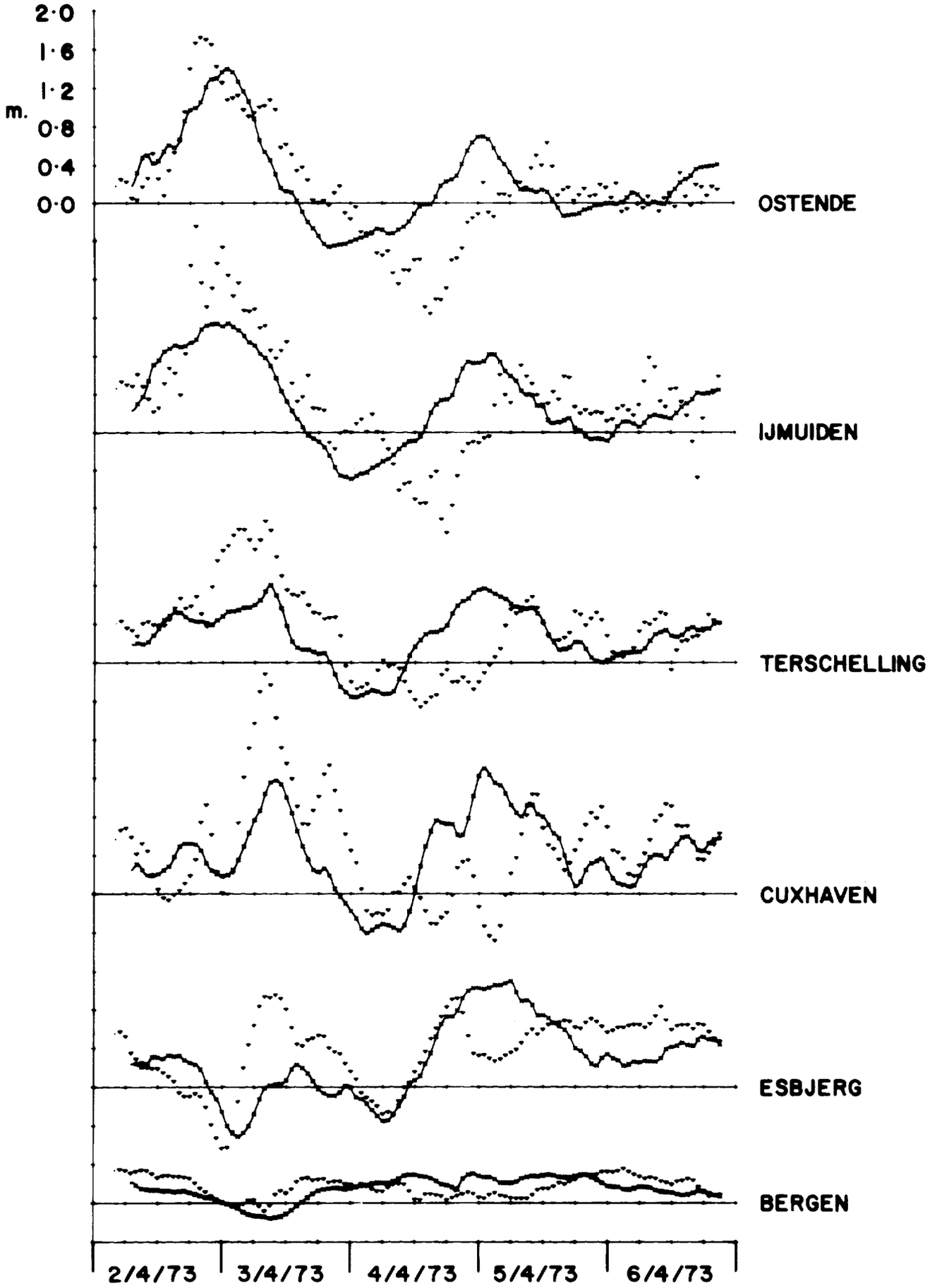

Figure 2b : Storm surges at continental ports ; ——— original solution (O) ; ▾▾▾▾▾▾ observed.

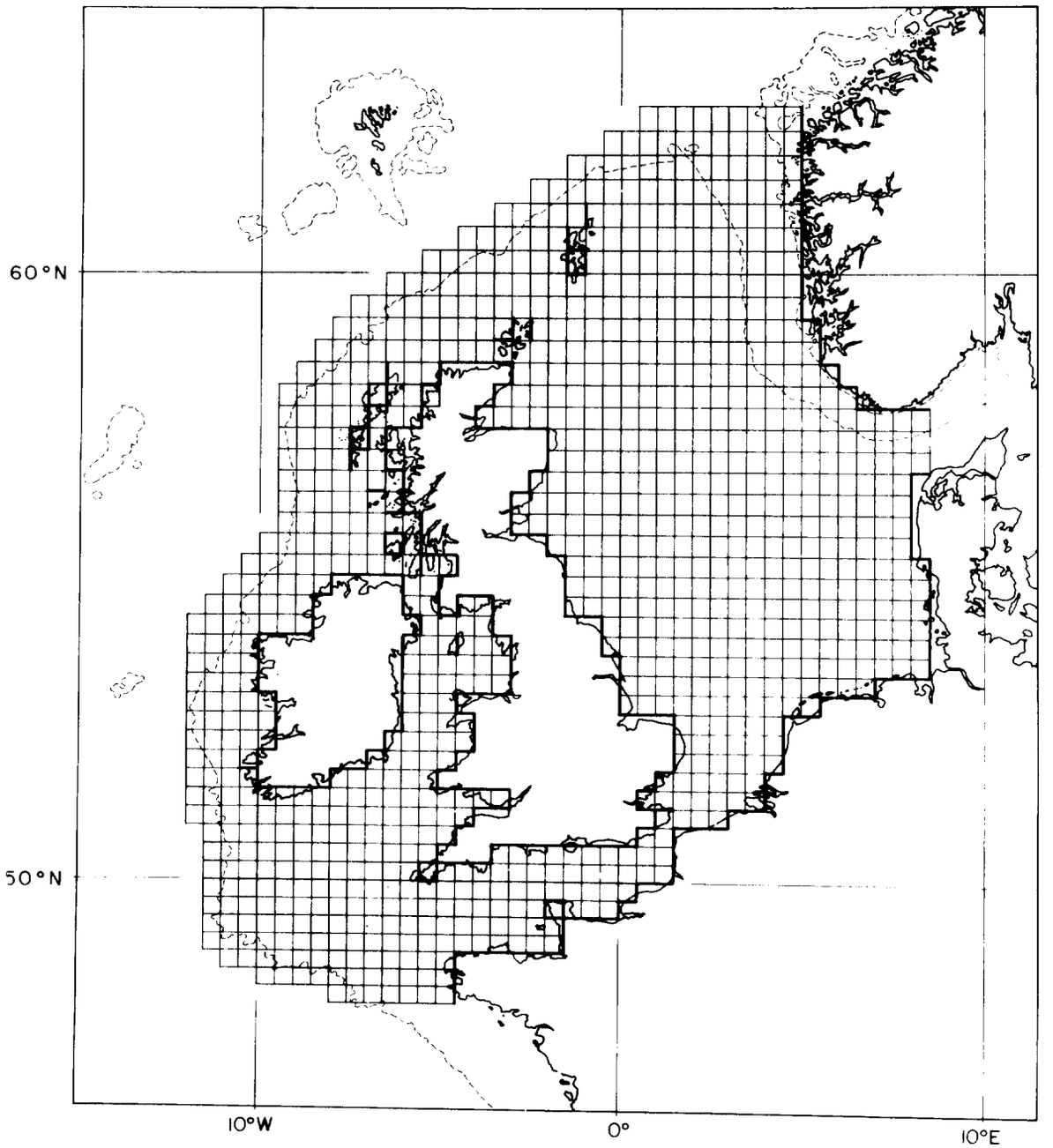

FIGURE 3 : FINITE DIFFERENCE GRID FOR THE NORTH SEA AND CONTINENTAL SHELF ;
------- 100 FATHOM DEPTH CONTOUR.

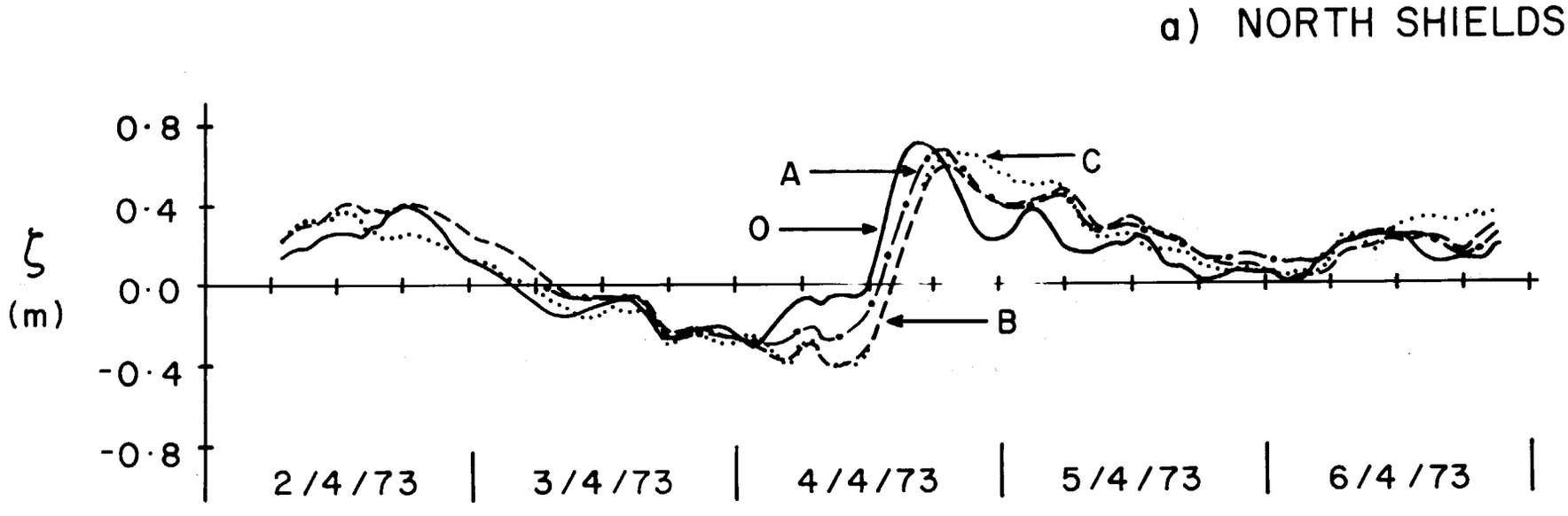

FIGURE 4 : Solutions O, A, B, C compared

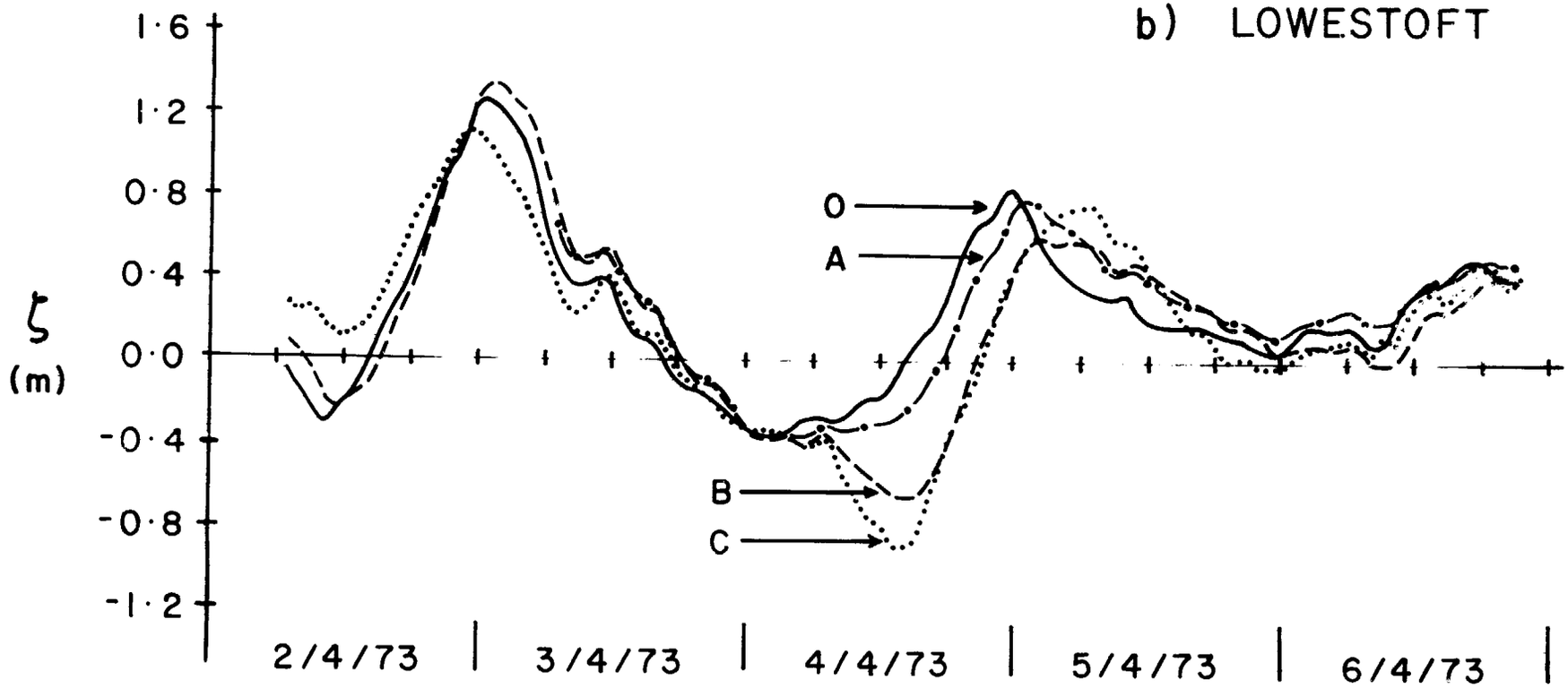
b) LOWESTOFT
1·6
1·2
0·8
0·4
0·0
-0·4
-0·8
-1·2
ζ
(m)
O
A
B
C
2/4/73
3/4/73
4/4/73
5/4/73
6/4/73

FIGURE 4

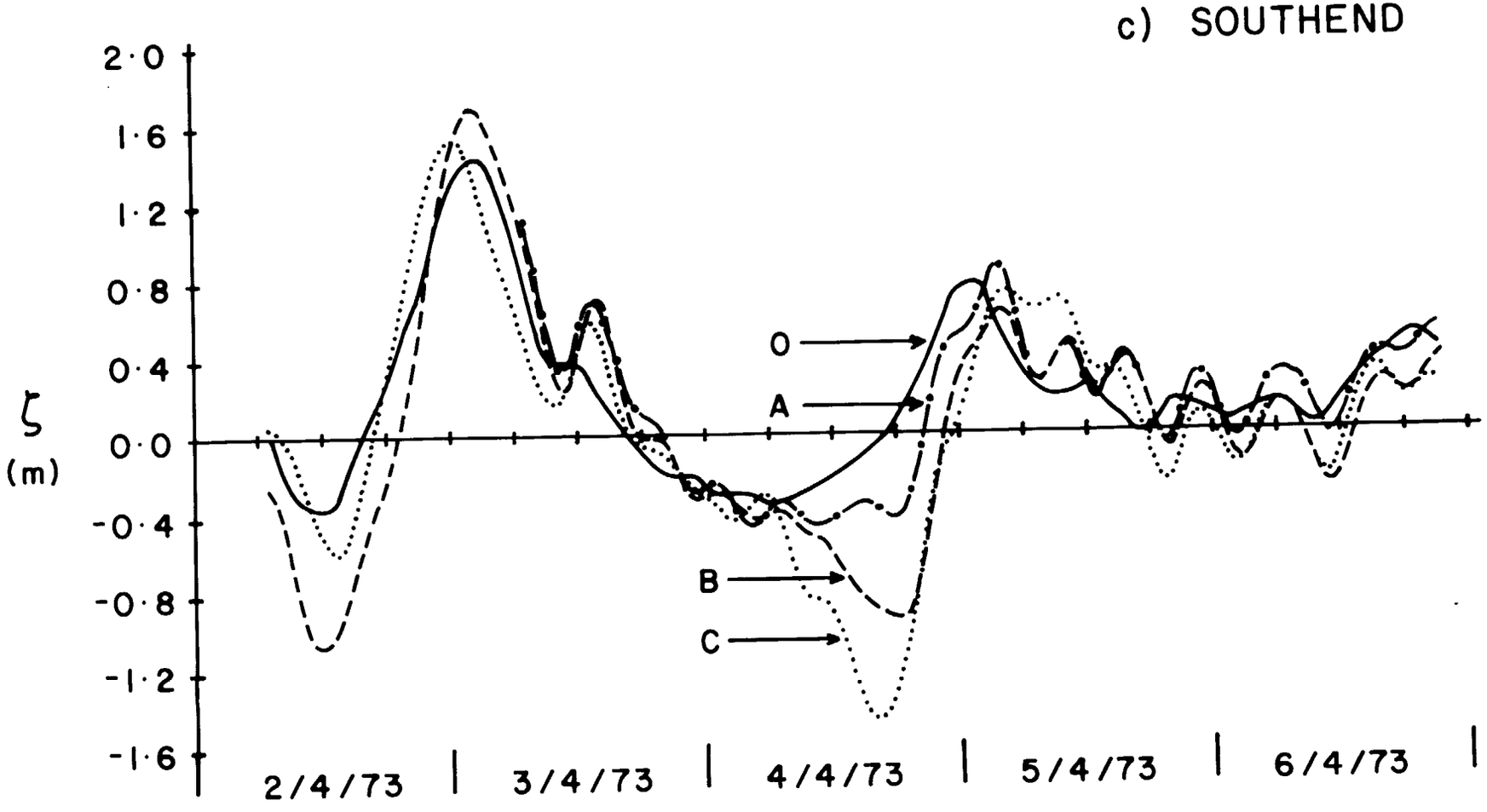
c) SOUTHEND
2·0
1·6
1·2
0·8
0·4
0·0
-0·4
-0·8
-1·2
-1·6
ζ
(m)
O
A
B
C
2/4/73
3/4/73
4/4/73
5/4/73
6/4/73

FIGURE 4

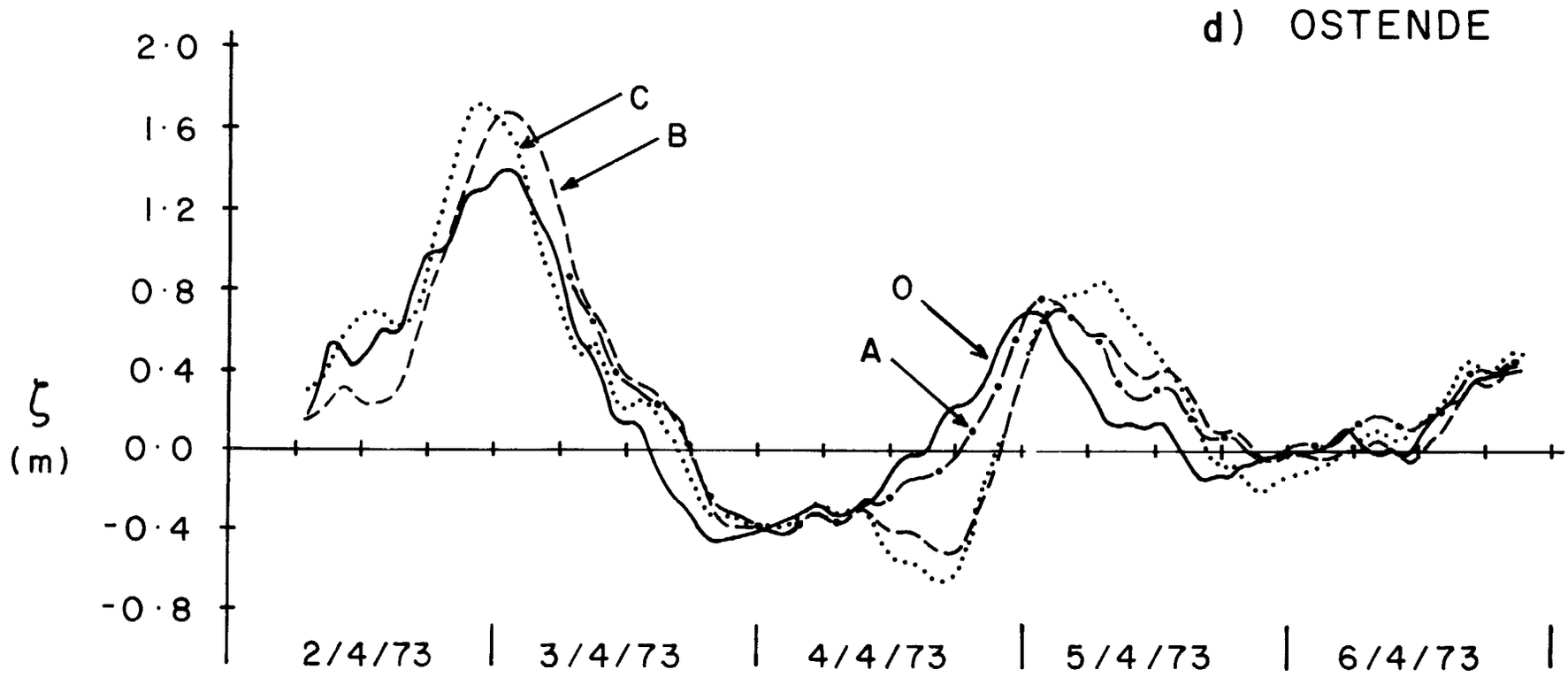
d) OSTENDE
2·0
1·6
1·2
0·8
0·4
0·0
-0·4
-0·8
ζ
(m)
C
B
O
A
2/4/73
3/4/73
4/4/73
5/4/73
6/4/73

FIGURE 4

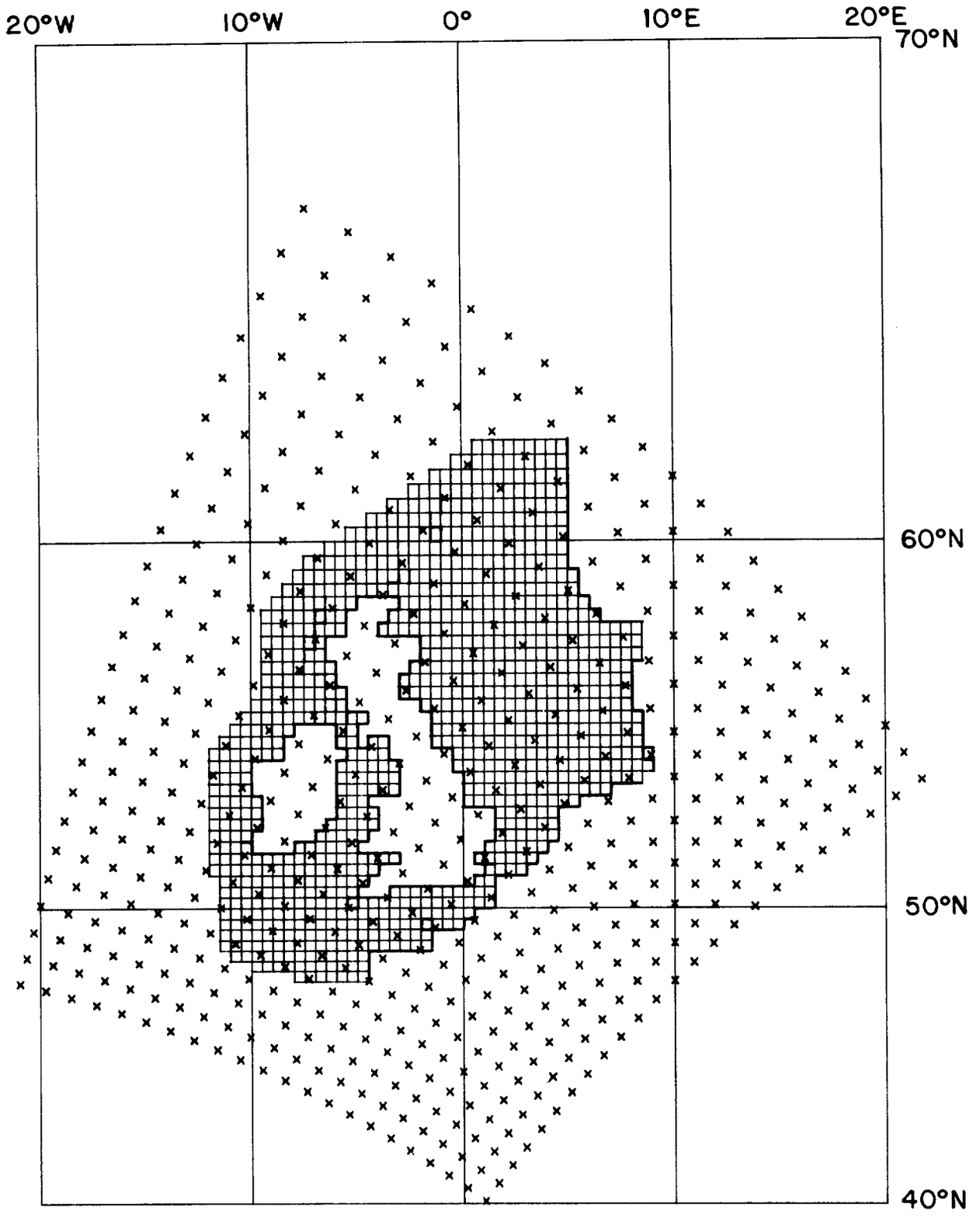

Figure 5 : Revised finite difference grid for the continental shelf with mesh points of the 10-level model (×).

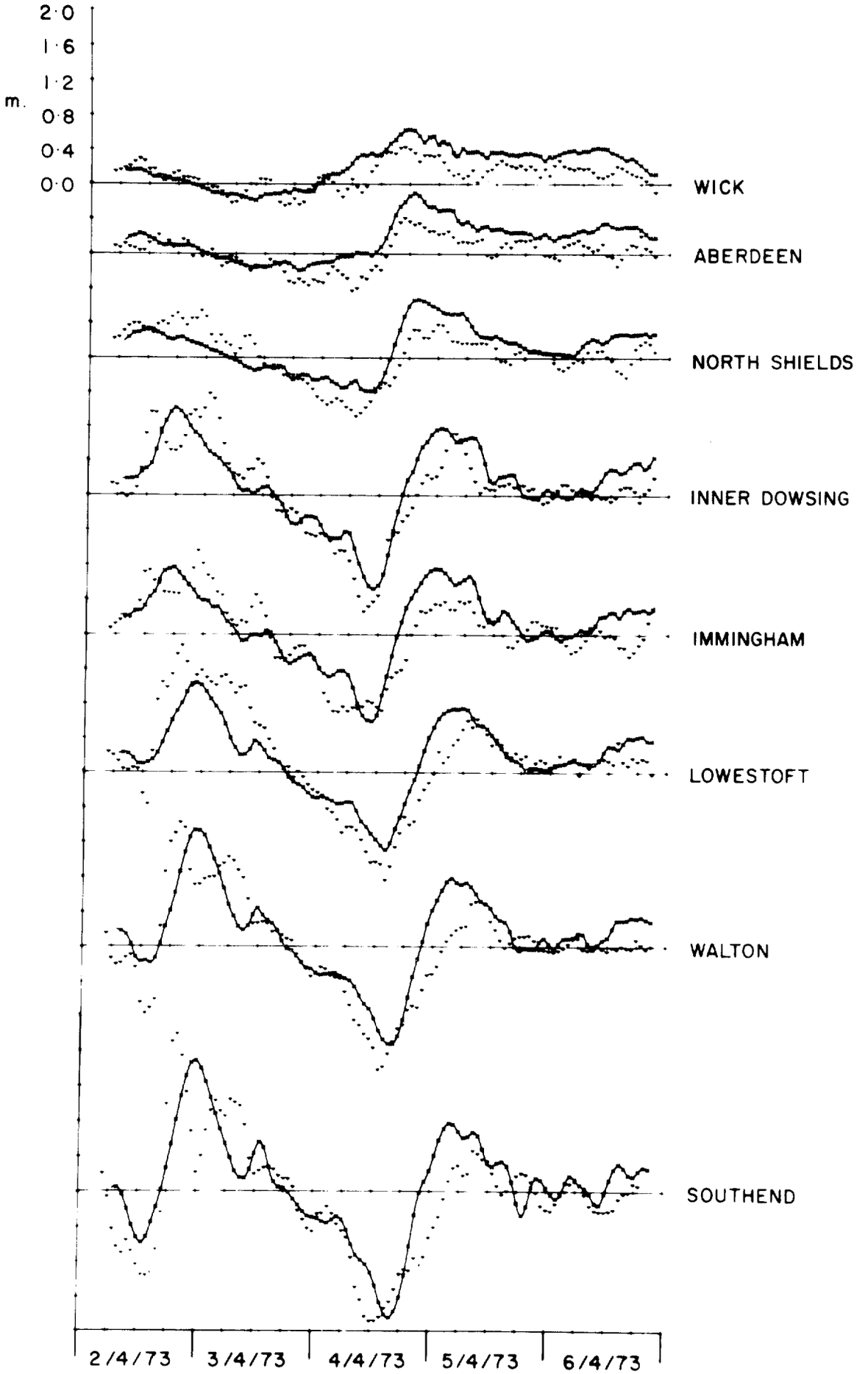

Figure 6a : Storm surges at UK ports ; ——— solution D ; ▾▾▾▾▾▾▾ observed.

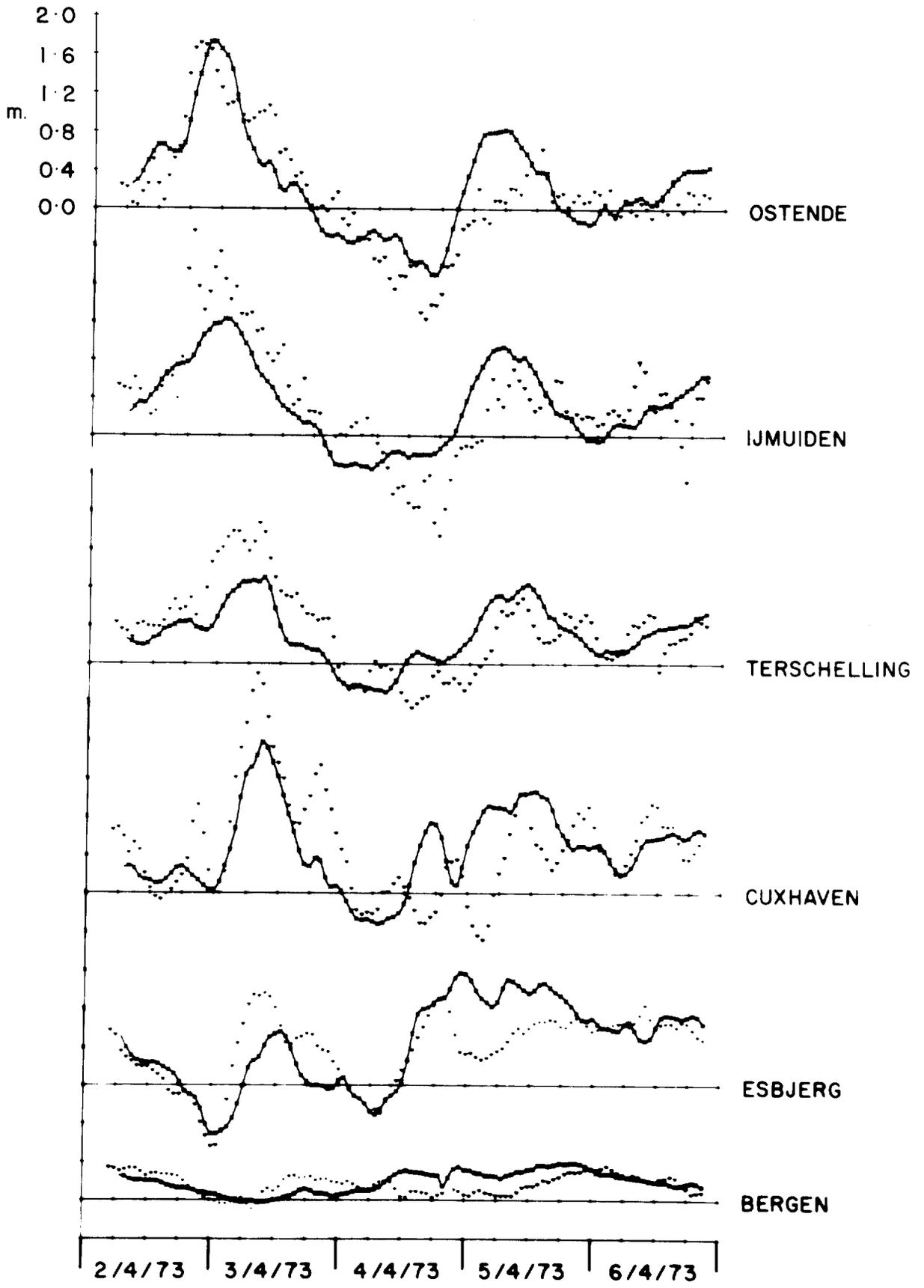

Figure 6b : Storm surges at continental ports ; ——— solution D ; ▼▼▼▼▼▼▼ observed.

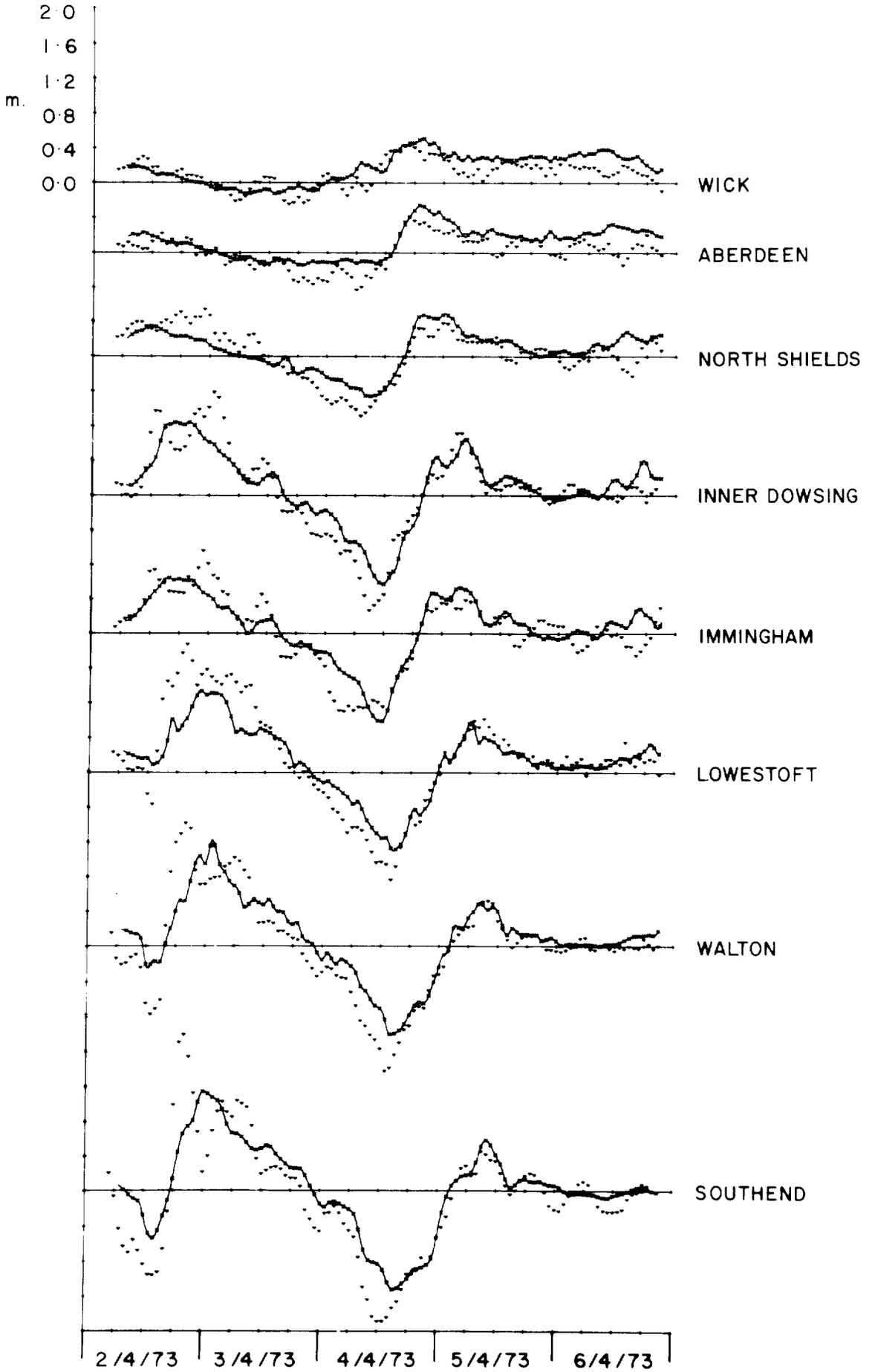

Figure 7a : Storm surges at UK ports ; ——— solution E ; ▾▾▾▾▾▾▾ observed.

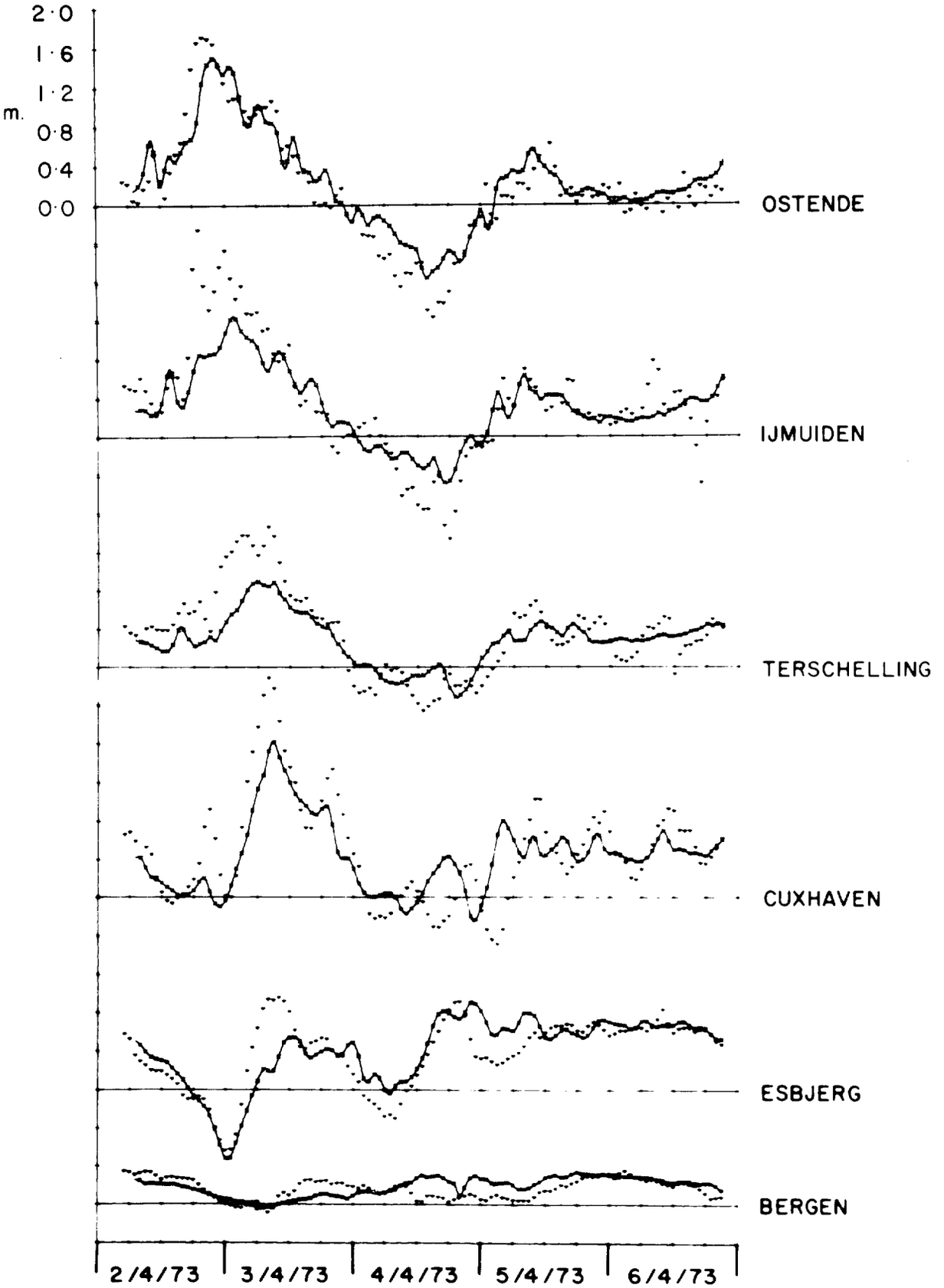

Figure 7b : Storm surges at continental ports ;

——— solution E ; ▾▾▾▾▾▾▾ observed.

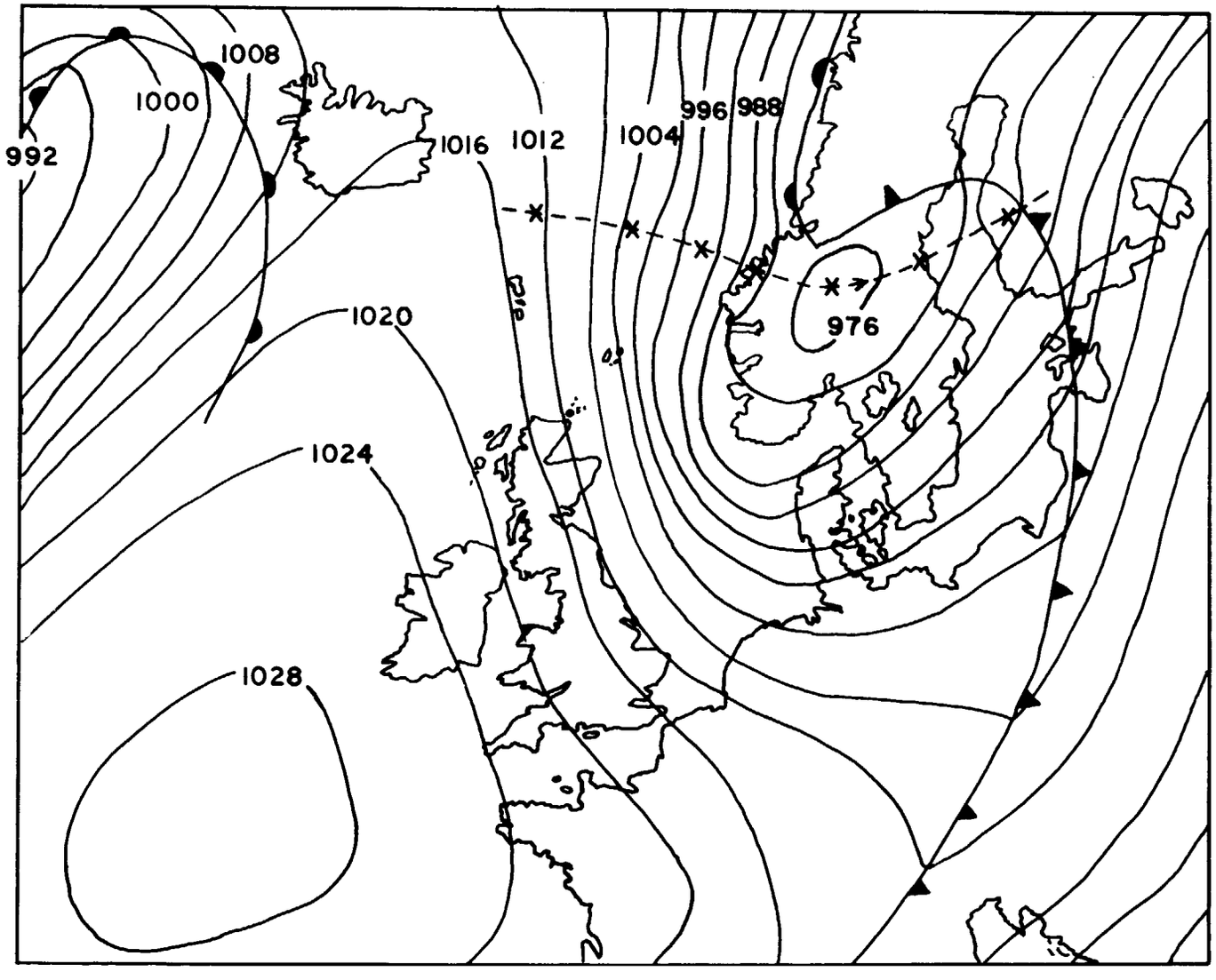

FIGURE 8a : WEATHER CHART FOR 0600h 6/11/73 WITH THE TRACK OF THE DEPRESSION (✱---✱→--✱); CROSSES INDICATE THE POSITION OF THE LOW EVERY 12 HOURS.

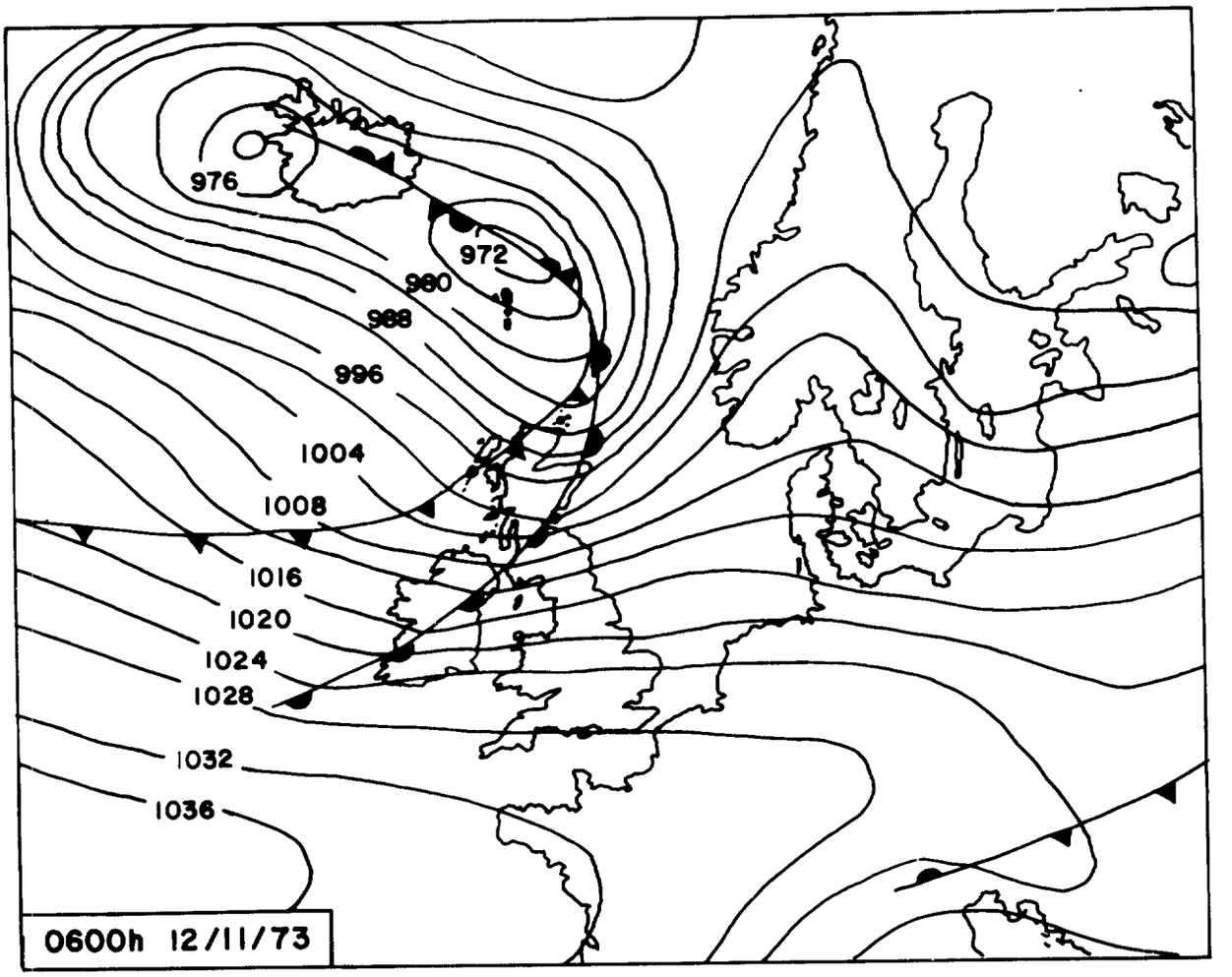

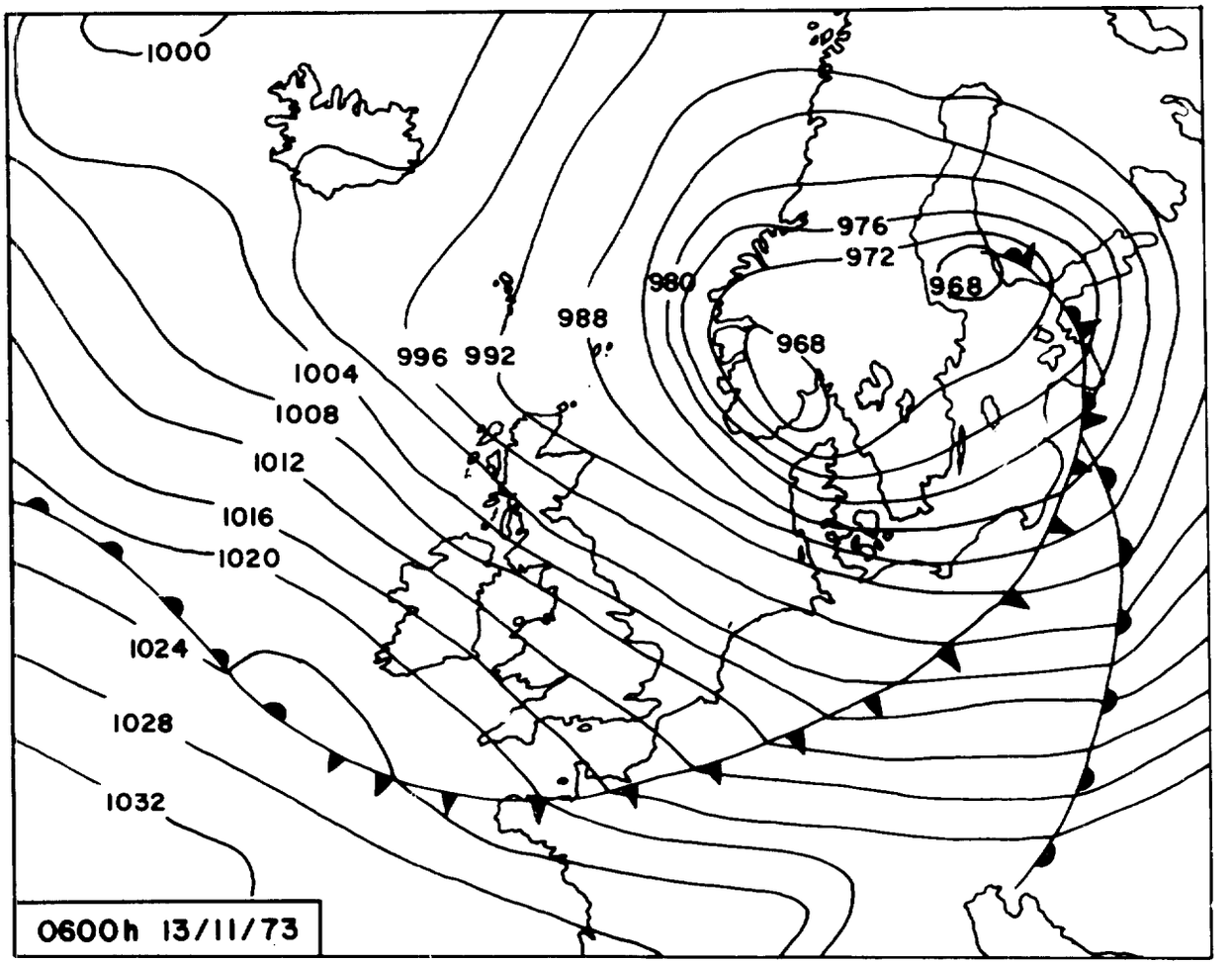

FIGURE 8b: **WEATHER CHARTS FOR 0600h 12 & 13/11/73**

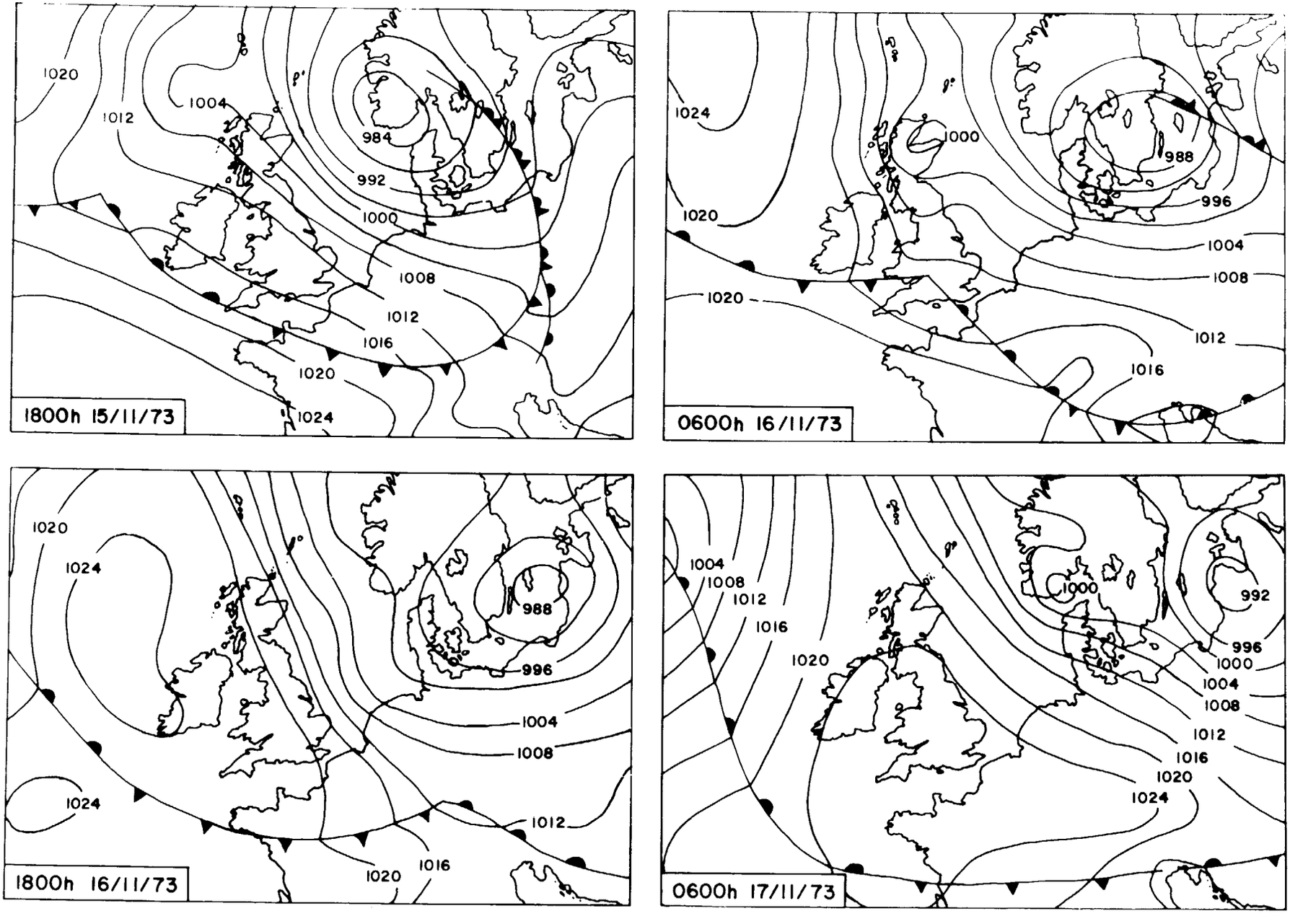

FIGURE 8c : WEATHER CHARTS FOR 15 - 17/11/73

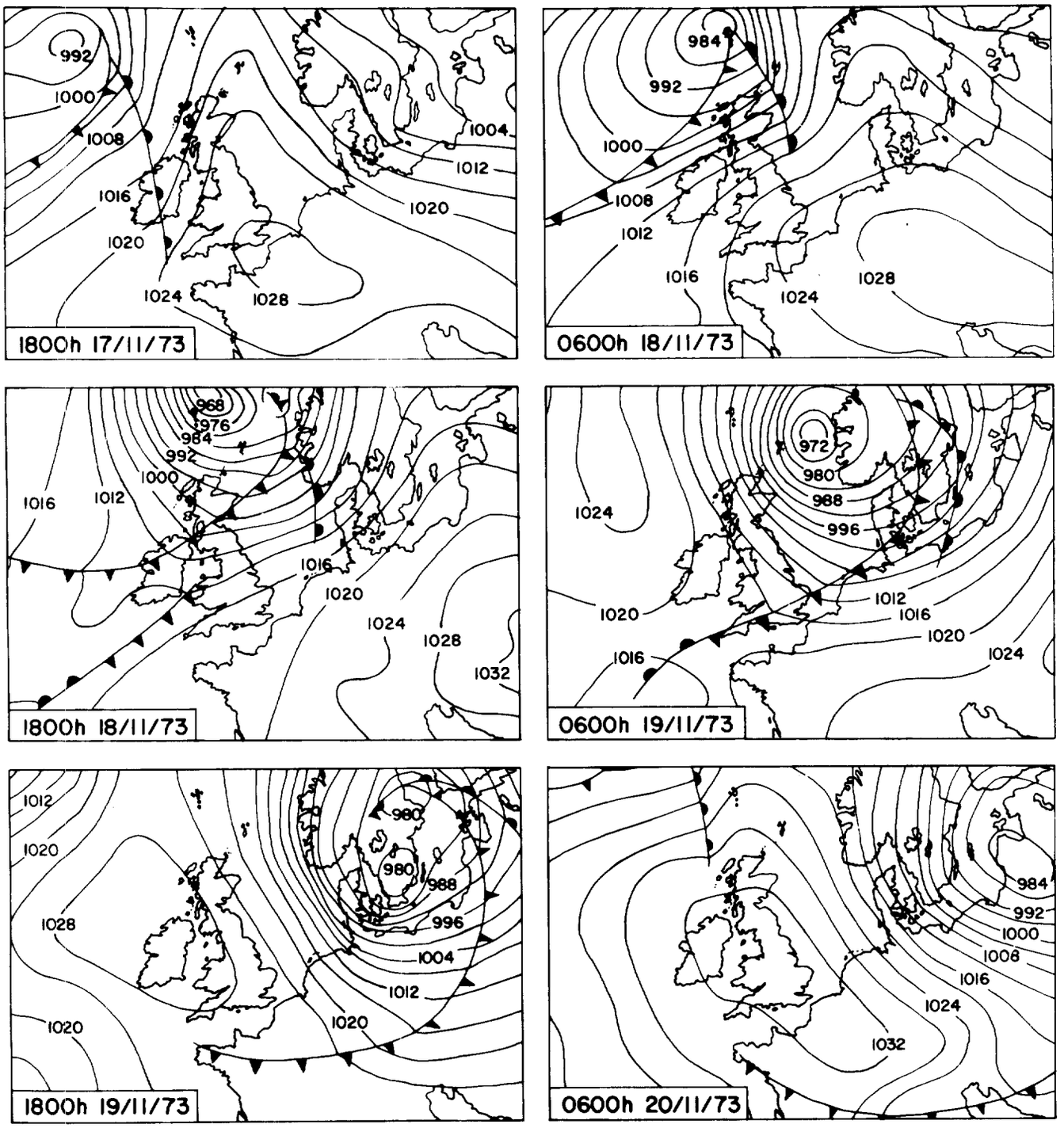

FIGURE 8d: WEATHER CHARTS FOR 17-20/11/73

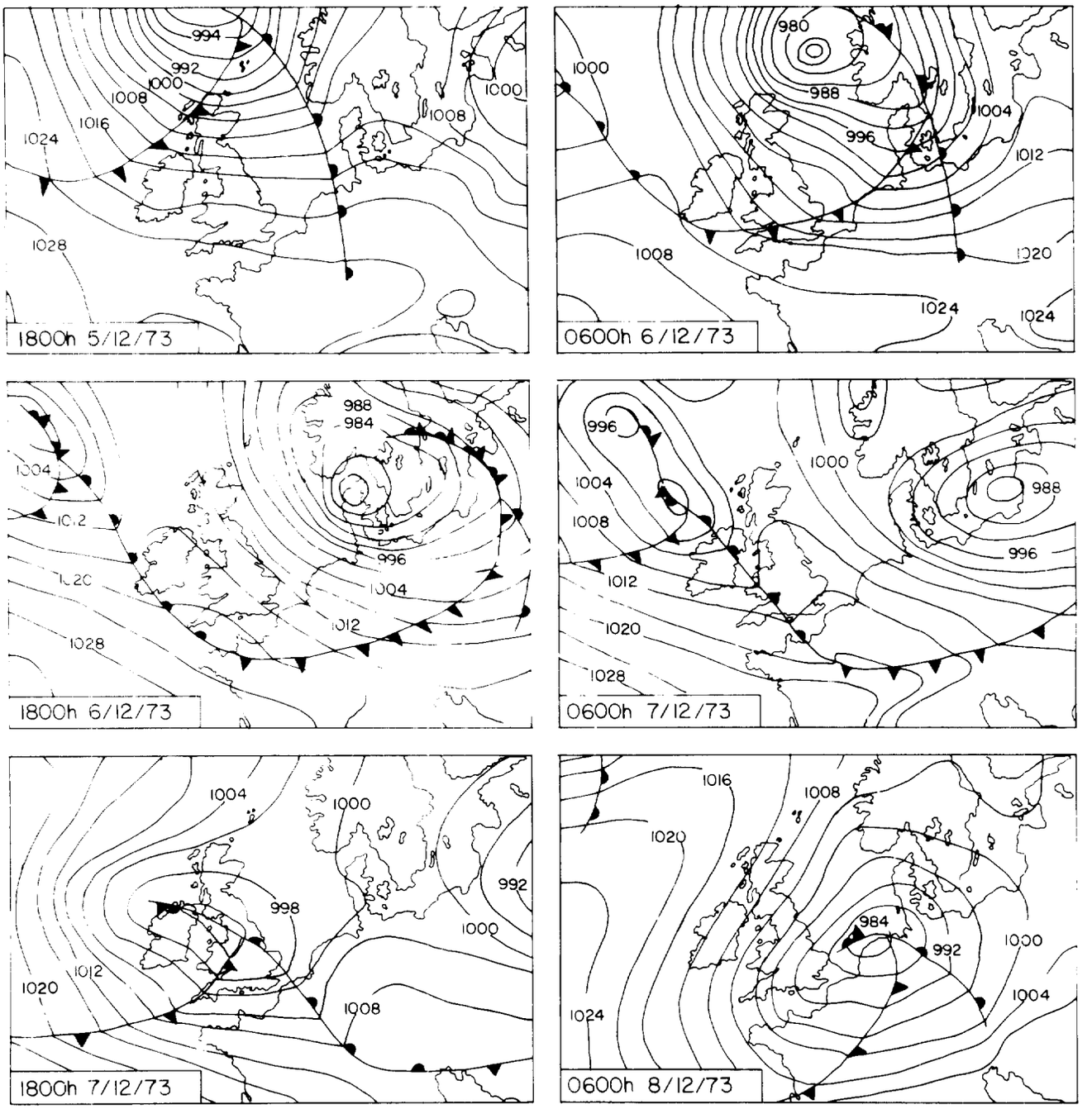

FIGURE 8e: WEATHER CHARTS FOR 5-8/12/73

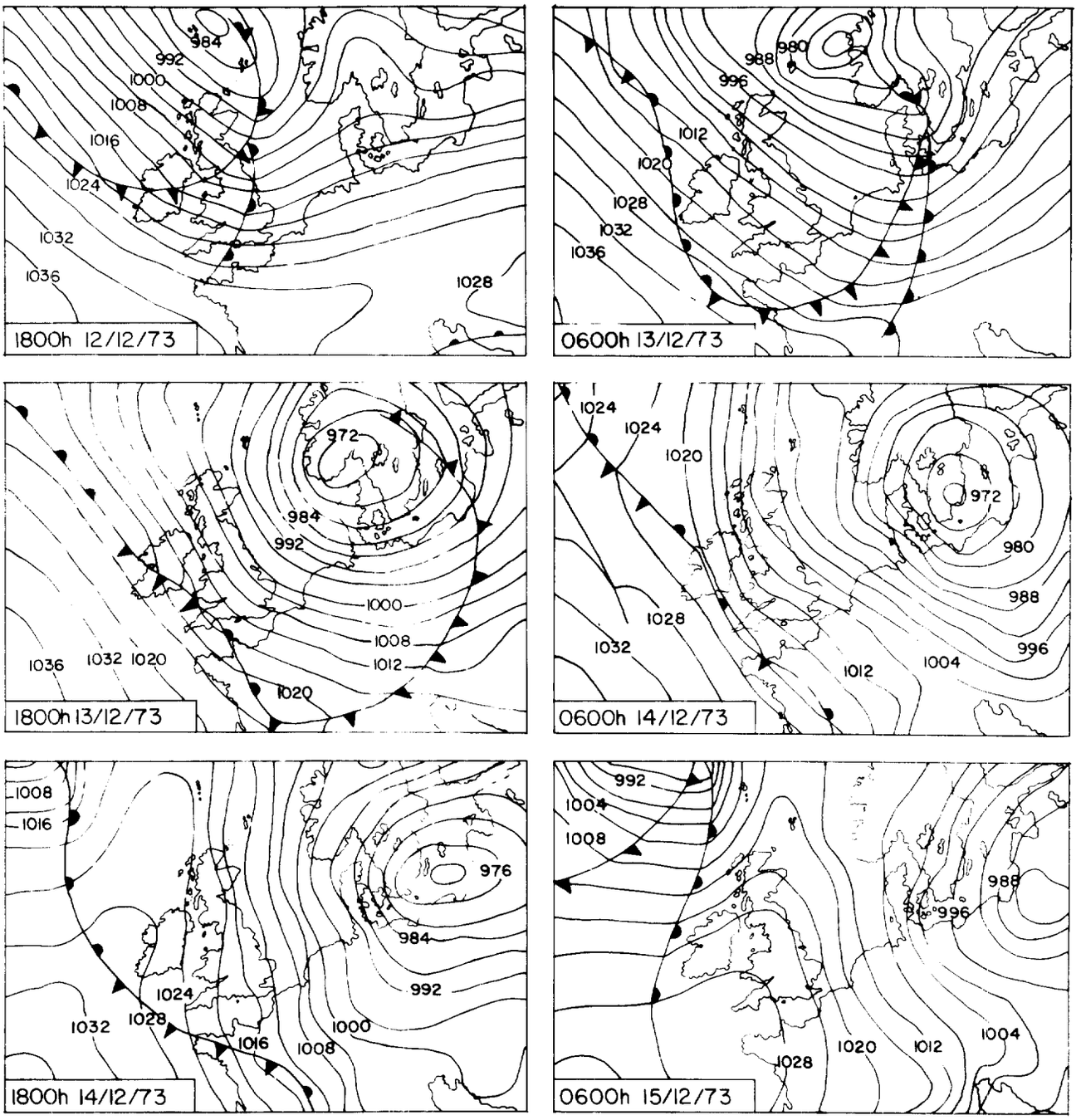

FIGURE 8f : WEATHER CHARTS FOR 12-15/12/73

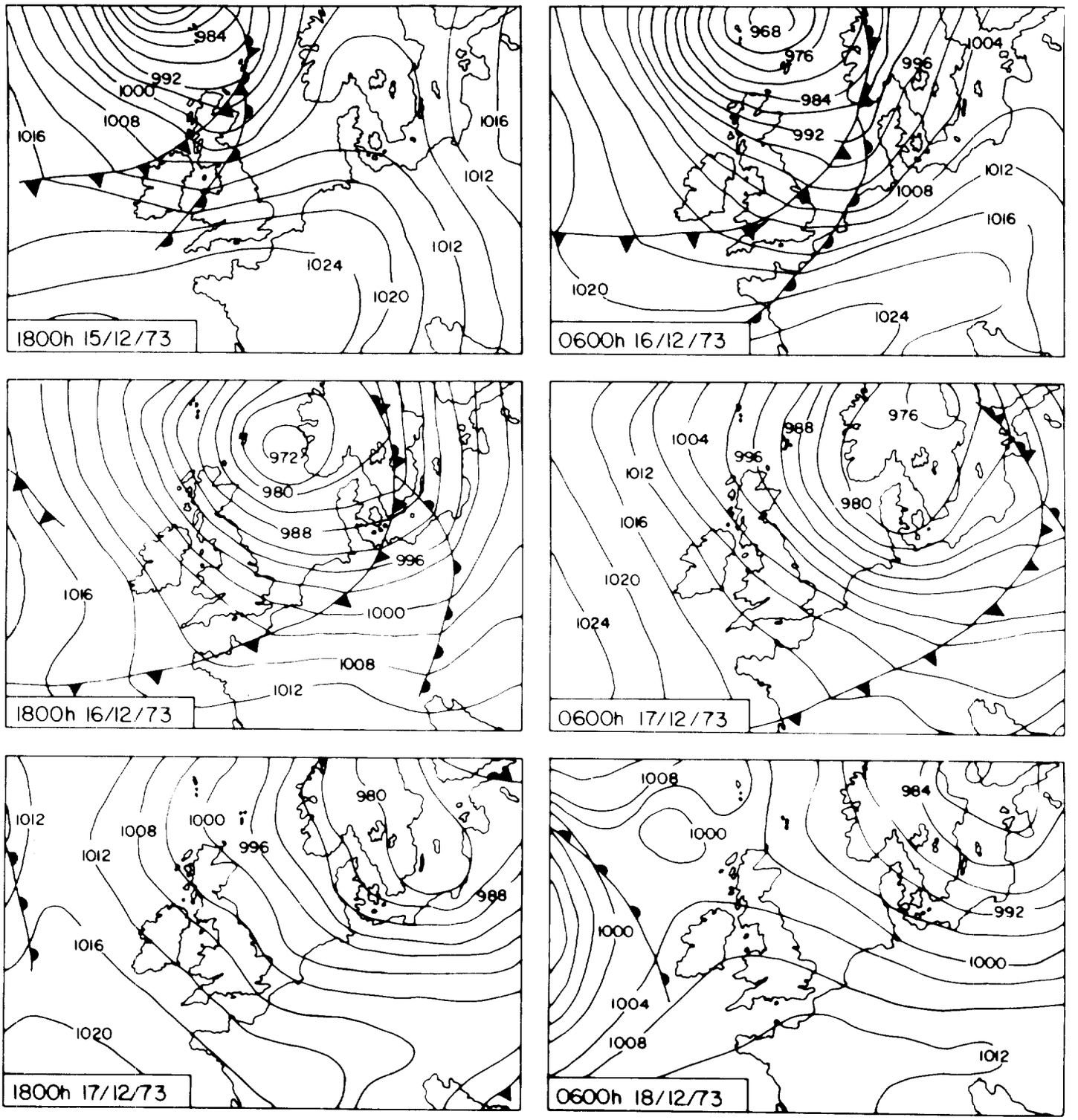

FIGURE 8g : WEATHER CHARTS FOR 15-18/12/73

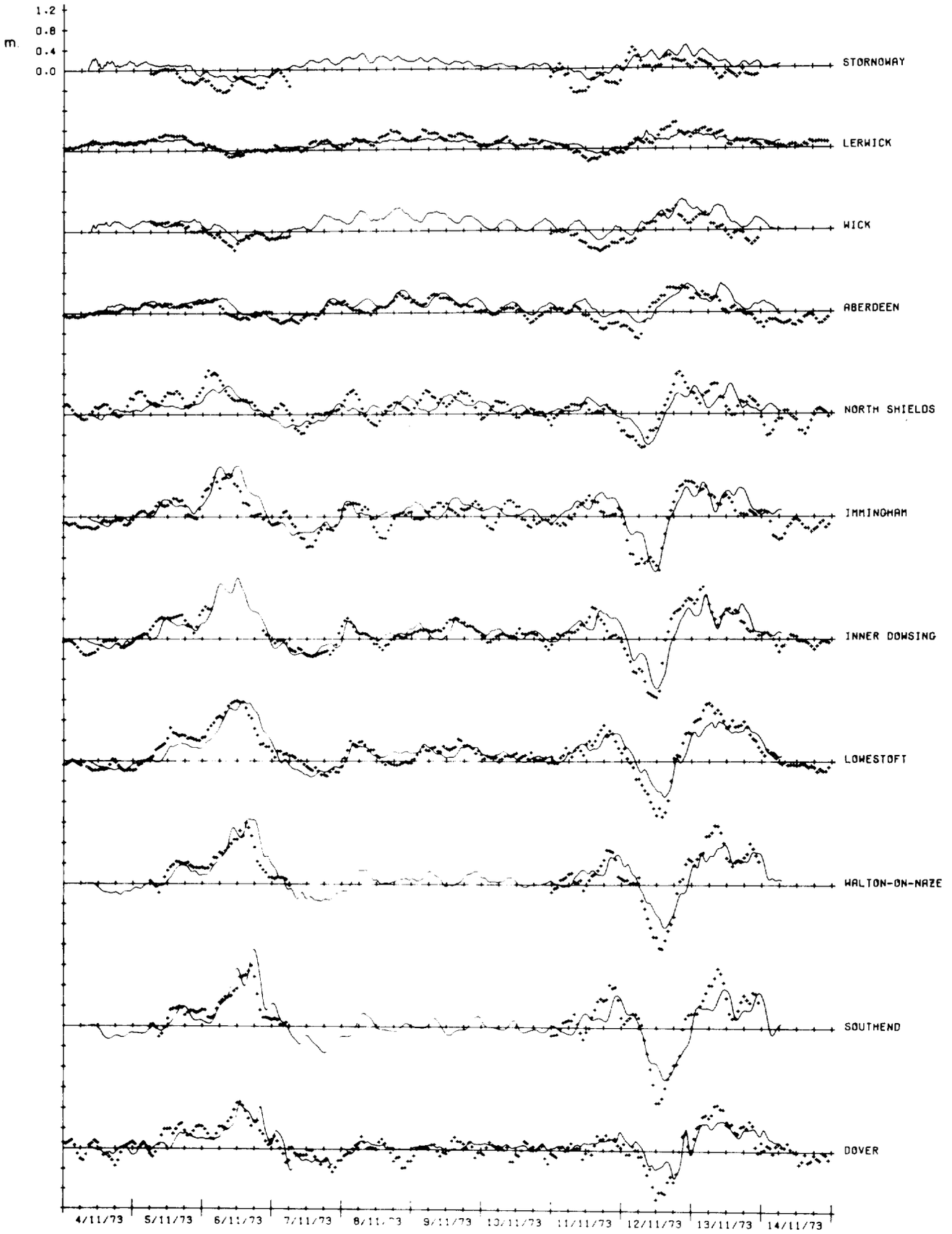

FIGURE 9a: STORM SURGES AT UK PORTS. COMPUTED (——————): OBSERVED (++++++).

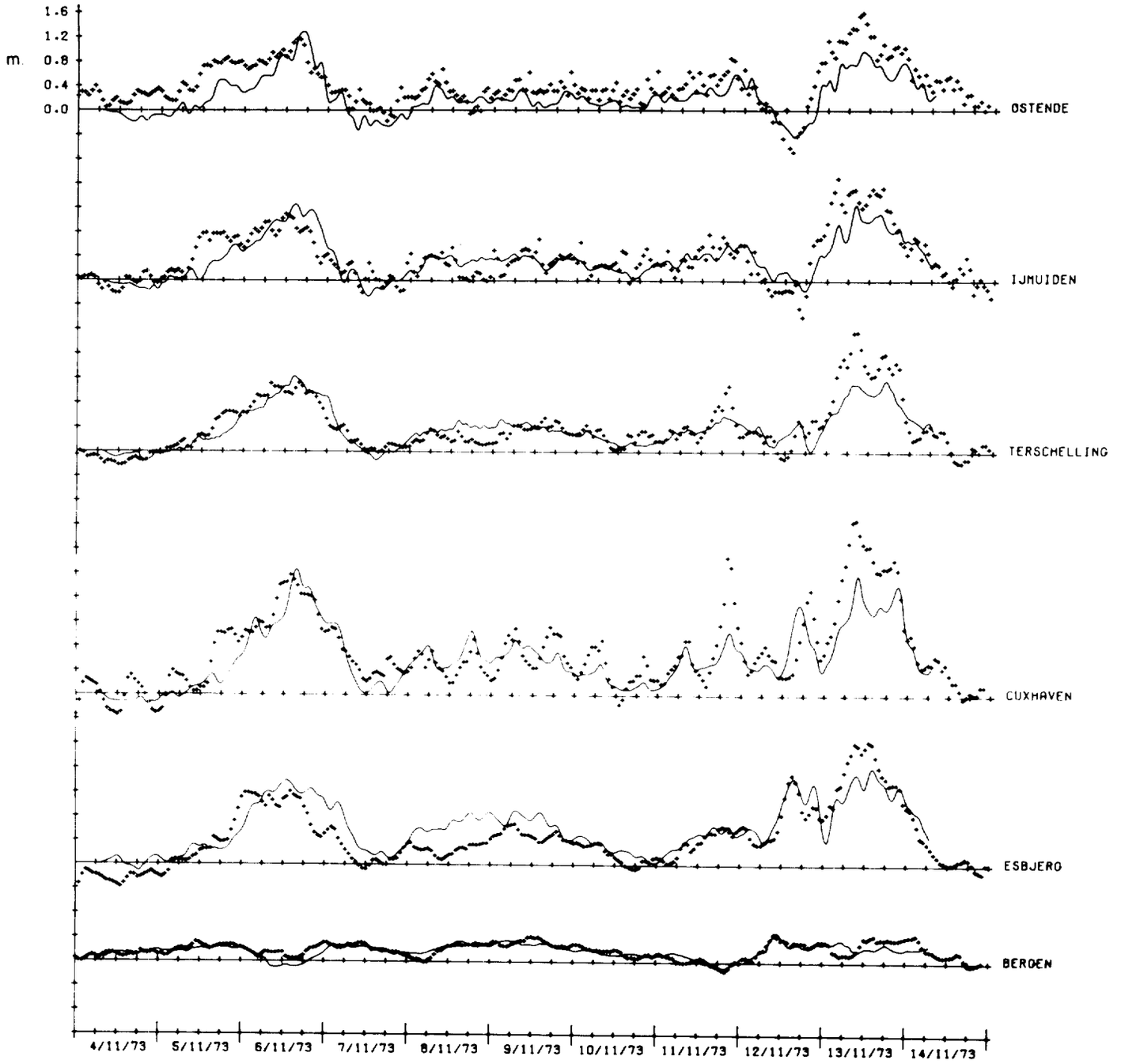

FIGURE **9b** : STORM SURGES AT CONTINENTAL PORTS. COMPUTED (———); OBSERVED (++++++).

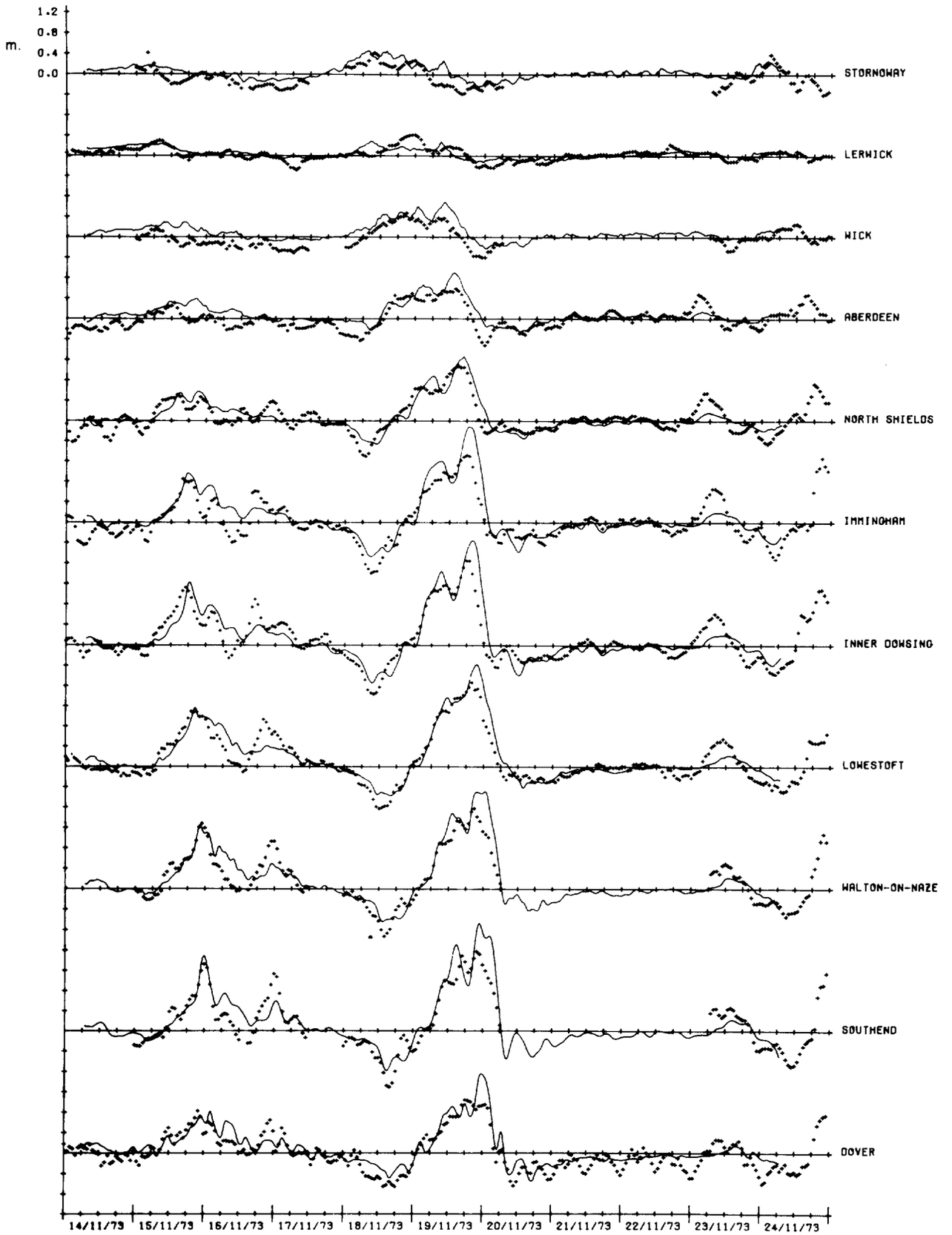

FIGURE 10a: STORM SURGES AT UK PORTS. COMPUTED (———); OBSERVED (++++++).

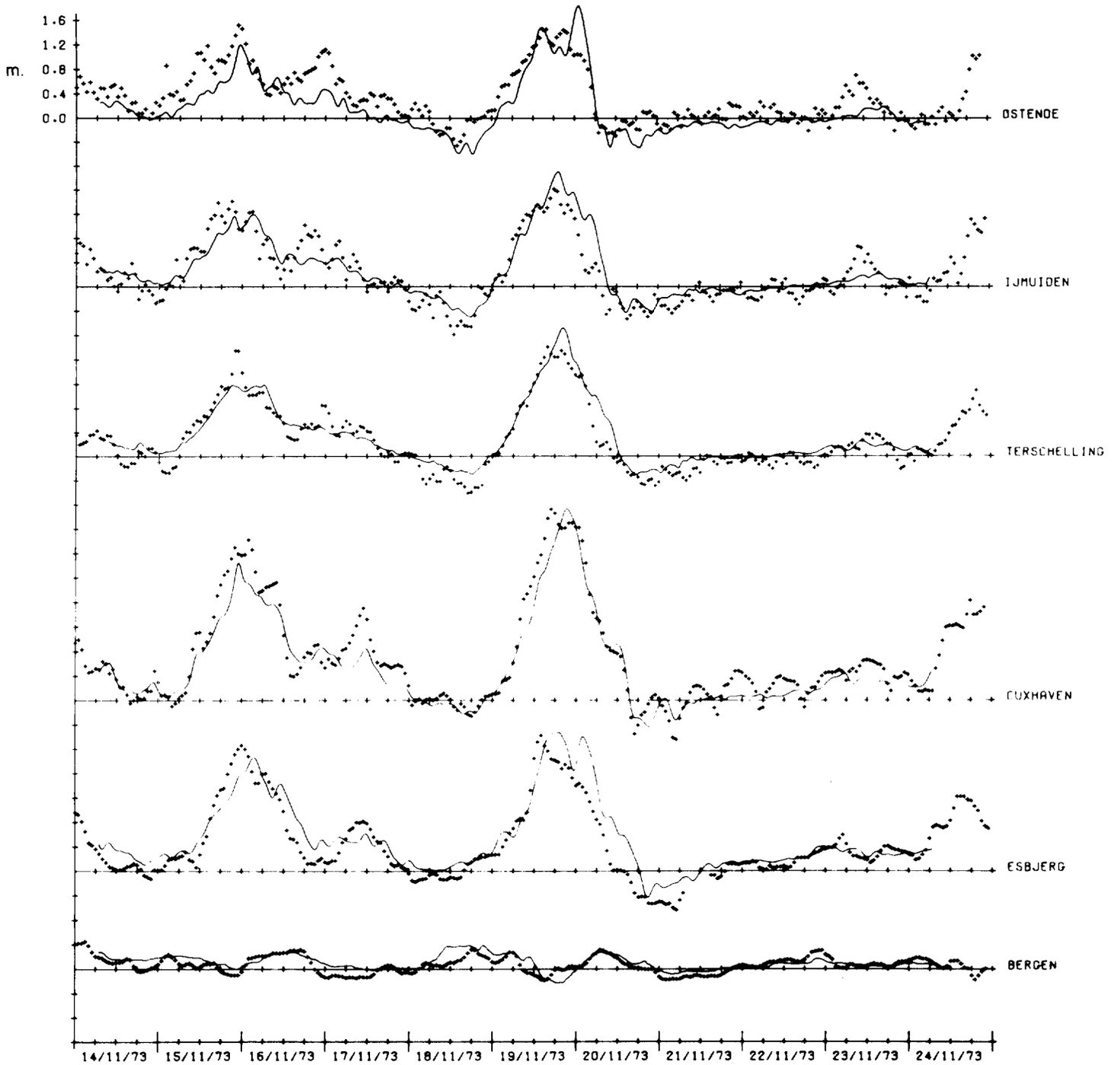

FIGUREIOb: STORM SURGES AT CONTINENTAL PORTS. COMPUTED (———): OBSERVED (++++++).

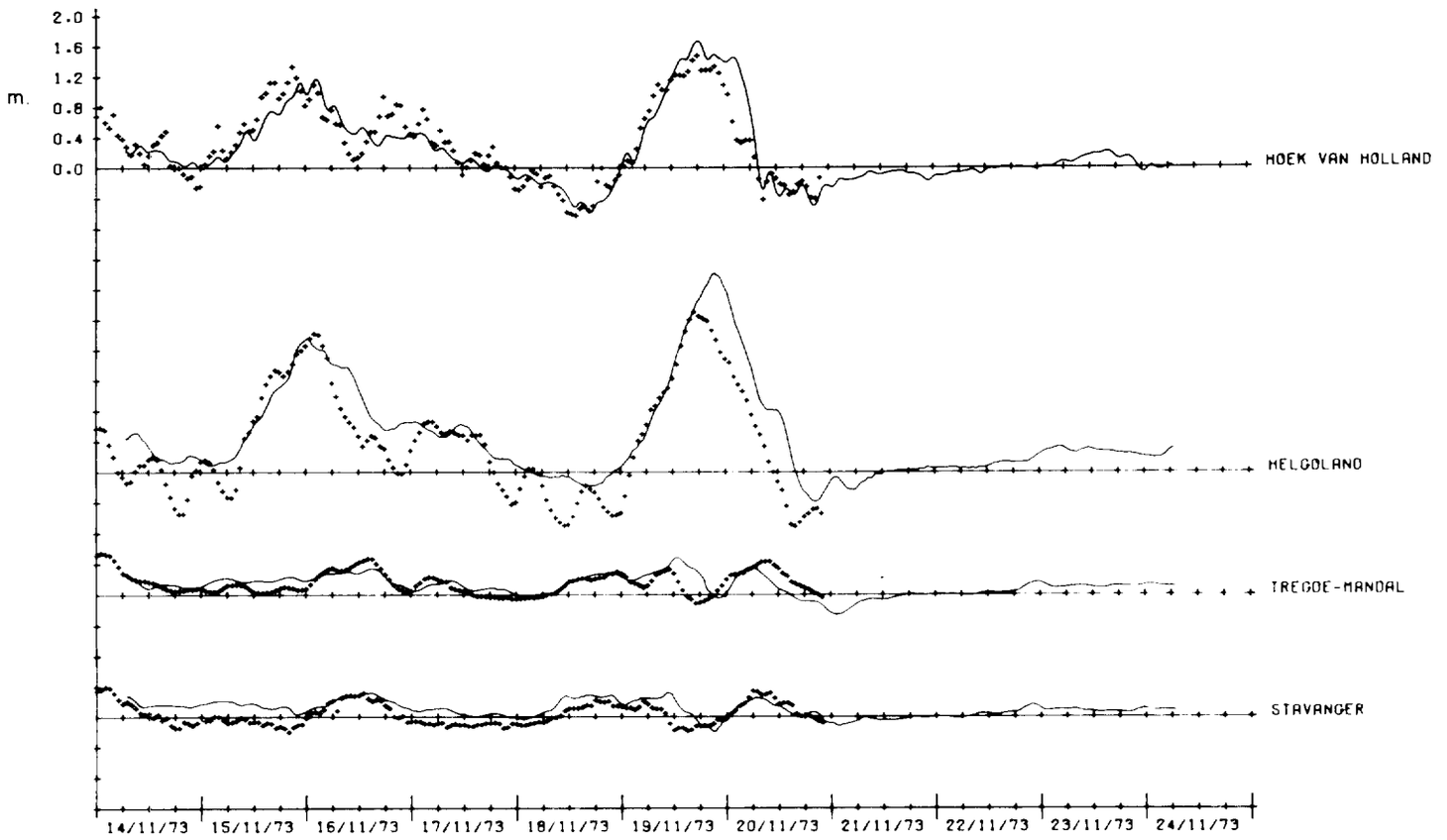

FIGURE 10c: STORM SURGES AT ADDITIONAL PORTS. COMPUTED (———); OBSERVED (++++++).

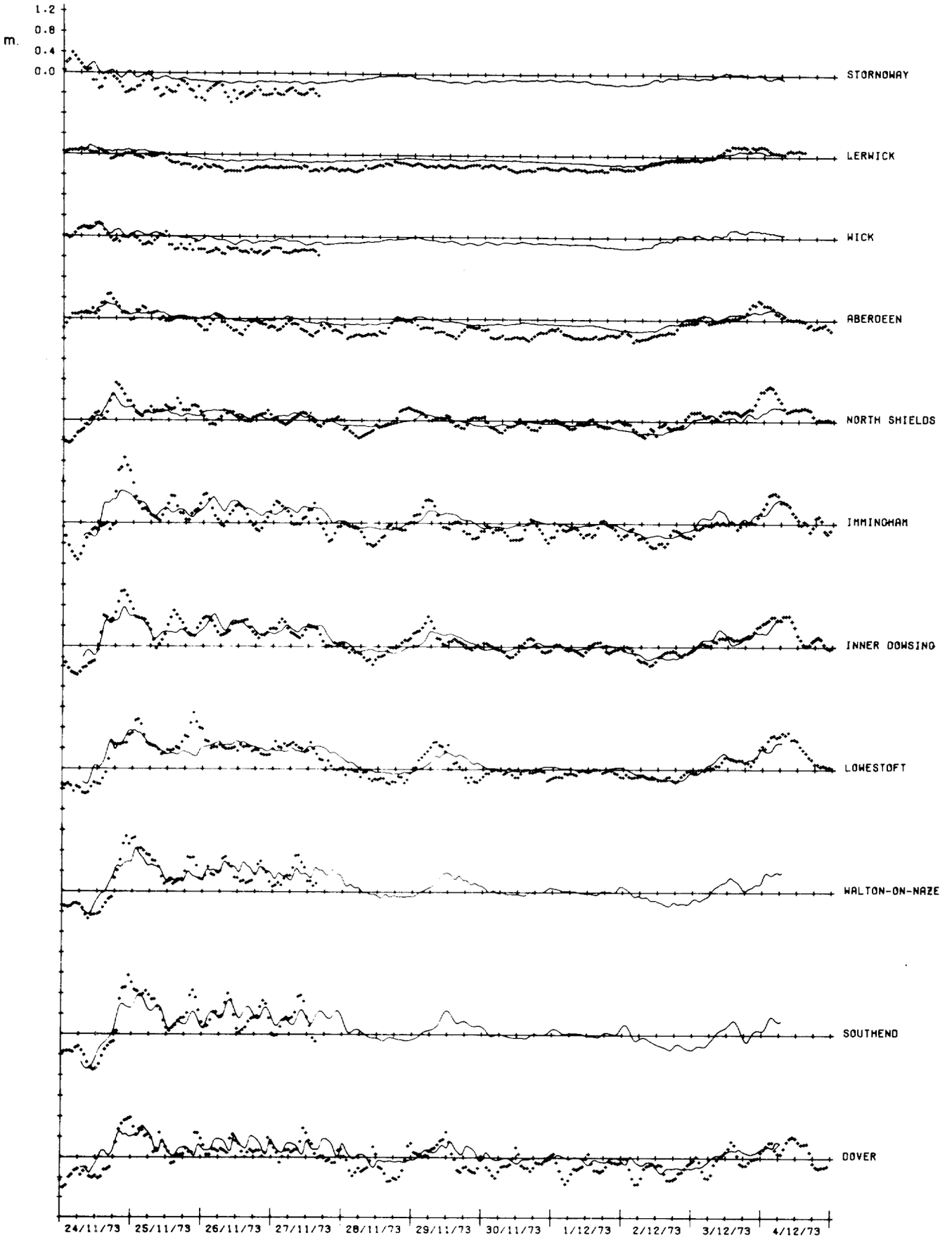

FIGURE IIa: STORM SURGES AT UK PORTS, COMPUTED (———); OBSERVED (++++++).

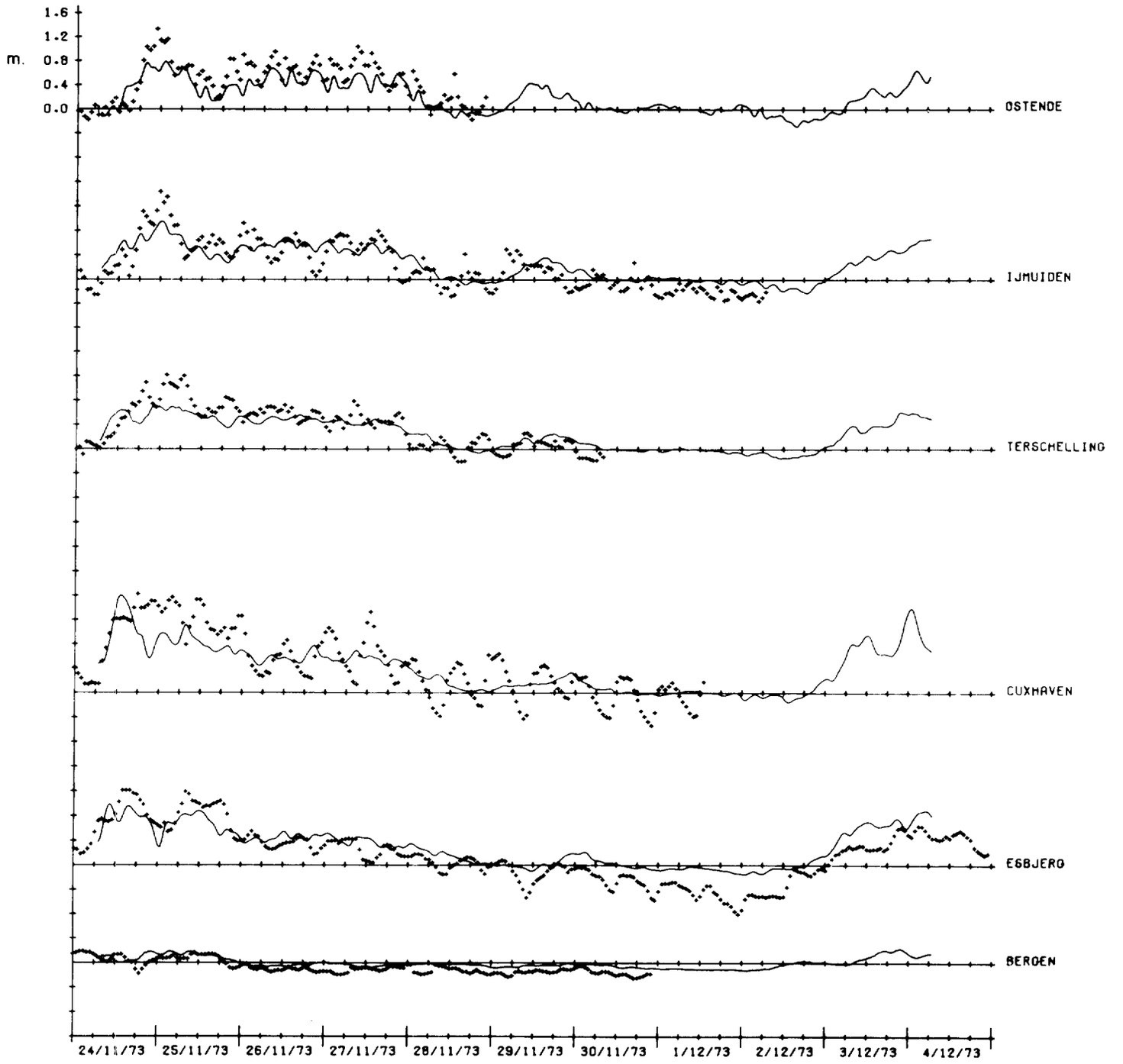

FIGURE IIb : STORM SURGES AT CONTINENTAL PORTS. COMPUTED (———); OBSERVED (++++++).

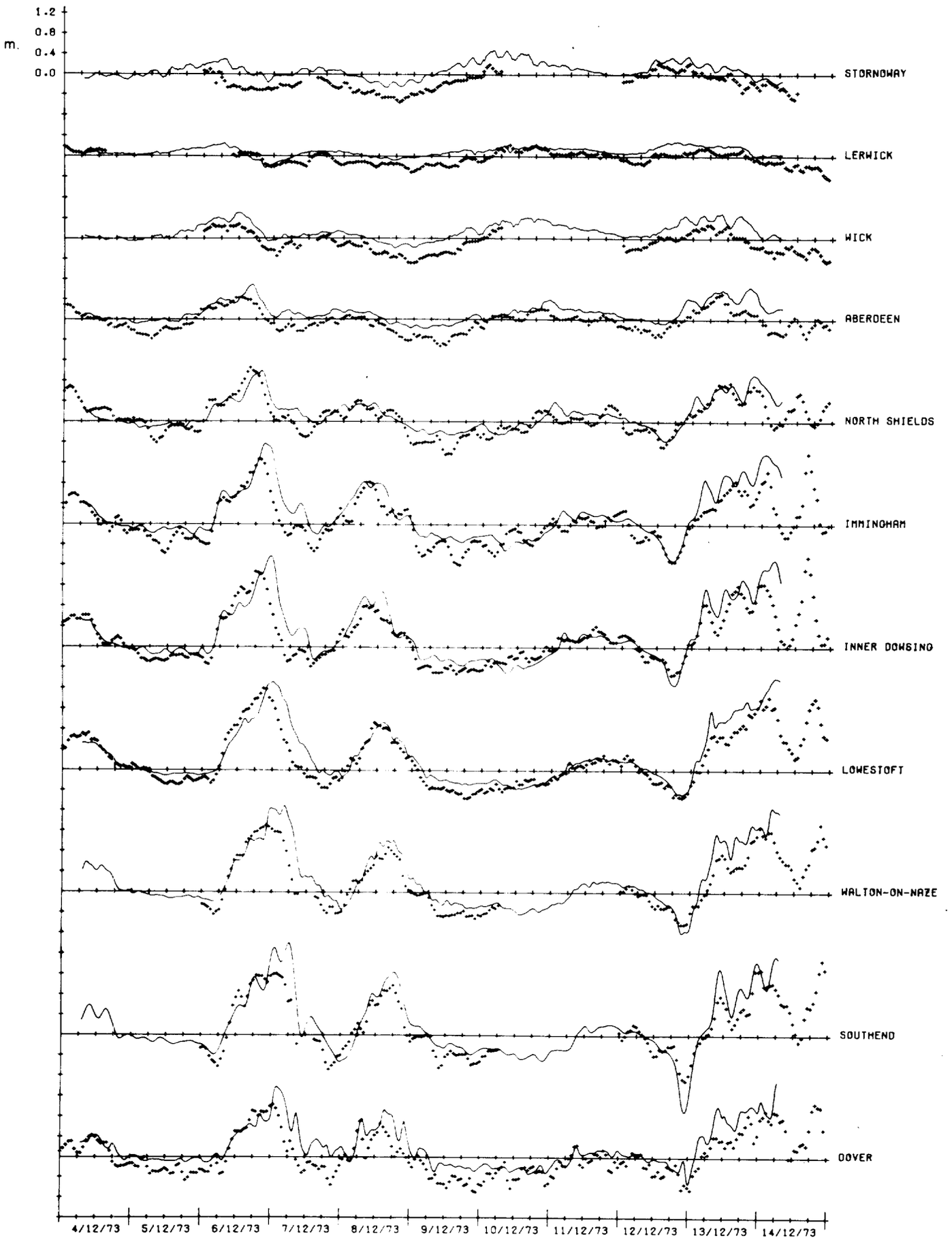

FIGURE 12a: STORM SURGES AT UK PORTS, COMPUTED (———); OBSERVED (++++++).

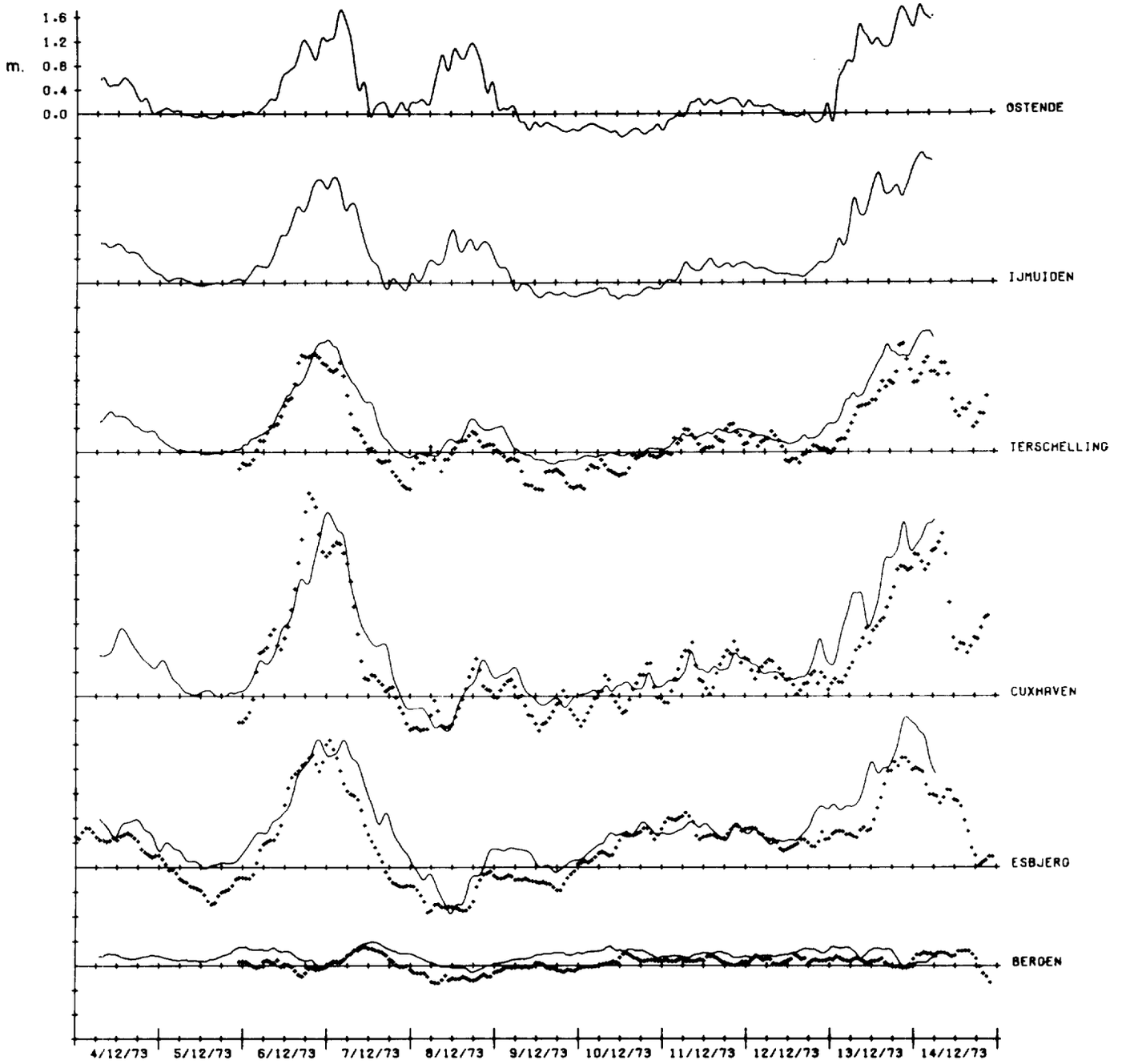

FIGURE 12b: STORM SURGES AT CONTINENTAL PORTS. COMPUTED (———); OBSERVED (++++++).

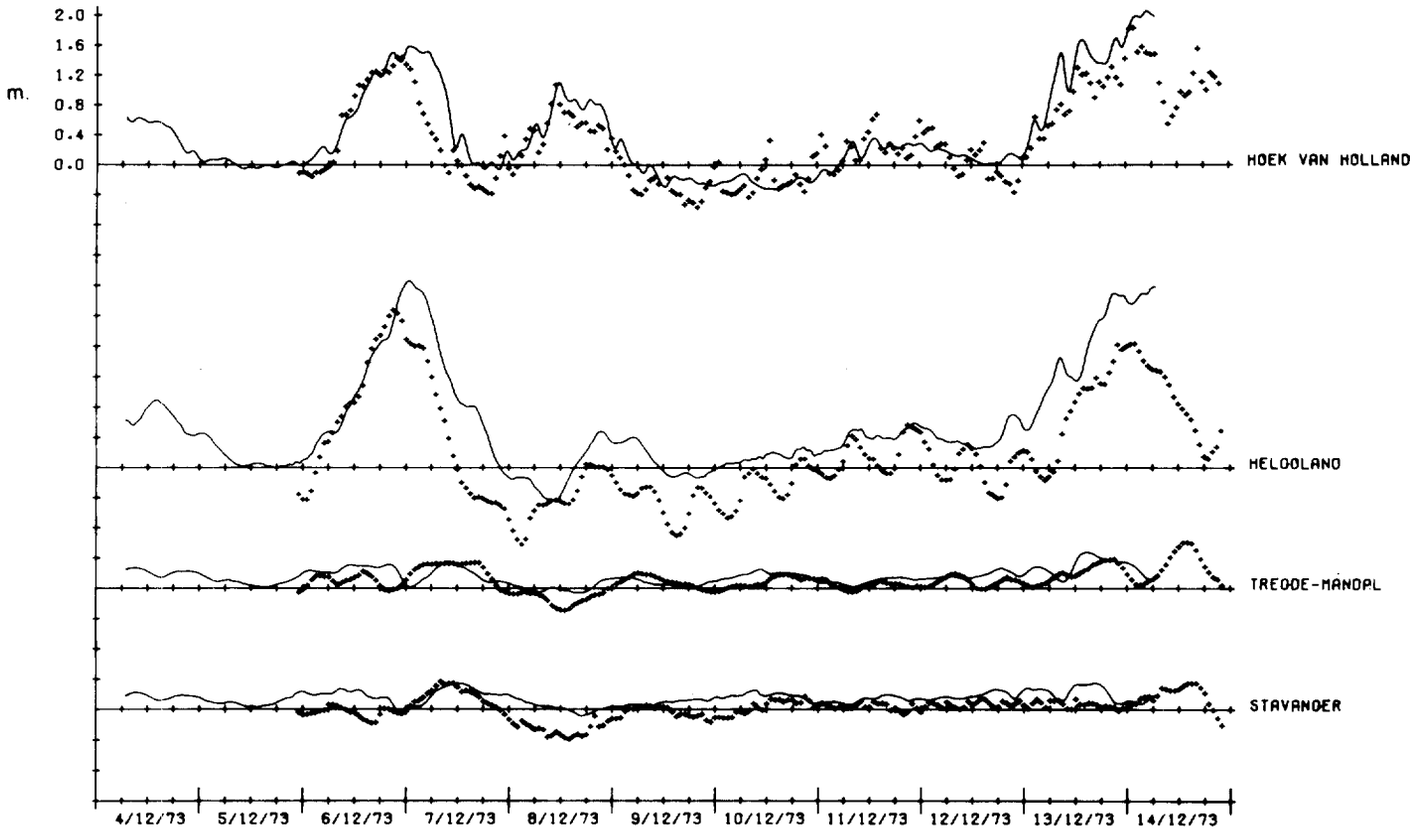

FIGURE 12c: STORM SURGES AT ADDITIONAL PORTS. COMPUTED (————); OBSERVED (++++++).

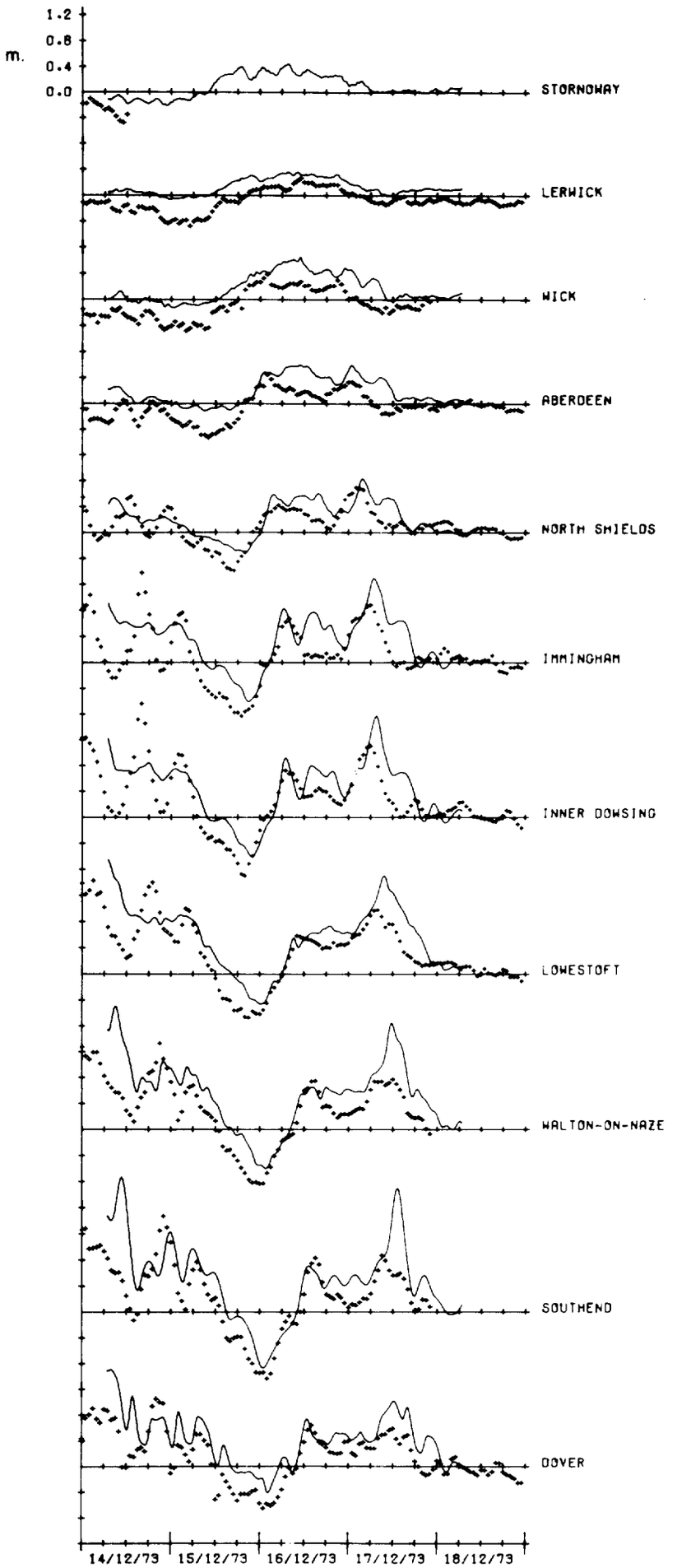

FIGURE 13a: STORM SURGES AT UK PORTS, COMPUTED (———); OBSERVED (++++++).

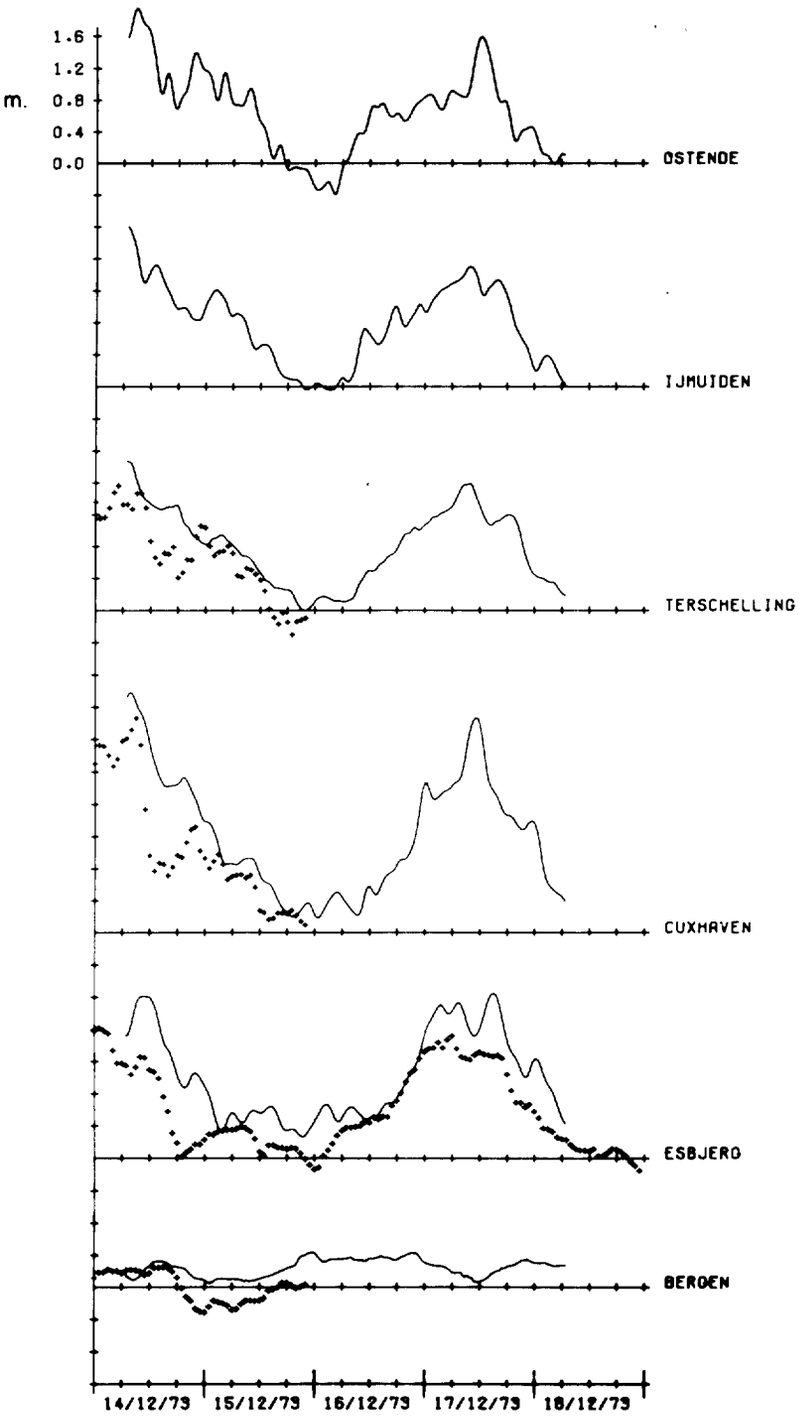

FIGURE 13b: STORM SURGES AT CONTINENTAL PORTS. COMPUTED (————); OBSERVED (++++++)

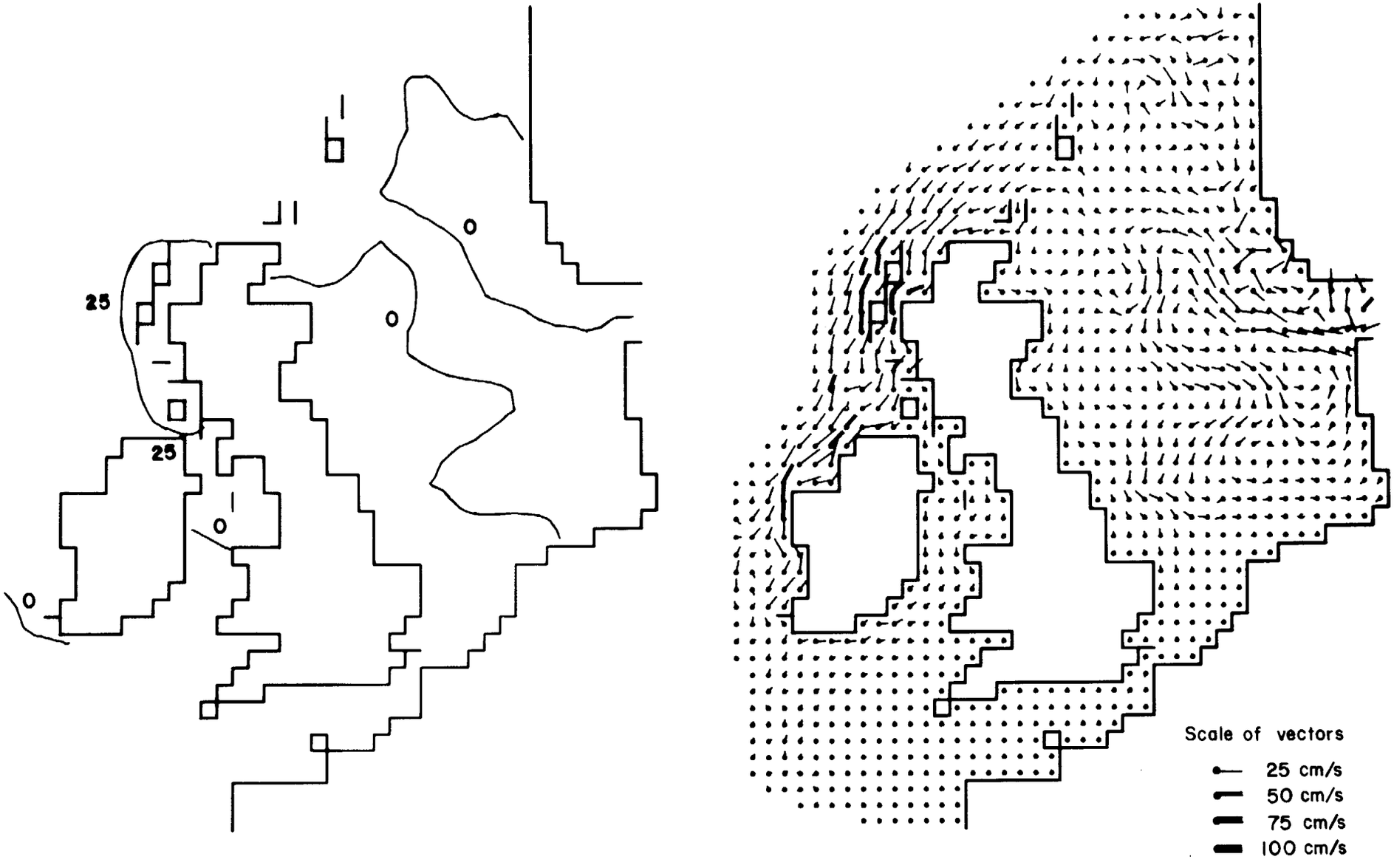

Figure 14a : The storm surge of 18-20/11/73 . Contours of surface elevation (cm) and current vectors at

0100 18/11/73

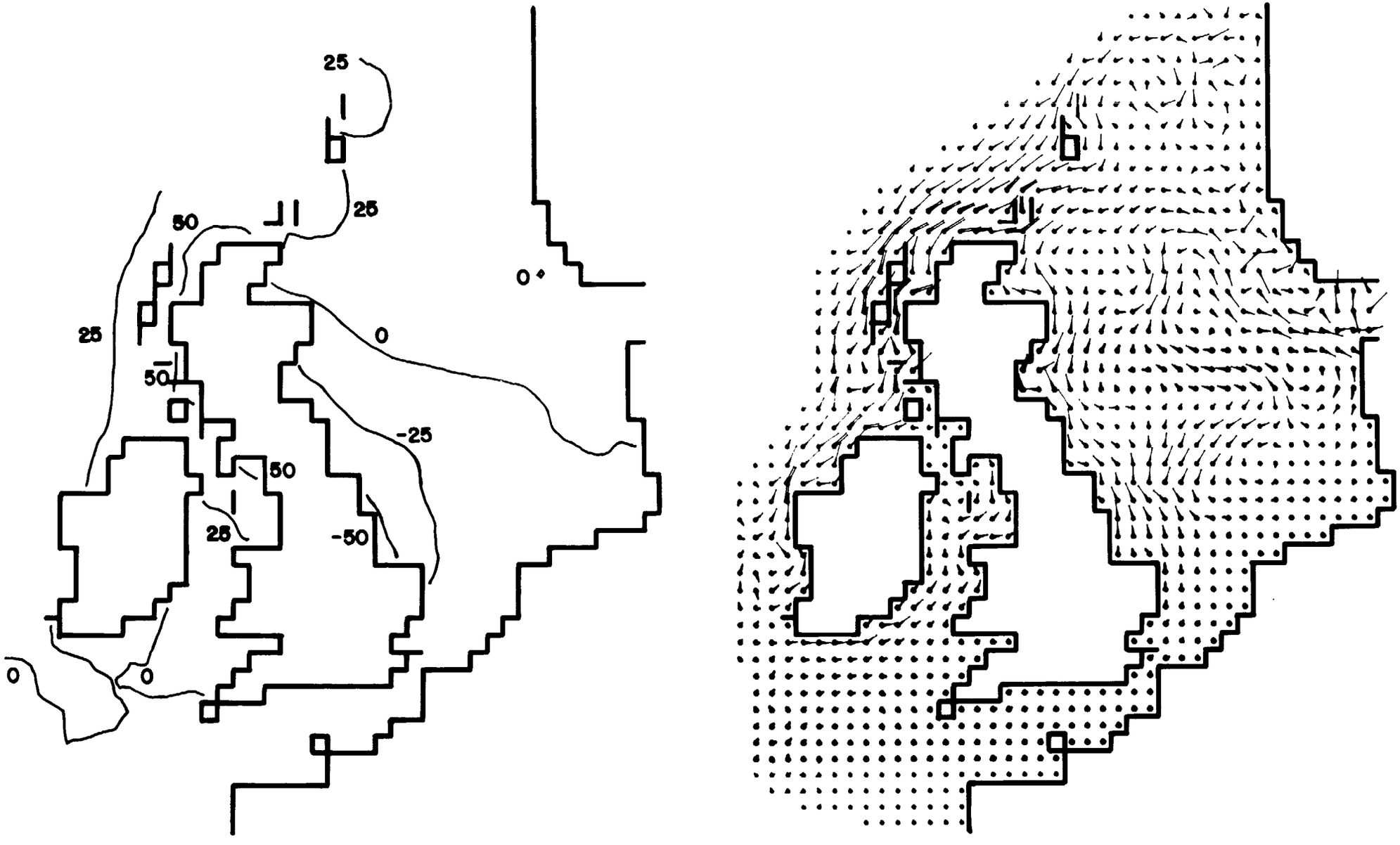

Figure 14b 0700 18/11/73

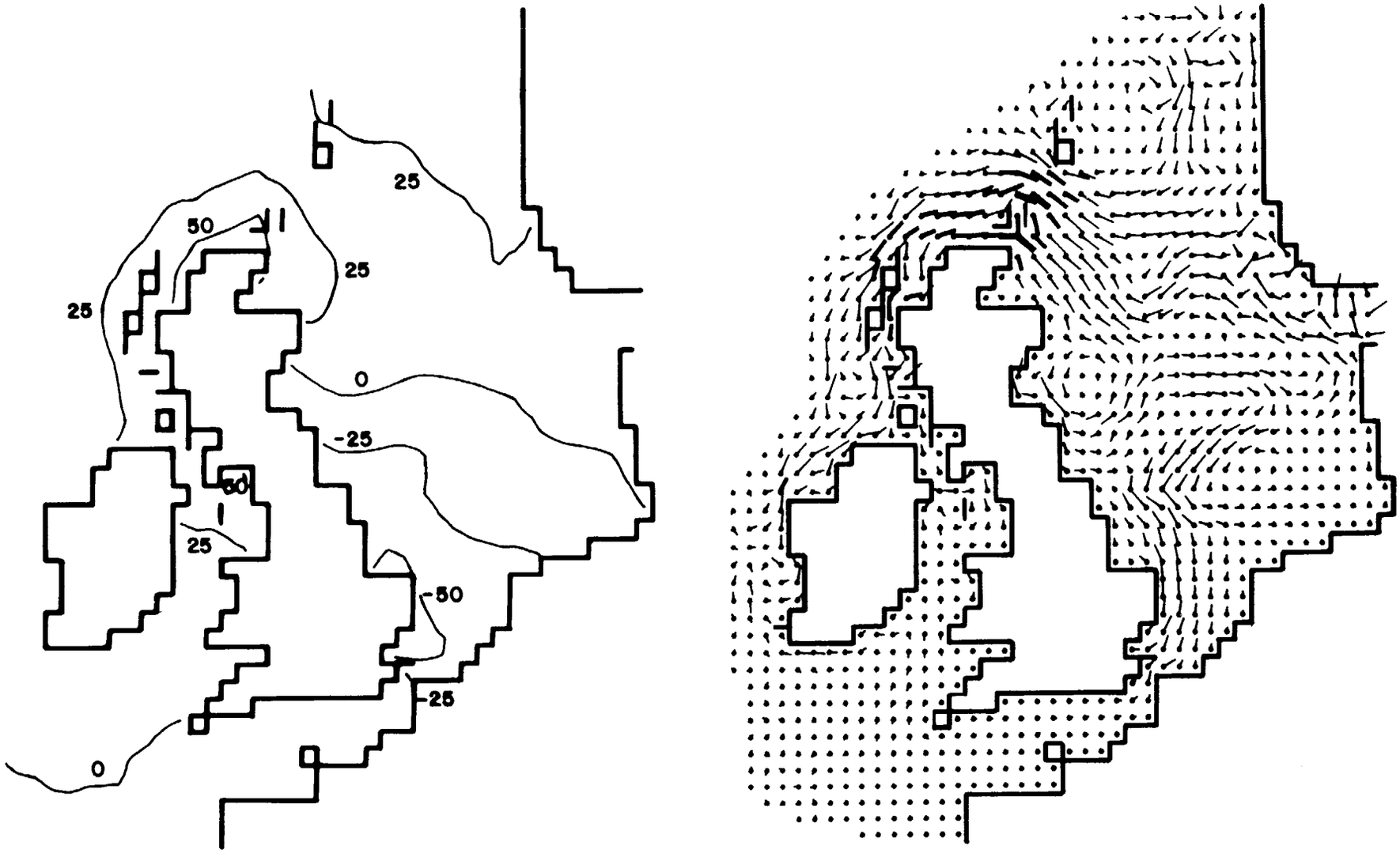

Figure 14c 1300 18/11/73

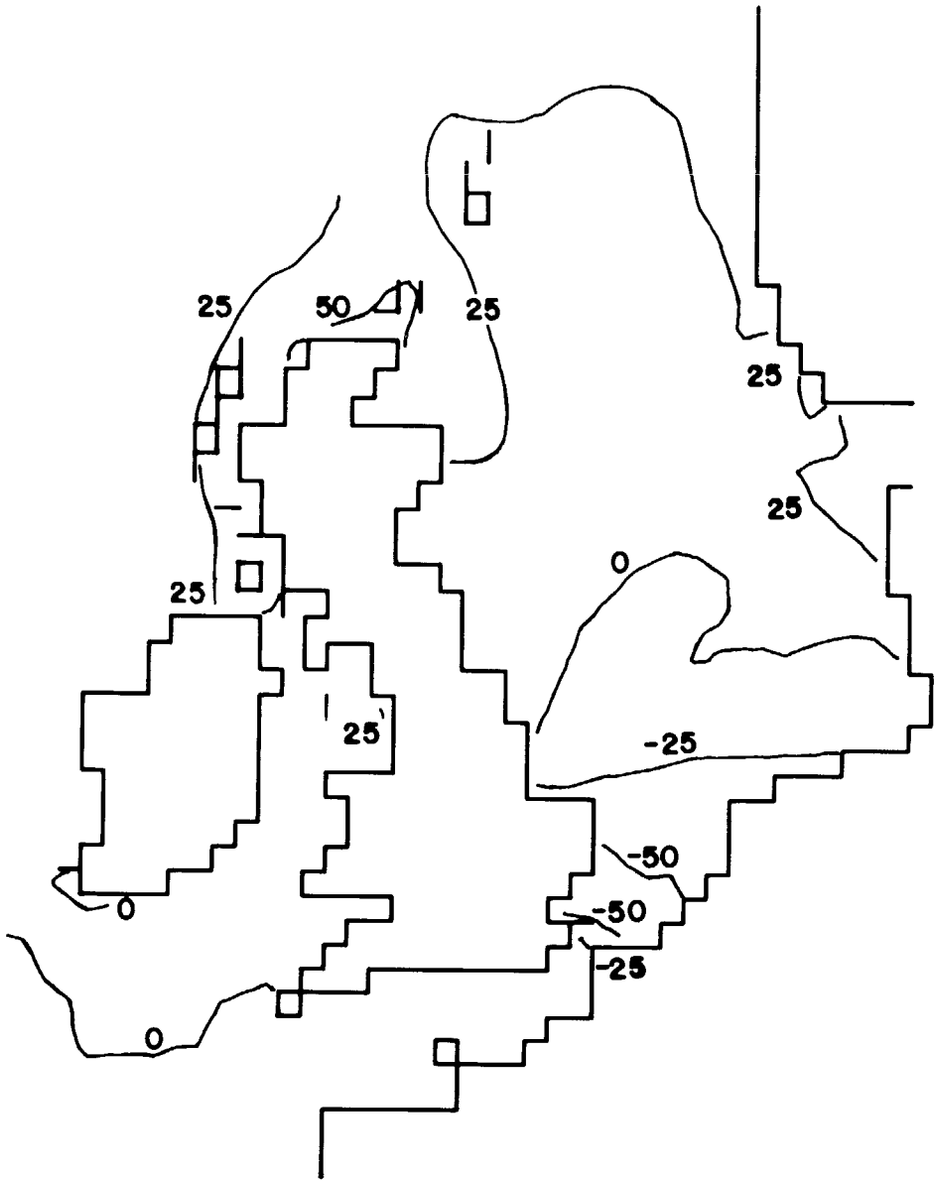

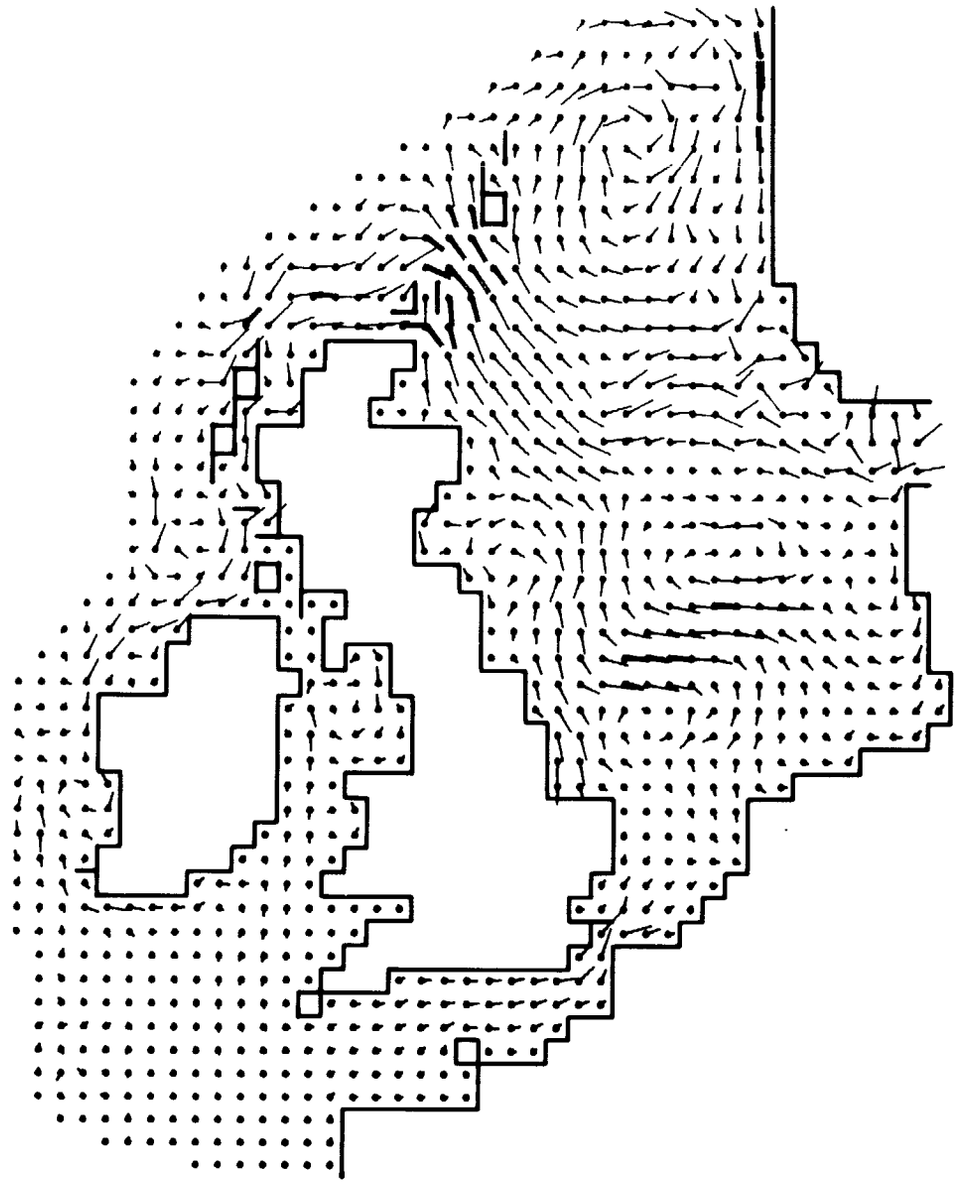

Figure 14 d 1900 18/11/73

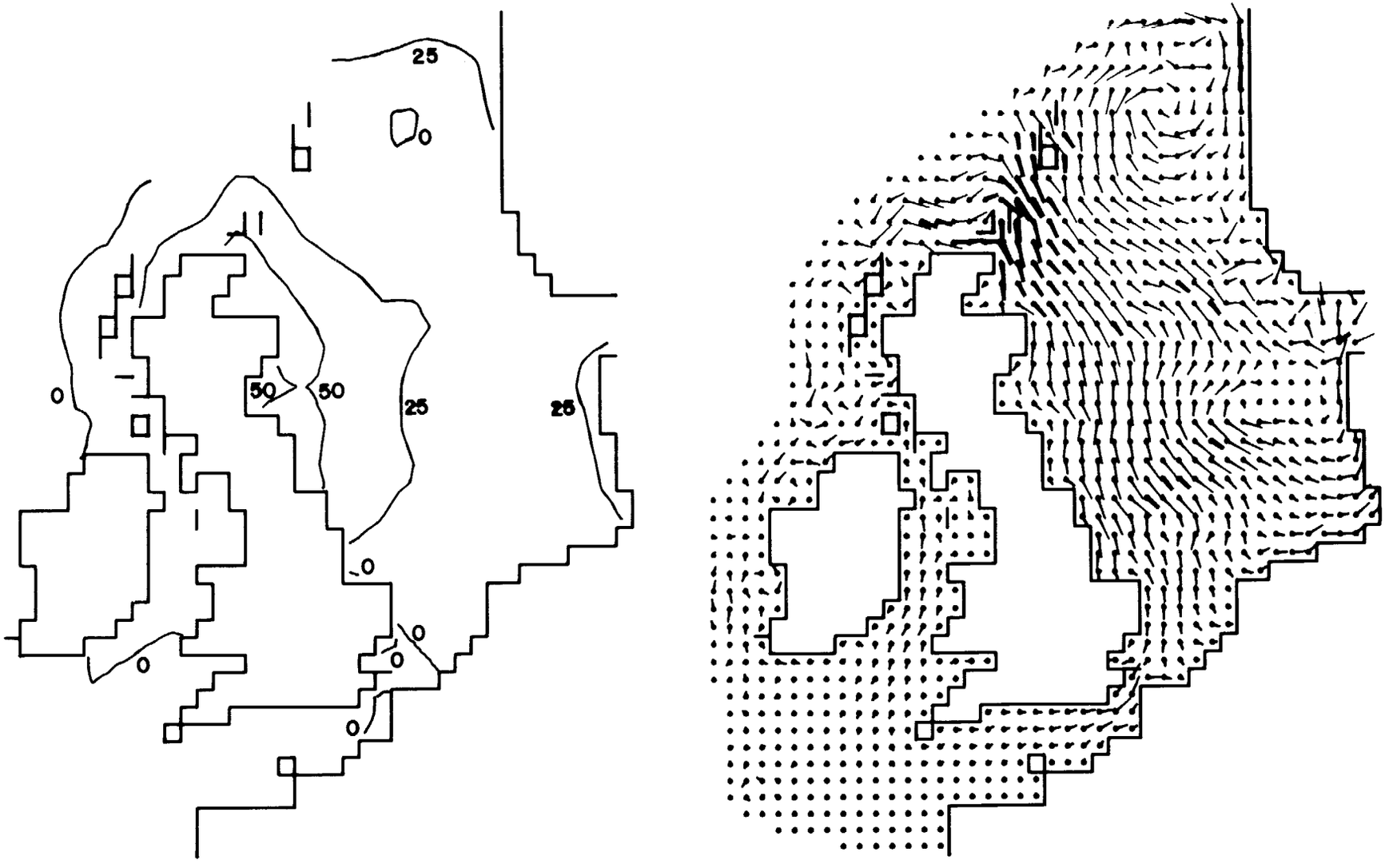

Figure 14e 0100 19/11/73

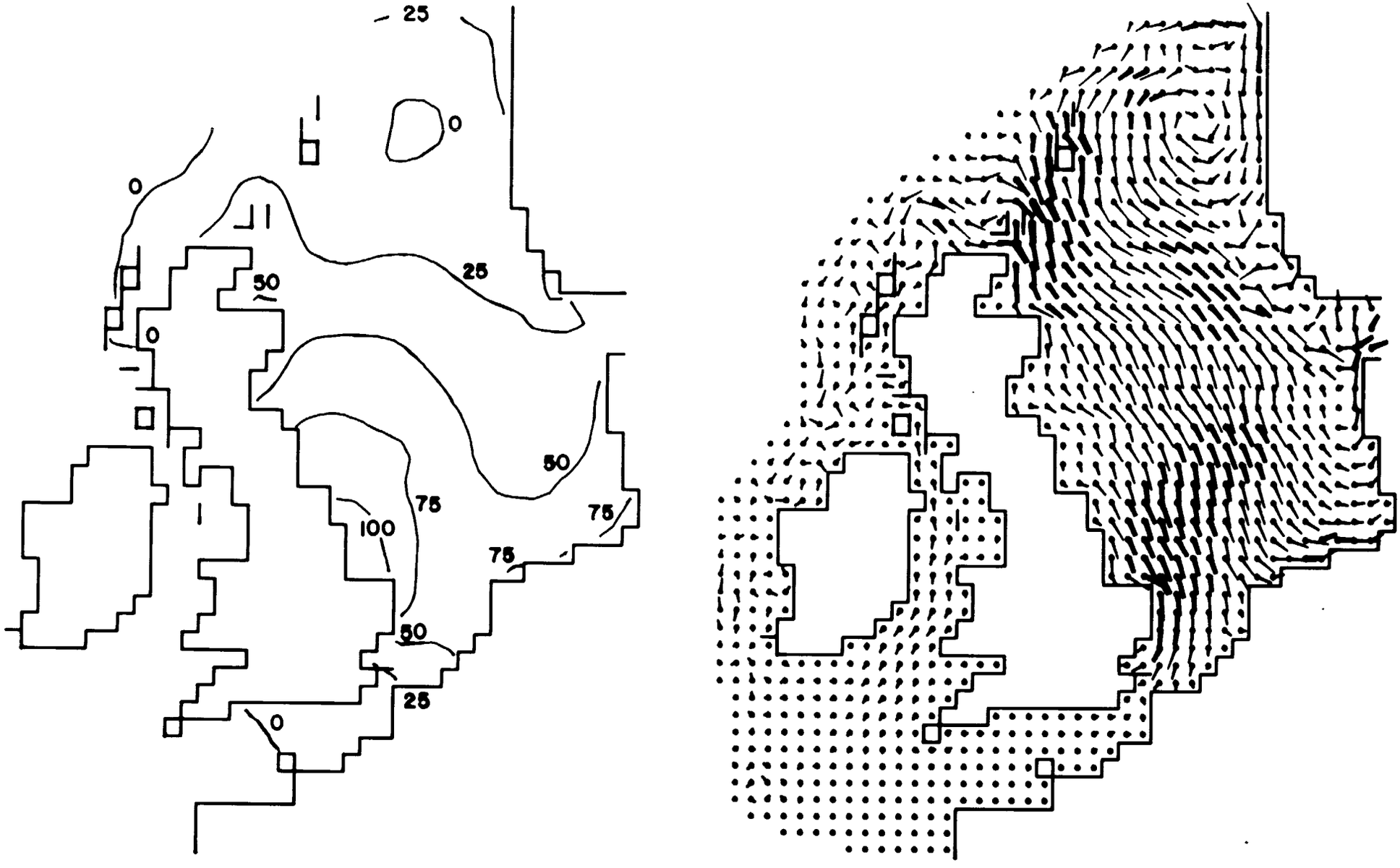

Figure 14f 0700 19/11/73

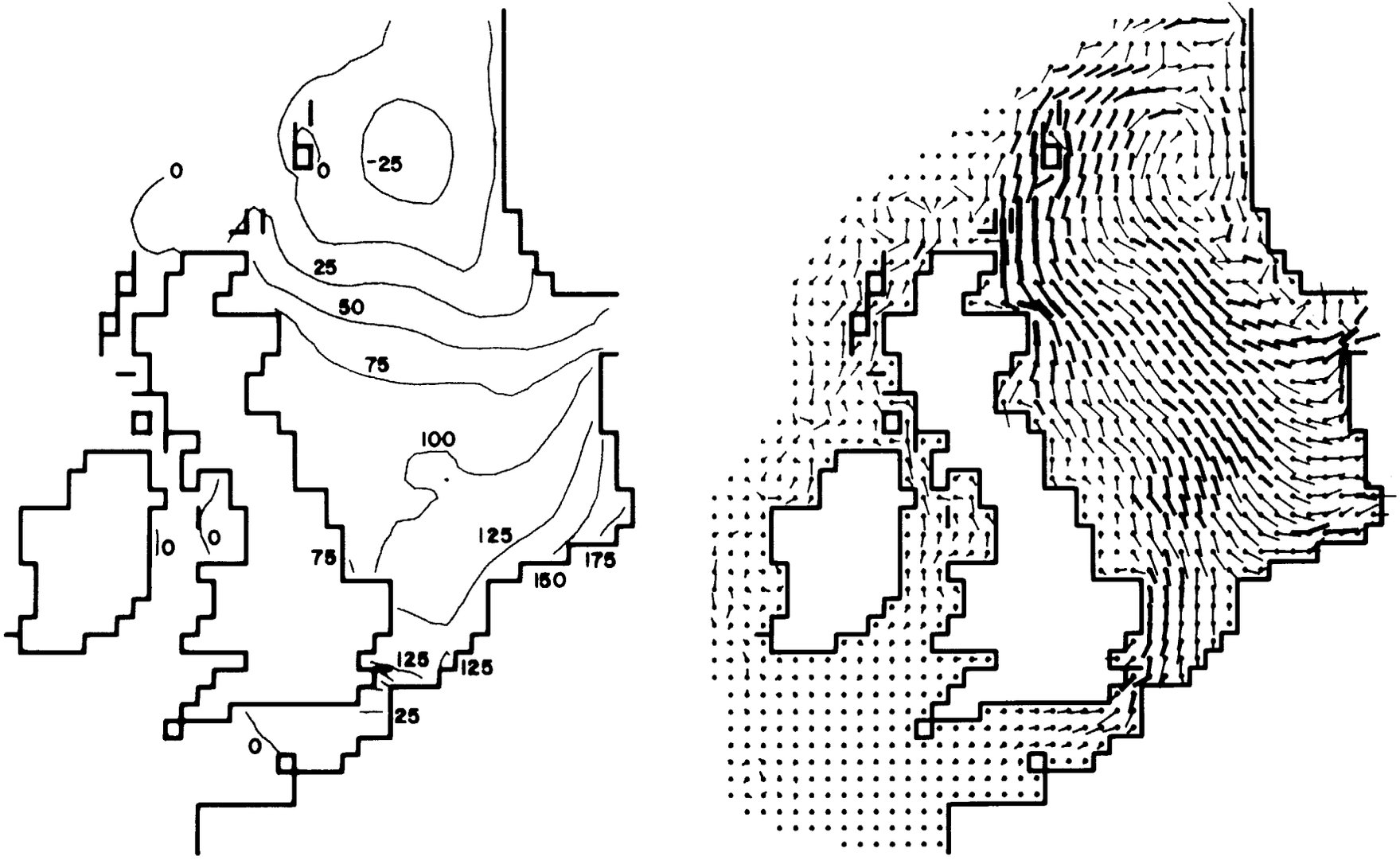

Figure 14 g 1300 19/11/73

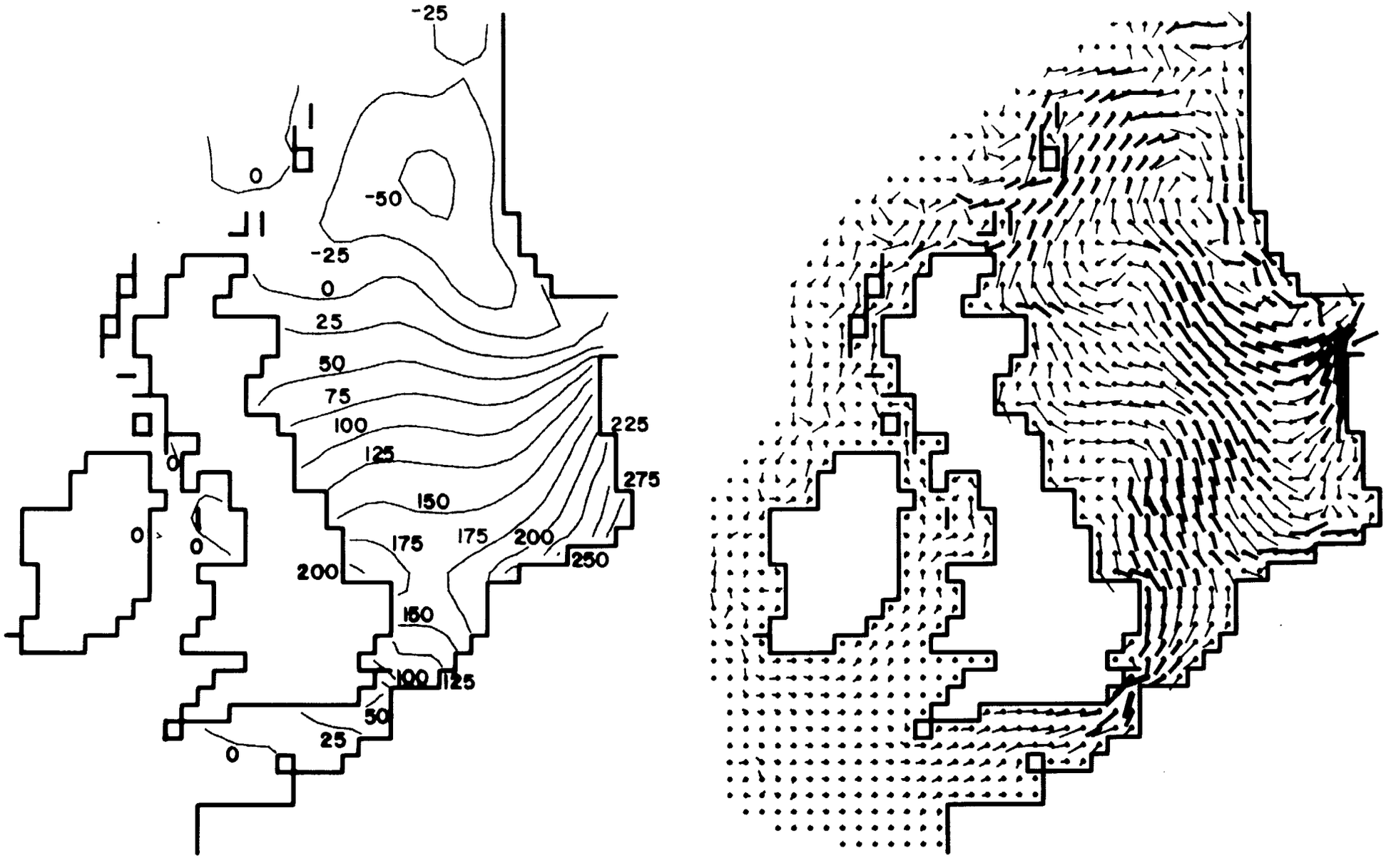

Figure 14h 1900 19/11/73

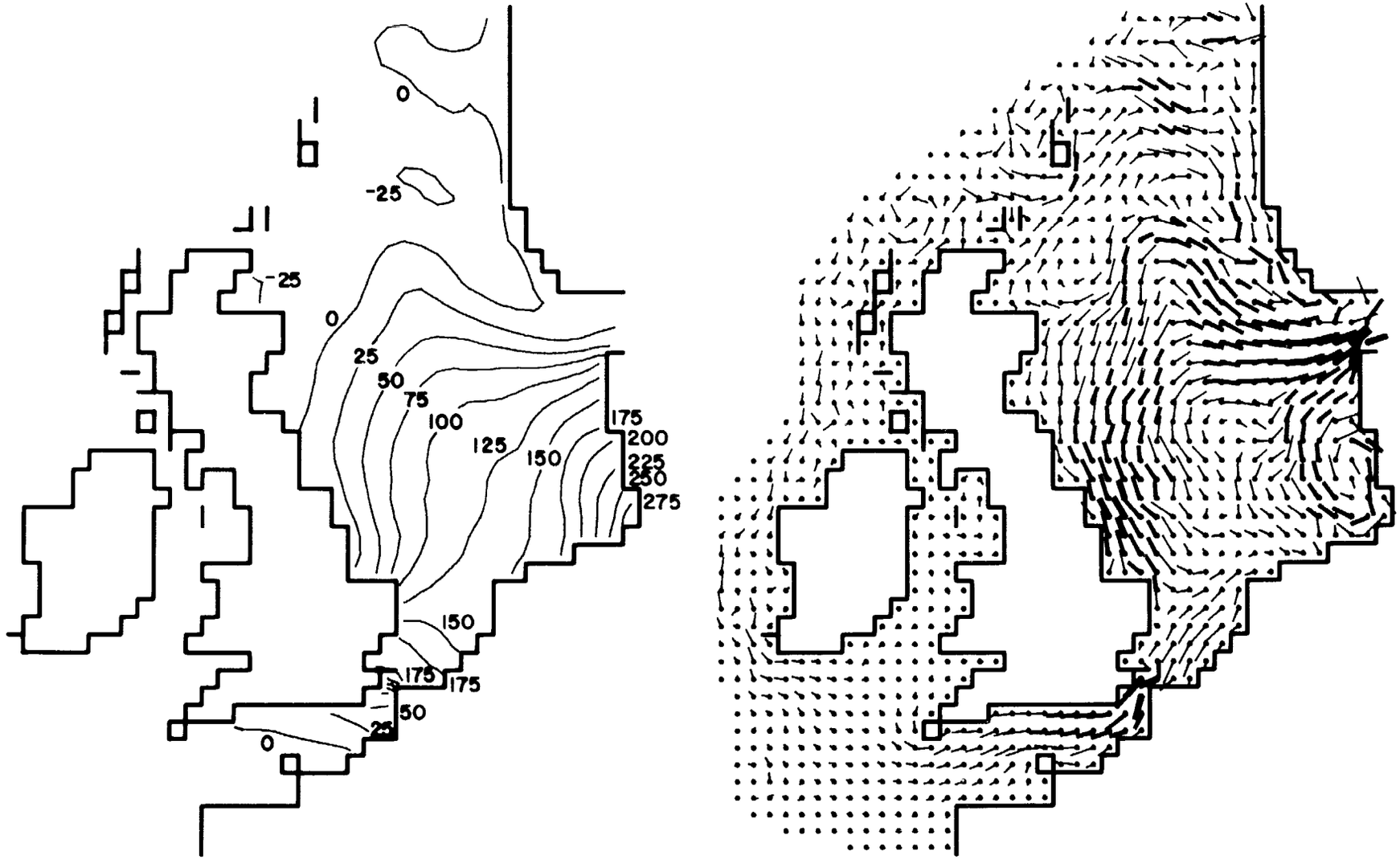

Figure 141 0100 20/11/73

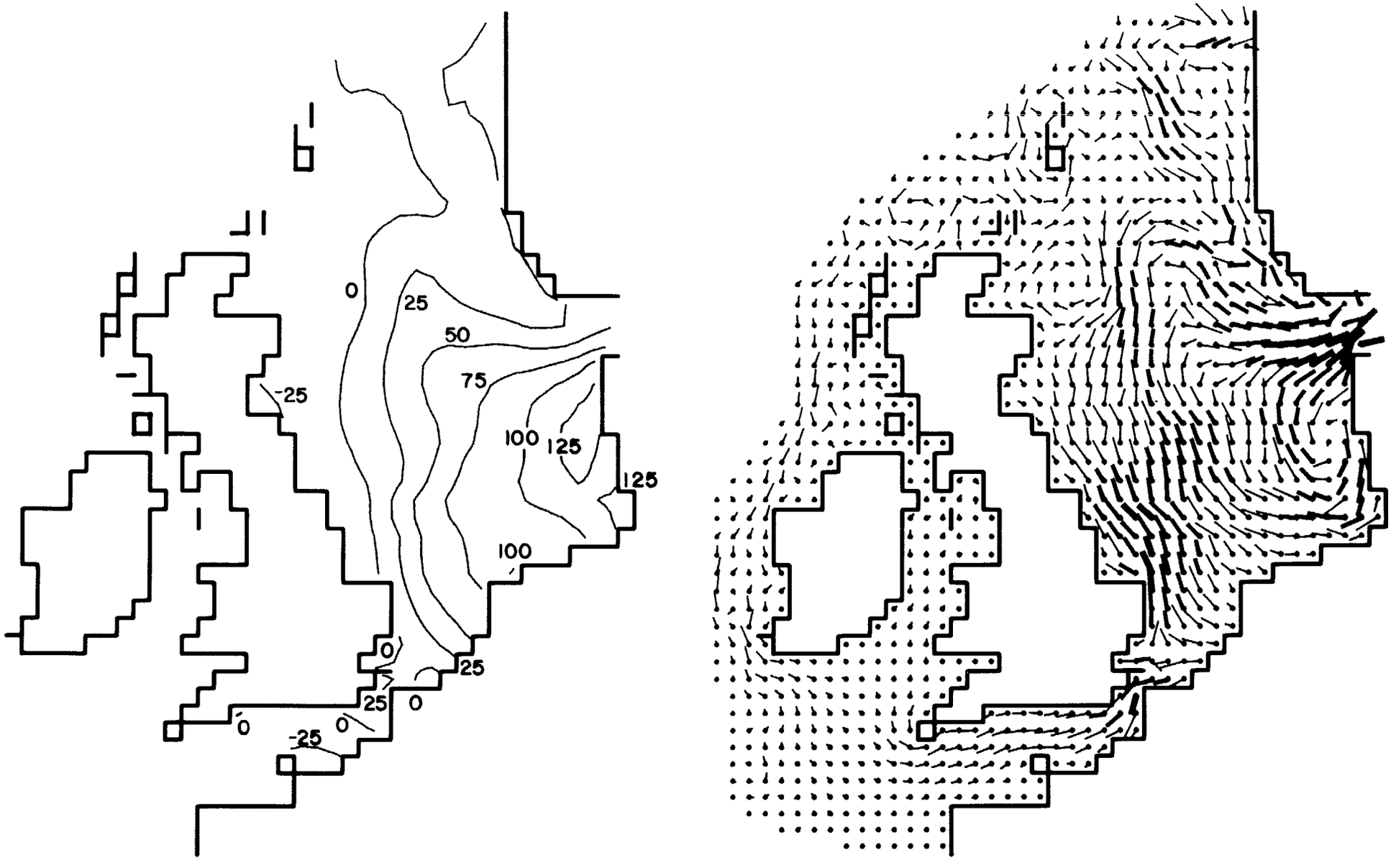

Figure 14j 0700 20/11/73

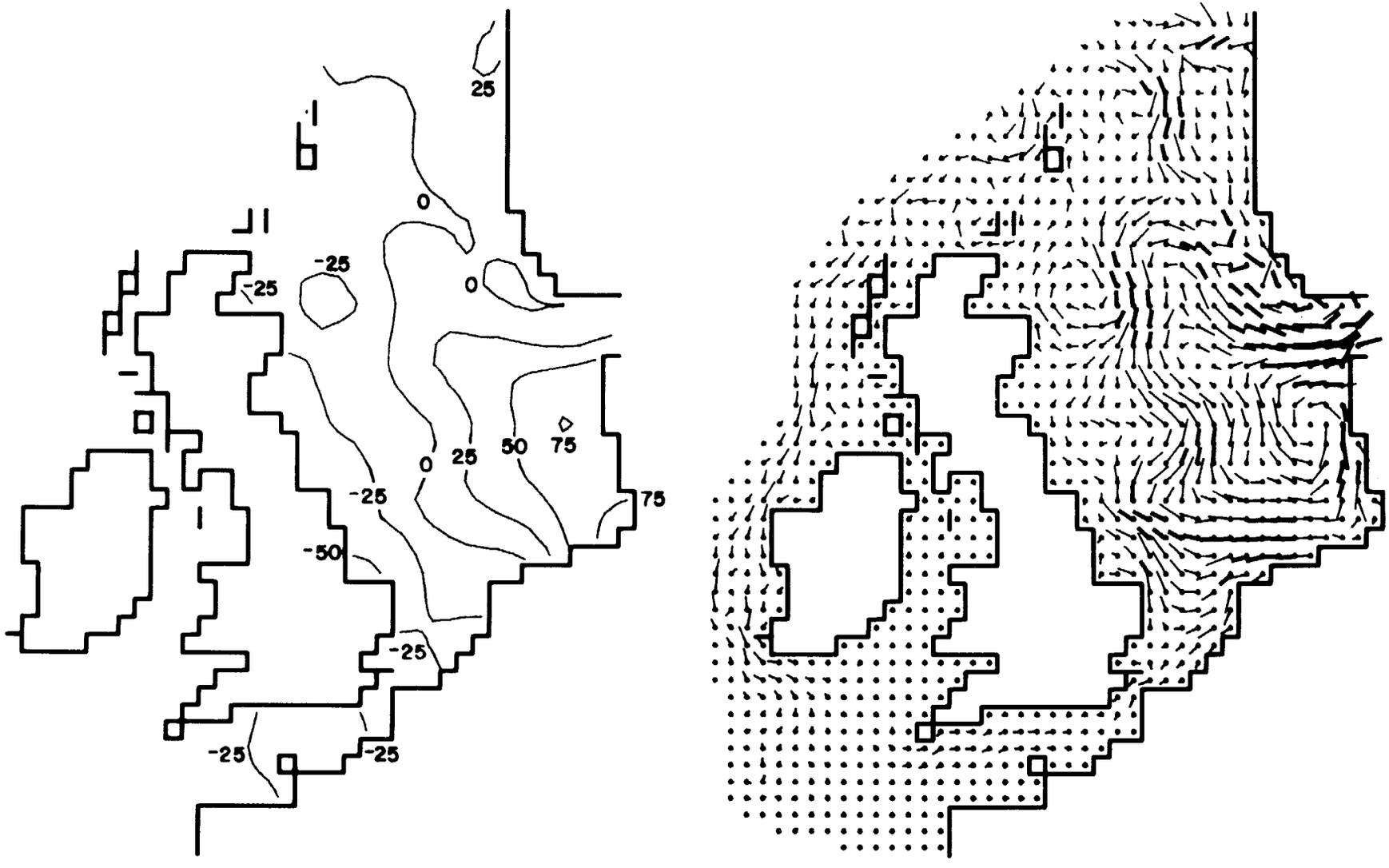

Figure 14k 1300 20/11/73

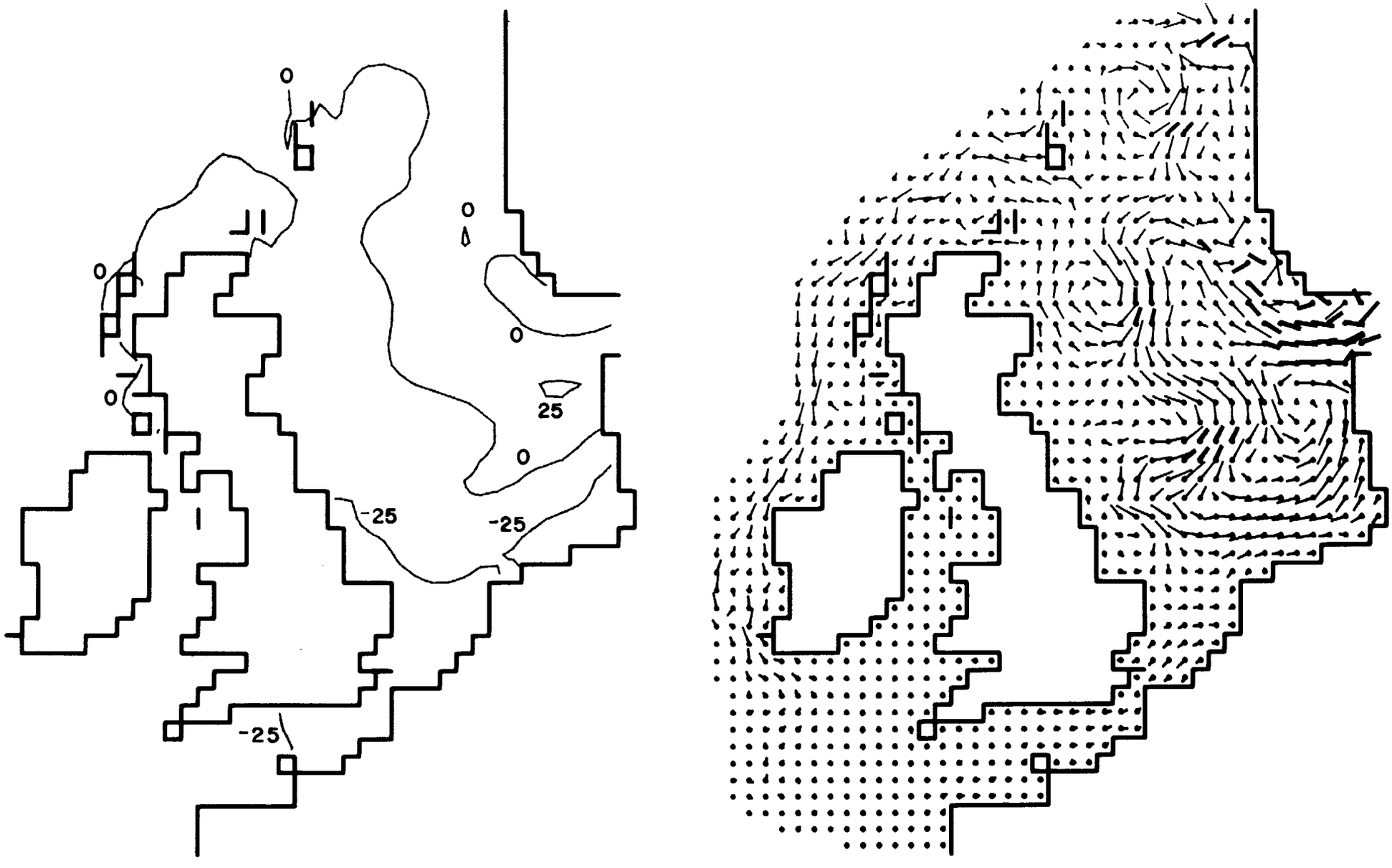

Figure 141 1900 20/11/73